Università degli Studi di Padova

Dipartimento di Biologia

SCUOLA DI DOTTORATO DI RICERCA IN: Bioscienze e Biotecnologie

INDIRIZZO: Biochimica e Biofisica

CICLO XXVIII

In Vitro and In Vivo Study Of The Role Of The Mitochondria – Shaping Protein Opa1 In Cancer

Direttore della scuola : Ch.mo Prof. Paolo Bernardi

Coordinatore d'indirizzo: Ch.mo Prof. Fabio Di Lisa

Supervisore: Ch.mo Prof. Luca Scorrano

Dottoranda: Dijana Samardžić

31 GENNAIO 2016

TABLE OF CONTENTS

1. RIASSUNTO DELL' ATTIVITA SVOLTA

I mitocondri sono organelli cellulari che svolgono un ruolo cruciale nella produzione di ATP, nel metabolismo, nella regolazione di segnali cellulari e nell'amplificazione della morte cellulare programmata (Wasilewski e Scorrano, 2009). Nel processo di apoptosi i mitocondri rilasciano citocromo *c* e altri cofattori necessari ad amplificare la morte cellulare (Li et al., 1997). Il rilascio completo del citocromo *c* dipende dai cambiamenti nella forma e nell'ultrastruttura dell'organello, poiché durante questi processi la complessa rete mitocondriale subisce frammentazione, accompagnata dall'alterazione strutturale e dall'ampliamento delle giunzioni delle creste mitocondriali (Frank et al, 2001;. Scorrano et al., 2002). Da notare che una mancata o alterata regolazione dell'apoptosi rappresenta una delle caratteristiche tipiche del cancro, poiché le cellule tumorali sfruttano l'inibizione della via apoptotica mitocondriale per acquisire il fenotipo maligno (Thompson, 1995).

I mitocondri sono organelli dinamici. Tutti i processi che incidono sui cambiamenti nella forma e nell'ultrastruttura dell'organello sono controllati dall'azione coordinata di una coorte di proteine chiamate *mitochondria-shaping proteins*, le quali rappresentano grandi GTPasi che condividono omologia strutturale con la famiglia delle dinamine (Dimmer e Scorrano, 2006).

La forma mitocondriale nello stato stazionario è il risultato dell'azione equilibrata di eventi di fissione e fusione (Griparic e van der Bliek, 2001). Il processo di fissione mitocondriale è controllato dall'azione sincrona di una proteina citosolica Drp1 (*Dynamin-related protein* 1) (Cereghetti et al, 2008), che viene reclutata sulla membrana mitocondriale esterna dove interagisce con i suoi adattatori Fis1 (*Fission - 1*), MFF (*Mitochondrial Fission Factor*), Mid49 e

Mid51 (*Mitochondrial Division 49* e *Mitochondrial Division51*) e partecipa alla divisione dei mitocondri (Palmer et al., 2011). La fusione mitocondriale, invece, è un processo controllato dalle Mitofusine (Mfn1 e MFN2) - proteine localizzate nella membrana mitocondriale esterna – e da *Optic Atrophy 1* (Opa1), la sola GTPasi responsabile della forma mitocondriale localizzata nella membrana mitocondriale interna (Santel e Fuller, 2001; Chen et al., 2003; Cipolat et al, 2004).

Negli esseri umani, lo *splicing* alternativo di Opa1 dà luogo a 8 varianti di *splicing* diverse. Queste varianti di splicing possono essere ulteriormente modificate a livello post-trascrizionale dall'azione di proteasi che danno luogo a 2 forme lunghe e 3 forme brevi di Opa1 (Olichon et al, 2007;. Duvezin-Caubet et al., 2007).

Opa1 è una proteina multifunzionale: indipendentemente dalla sua funzione nel promuovere la fusione dei mitocondri, svolge anche un ruolo nel controllo dell'apoptosi, mantenendo sotto controllo la struttura e la forma delle creste mitocondriali, formando complessi multimerici localizzati alle giunzioni delle creste stesse (Cipolat et al., 2004; Frezza et al, 2006; Cipolat et al, 2006). Un altro ruolo importante di Opa1 è nel controllo del metabolismo mitocondriale, perché favorisce l'associazione dei complessi della catena respiratoria mitocondriale in supercomplessi, aumentando in questo modo l'efficienza della fosforilazione ossidativa (Cogliati et al., 2013). Tutte queste funzioni concorrono a determinare il risultato benefico di una sua lieve sovraespressione in vivo, che, infatti, è protettiva in caso di ischemia cerebrale o cardiaca, atrofia muscolare indotta da denervazione e in caso di epatite fulminante (Varanita et al., 2015). Inoltre, la sovraespressione di OPA1 corregge alcuni modelli murini di disfunzione

mitocondriale primaria causata da difetti nei componenti della catena respiratoria (Civiletto et al., 2015).

Tuttavia, tutti questi effetti benefici hanno una controparte negativa. Infatti, alcuni studi hanno mostrato come Opa1 sia sovraespressa in diversi tumori umani, in cui elevati livelli di Opa1 sono correlati ad una peggiore prognosi e una risposta alterata alle terapie anti-tumorali (Fang et al., 2012). Al contrario, la riduzione dell'espressione di Opa1 è stata associata all'induzione di apoptosi nelle cellule tumorali tramite la via mitocondriale e ad un migliore esito clinico (Zhao et al, 2013).

In questa Tesi abbiamo deciso di investigare quale ruolo biologico giochi Opa1 nell'acquisizione e nel mantenimento del fenotipo tumorale, sia in modelli cellulari che animali, ipotizzando che una possibile spiegazione per la mancata sovraespressione costitutiva di Opa1 sia che tale sovraespressione potrebbe essere legata ad un aumento di suscettibilità allo sviluppo e/o progressione di forme tumorali.

Abbiamo utilizzato linee cellulari, derivanti da pazienti con diagnosi di linfoma diffuso a grandi cellule B (DLBCL) come sistema modello in vitro. I linfomi diffusi a grandi cellule B (DLBCL) sono tra le forme più comuni di neoplasie linfoidi non-Hodgkin negli adulti (Lohr et al., 2012). Sono un gruppo geneticamente eterogeneo di tumori che possono essere ulteriormente suddivisi in diversi sottogruppi in base a caratteristiche molecolari distinte (Alizadeh et al., 2000). Attraverso un approccio basato su *Genome wide array* e molteplici algoritmi di *clustering* sono stati caratterizzati due gruppi di linfomi: il primo presenta la sovraespressione di geni che codificano per i componenti del recettore delle cellule B – BCR (BCR-DLBCL), il secondo è

rappresentato da un gruppo arricchito in geni coinvolti nella fosforilazione ossidativa mitocondriale (OxPhosS-DLBCL). Il sottoinsieme OxPhos manca di una rete intatta di segnalazione a valle del BCR, suggerendo la dipendenza da meccanismi di sopravvivenza alternativi, che non sono stati ancora definiti (Monti et al., 2005; Caro et al, 2012.). Attraverso un approccio di proteomica, volto a comprendere con cura i componenti del proteoma mitocondriale del gruppo BCR nei confronti del gruppo OxPhos, è stato osservato che i livelli di Opa1 nelle cellule OxPhos sono più alti (Danial N, manoscritto in preparazione). Per tale ragione abbiamo voluto chiarire quale ruolo giochi Opa1 in questi sottoinsiemi di cellule di cancro.

Al fine di verificare se la sovraespressione di Opa1 contribuisca allo sviluppo e alla progressione del cancro in vivo, abbiamo utilizzato un modello noto e caratterizzato di linfoma in topo, il topo transgenico Eμ-myc (Adams et al., 1985). I topi Eμ-myc sono stati ulteriormente incrociati con un modello murino di sovraespressione Opa1, recentemente generato nel nostro laboratorio (Cogliati et al., 2013). Il risultato di questo incrocio ha generato il modello di topo che abbiamo usato nel nostro studio.

In questa Tesi presentiamo prove che Opa1 è processata in forme più brevi nel sottoinsieme di DLBCL caratterizzato dalla sovraespressione di componenti del BCR e che, come risultato, la morfologia mitocondriale, il metabolismo e l'ultrastruttura sono diversi tra i sottoinsiemi BCR e OxPhos. Inoltre, mostriamo anche la prova di una marcata sinergia tra *Opa1 e c-Myc* in modelli murini transgenici, dove la sovraespressione di Opa1 contribuisce e aggrava lo sviluppo di cancro nel modello murino Eμ-Myc. Il lavoro svolto in questa Tesi mette in evidenza un ruolo per Opa1 nel definire le caratteristiche dei linfomi diffusi a grandi cellule B (DLBCL) e nella progressione dei tumori in vivo. In conclusione, i nostri dati indicano che Opa1 mostra

caratteristiche pro-oncogeniche e che può essere presa in considerazione come nuovo bersaglio terapeutico per il trattamento del cancro.

2. SUMMARY

Mitochondria are double membrane–enclosed organelles that play a crucial role in ATP production, metabolism, regulation of cellular signaling and amplification of programmed cell death (Wasilewski and Scorrano, 2009). In the process of apoptosis mitochondria release cytochrome c and other cofactors that are required to amplify cell death (Li et al., 1997). The complete release of cytochrome c depends on the changes in the shape and in the ultrastructure of the organelle, since during these processes mitochondrial network undergoes fragmentation, that is accompanied by cristae remodeling and widening of cristae junctions (Frank et al., 2001; Scorrano et al., 2002). Of note, deregulation of apoptosis represents a typical hallmark of cancer, since cancer cells exploit the inhibition of the mitochondrial arm of apoptosis to acquire the malignant phenotype (Thompson, 1995).

Mitochondria are dynamic organelles, and all processes that impinge on the changes in the shape and in the ultrastructure of the organelle are controlled by a regulated action of mitochondria shaping proteins, which represent large GTPases that share structural homology with the dynamin protein family (Dimmer and Scorrano, 2006).

Mitochondrial shape in the steady state is a result of the balanced action of fission and fusion events (Griparic and van der Bliek, 2001). The process of mitochondrial fission is controlled by a synchronized action of a cytosolic protein Drp1 (Dynamin – related protein 1) (Cereghetti et al., 2008), that is recruited to the outer mitochondrial membrane where it binds its adaptors Fis1 (Fission – 1), MFF (Mitochondrial fission factor), Mid49 and Mid51 (Mitochondrial division), and participates in the division of mitochondria (Palmer et al., 2011). Mitochondrial fusion, on the

other hand, is a process controlled by mitofusins (Mfn1 and Mfn2), proteins located in the outer mitochondrial membrane, together with the only inner membrane GTPase - Optic Atrophy 1 (Opa1) (Santel and Fuller, 2001; Chen et al., 2003; Cipolat et al., 2004).

In humans, alternative splicing of Opa1 gives rise to 8 mRNA splice variants which further get processed by proteolytic proteases giving rise to 2 long and 3 short forms of Opa1 (Olichon et al., 2007; Duvezin-Caubet et al., 2007).

Opa1 is a multifunctional protein: apart from its function in promoting mitochondrial fusion (Cipolat et al., 2004), it also plays a role in the control of apoptosis by keeping in check the cristae remodeling pathway, by forming multimeric complexes at the cristae junctions, keeping in shape the size of these junctions (Frezza et al., 2006; Cipolat et al., 2006). Another important role of Opa1 is in the control of mitochondrial metabolism, because Opa1 favors the superassembly of respiratory chain complexes into supercomplexes, increasing the efficiency of oxidative phosphorilation (Cogliati et al., 2013). All these functions concur to determine the beneficial outcome of its mild overexpression in vivo, which protects from heart and brain ischaemia, denervation-induced muscular atrophy and fulminant hepatitis (Varanita et al., 2015). Furthermore, it corrects mouse models of primary mitochondrial dysfunction caused by defects in components of the respiratory chain (Civiletto et al., 2015).

However, all these beneficial effects come with a counterpart, since a handful of studies reported that Opa1 is overexpressed in several human cancers where high levels of Opa1 correlated with a worst prognosis and an impaired response to therapy (Fang et al., 2012), while blocking its

expression was associated with an induction of the mitochondria - associated apoptotic pathway in the cancer cell and a better clinical outcome (Zhao et al., 2013).

In this Thesis we set out to understand what role does Opa1 play in the acquisition and maintenance of the cancer phenotype, both in cellular and animal models, while reasoning that a possible explanation why we don't have constitutively high Opa1 levels is the fact that the trade off of Opa1 overexpression could be an increased susceptibility to cancer development/progression.

Well established cell lines, initially deriving from patients diagnosed with diffuse large B cell lymphoma (DLBCL) served as our in vitro model system. DLBCLs are one of the most common adult non-Hodgkin lymphoid malignancies today (Lohr et al., 2012). They are a genetically heterogeneous group of tumors that can be further divided in several subsets, identified by their distinct molecular signatures (Alizadeh et al., 2000). Genome wide arrays and multiple clustering algorithms defined a B cell receptor (BCR)/proliferation cluster (BCR–DLBCL), which displays upregulation of genes encoding BCR signaling components, and an OxPhos cluster (OxPhos–DLBCL) which is enriched in genes involved in mitochondrial oxidative phosphorylation. The OxPhos subset lacks an intact BCR signaling network, suggesting dependence on alternative survival mechanisms, which are not yet defined (Monti et al., 2005; Caro et al., 2012). Since a proteomic approach, aimed at carefully dissecting components of the mitochondrial proteome in the BCR versus OxPhos cell group, identified increased levels of Opa1 in the OxPhos (Danial N, manuscript in preparation), we wished to elucidate what role does Opa1 play in these cancer cell subsets.

In order to test whether Opa1 overexpression contributes to the development and progression of cancer in vivo, we reached out to an already established mouse lymphoma model, the Eμ-myc transgenic mouse (Adams et al., 1985), that we further crossed with a mouse model of controlled Opa1 overexpression that was recently generated in our lab (Cogliati et al., 2013), and the net result of this cross gave rise to the mouse model we used in our study.

In this Thesis we present evidence that Opa1 is increasingly processed in the BCR subset of diffuse large B cell lymphoma, and that mitochondrial morphology, metabolism, and ultrastructure are different between the BCR and the OxPhos DLBCL subsets that display different levels of Opa1. Furthermore, we also show evidence of a marked synergy between *Opa1* and *c-Myc* in doubly transgenic mouse models, where Opa1 overexpression is contributing to the development of, and aggravating cancer in Eμ-Myc transgenic animals. The work performed in this thesis highlights a role for Opa1 in DLBCL features, and tumor progression in vivo. Thus, our data indicate that Opa1 displays oncogenic features and it can be taken into consideration as a novel therapeutic target for cancer treatment.

3. INTRODUCTION

3.1. Mitochondria

Mitochondria are double-membrane enclosed organelles found in most eukaryotic cells, where they play a key role due to their high involvement in processes necessary for cell life and cell death. Mitochondria are often referred to as “powerhouses” of the cells, since they are the main source of cellular ATP, generated through the process of oxidative phosphorylation. These organelles also host the tricarboxylic acid (TCA) cycle, participate in the metabolism of fatty acids and are involved in gluconeogenesis. Moreover, they are involved in regulating calcium and redox homeostasis, and during apoptosis, upon membrane permeabilization and cristae remodeling, they release various pro-apoptotic proteins, such as cytochrome c, SMAC/DIABLO, AIF, ENDO G, Omi-HTRA2 taking part in the process of cell demise (Corrado et al., 2012).

Mitochondria are dynamic organelles: in order to fulfil all their different functions, they come in various shapes and forms that emerge as a results of the dynamic balance between processes of fusion and fission (Scorrano, 2013). Mutations in the mitochondrial genome or dysregulation of any of the mitochondria-controlled processes can have detrimental consequences to the cell and can lead to disease. During recent years, much attention has been given to the mitochondrial component in the development and progression of cancer, due to the involvement of mitochondria in cell metabolism and apoptosis, two processes that are often dysregulated in cancer (Kroemer, 2006).

3.1.1. Mitochondrial ultrastructure

The characterization of the mitochondrial ultrastructure dates all the way back to 1950s, when with advances in electron microscopy, it became possible to study the structure of cellular organelles in more detail, thanks to higher magnifications and greater resolving powers of the instrument. Pioneer works describing mitochondrial ultrastructure, with the use of electron microscopy, have been made independently by scientists George Palade and Fritiof Sjostrand. The model described by Palade is the so-called “baffle model” (Figure 1A). According to this model, mitochondria are double membrane enclosed organelles, with an outer and an inner mitochondrial membrane that folds itself forming invaginations. These invaginations, called “cristae mitochondriales” are organized in a way that one end remains open towards the inter mitochondrial space, and the other end is folded and protrudes though out the mitochondrial matrix (Palade, 1952). On the other hand, the model proposed by Sjostrand, has somewhat a different interpretation of the inner mitochondrial membrane. This model called the “septa model”, implies that the inner mitochondrial membrane forms septa-like structures that span the matrix (SJOSTRAND, 1953). Models proposed by Palade and Sjostrand are mostly of historical value today, since with the advances in modern technology and availability of high-end electron microscopes, the analysis of mitochondrial ultrastructure dramatically improved. The current model, proposed by Mannella et al in 1994, is the results of the investigation of the ultrastructure of isolated rat liver mitochondria using a high-voltage transmission electron microscope (Figure 1.B) (Mannella et al., 1994). According to this model, mitochondria are composed of an outer mitochondrial membrane (OMM) and an inner mitochondrial membrane (IMM), that can be

further subdivided into an inner boundary membrane and cristae, bag-like structures that are connected to the inner membrane by narrow tubular junctions (Mannella et al., 1994).

In terms of composition the outer mitochondrial membrane resembles that of other eukaryotic membranes. It is a phospholipid bilayer permeable to different metabolites and small peptides up to 3000 Da, thanks to the presence of voltage-dependent anion channels (VDAC) (Colombini and Mannella, 2012). The OMM is also enriched in the import machinery proteins like Tom20, Tom22 and Tom70 that enable import of proteins to the mitochondria (Pfanner and Wiedemann, 2002). On the other hand, based on physical properties and composition, the inner mitochondrial membrane (IMM) has similarities to prokaryotic membranes. The IMM contains cardiolipin, a lipid found in membranes of bacteria, responsible for proper function of many enzymes acting in the IMM, and for generating curvatures in the IMM that impact on cristae formation. IMM contains complexes of the electron transport chain, ATP synthase, transport protein complexes such as TIM that allow transport from the IMM to the matrix (Pfanner and Meijer, 1997), or Oxa1 that translocates proteins into the membrane (Herrmann and Neupert, 2003).

Cristae do not represent simple invagination of the IMM, as initially suggested by Palade, but indeed represent independent structures that are separated from the IMM by tubular junctions, called cristae junctions (Perkins et al., 1997). Cristae are the major sites of mitochondrial respiration, since the respiratory chain complexes are located there, together with ATP synthase dimers (Gilkerson et al., 2003). This particular organization of respiratory chain elements makes cristae the main containers of cytochrome c (Scorrano et al., 2002). Cristae are dynamic structures, balancing between orthodox and condensed states depending on the current status of mitochondrial respiration in the cell (Hackenbrock et al., 1980).

The mitochondrial matrix is the place where the mitochondrial genome is located – a small autonomous circular DNA molecule containing 37 genes, from which 13 encode proteins of the respiratory chain, 22 encode mitochondrial tRNA and 2 encode rRNA (Attardi and Schatz, 1988). Mitochondrial DNA is maternally inherited (Sato and Sato, 2011). Its mutations cause several severe neuromuscular diseases.

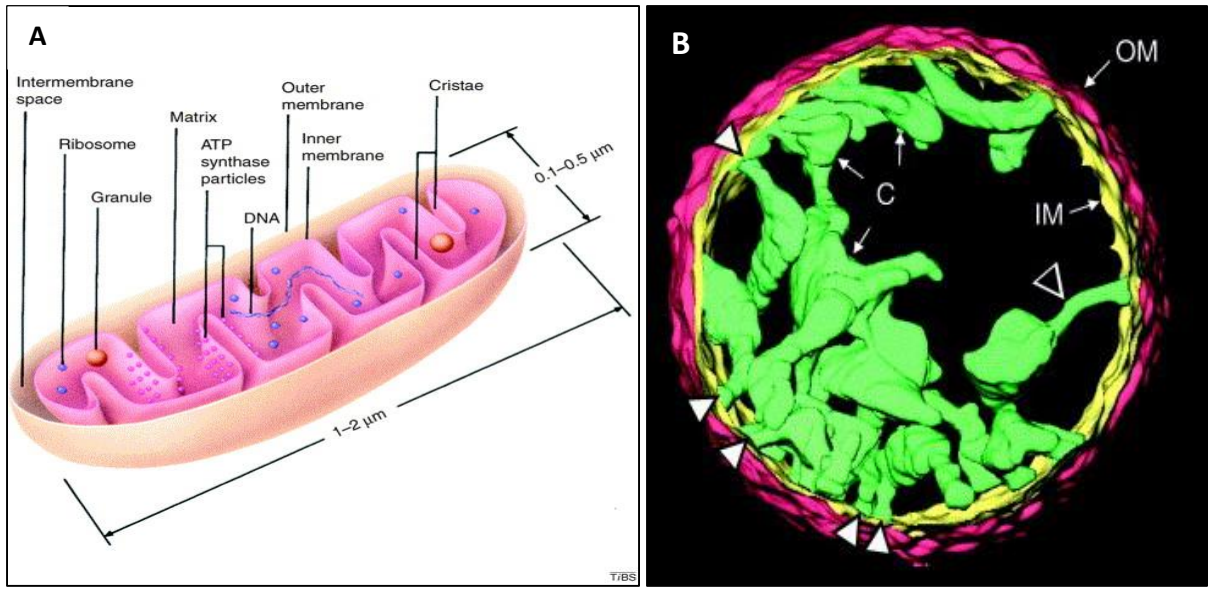

Figure 01. Mitochondrial ultrastructure. (A) Schematic representation of the "baffle"model. (B) 3D reconstruction of the isolated rat liver mitochondria acquired by high-voltage electron microscopy. OM: outer mitochondrial membrane, IM: inner mitochondrial membrane, C: cristae, Arrows point to cristae junctions. Bar 0.4 µm. Adapted from (Frey and Mannella, 2000)

3.1.2. Mitochondria – A dynamic organelle

Mitochondria are highly dynamic organelles, whose morphology and ultrastructure are continuously regulated by the balanced actions of fusion and fission (Figure 2). Thanks to the advances in live cell imaging, 3D reconstructions and electron tomography, the idea of

mitochondria as static organelles, as initially put forward by electron microscopy analyses, has been abandoned (Wasilewski and Scorrano, 2009).

Mitochondrial shape can range from different individual round organelles to very long interconnected filaments. Interestingly, mitochondrial morphology also differs from one cell type to another. For example, in epithelial cells mitochondria are tubular and form a tightly interconnected network, where on the other hand in cells like hepatocytes individual spheroid organelles are retrieved. The mitochondrial morphology can vary even within the same cell. A good example for this are skeletal muscle cells: in myocytes, in the perinuclear space the shape of mitochondria is mostly globular, whereas in the sarcolemma they are shaped like rods. In the acinar cells of the pancreas there are even three different groups of mitochondria, differently positioned around the periphery and the nucleus. The versatility in mitochondrial shape, even in the same cell further pinpoints the importance for a highly regulated process of mitochondrial shaping, necessary for satisfying all the functional needs of a cell (Collins et al., 2002).

Steady state mitochondrial shape depends on the balance between fusion and fission events. If one of these processes is blocked, the final shape of the mitochondria is governed by the unopposed process progressing towards the other side of the equilibrium. Mechanisms of mitochondrial fusion and fission are complex and require the action of many mitochondria shaping proteins, which are large GTPases sharing structural homology with the family of dynamins (Wasilewski and Scorrano, 2009).

3.1.2. Mechanisms of mitochondrial fission

Mitochondrial fission in mammalian cells is a process that largely depends on the activity of the dynamin-related protein 1 (Drp1). Drp1 is a large GTPase located in the cytosol and involved in the fragmentation of mitochondria, peroxisomes and the endoplasmic reticulum (Schrader, 2006). Mechanisms that enable translocation of Drp1 from the cytoplasm to the mitochondria involve dynamic processes of phosphorylation/dephosphorylation. Right after mitochondrial dysfunction, intracellular calcium levels rise, leading to the activation of calcineurin, which dephosphorylates the conserved Ser637 on Drp1, a signal that induces Drp1 translocation to the mitochondria (Cereghetti et al., 2008). However, opposing data exists regarding the kinase which is responsible for the phosphorylation of this residue that can be phosphorylated by protein kinase A (which then connects mitochondrial morphology to the second messenger cAMP), or by the calmodulin – independent protein kinase Iα (but in this case the phosphorylation of Drp1 links it to its mitochondrial localization) (Cribbs and Strack, 2007; Chang and Blackstone, 2007). The phosphorylation status of this site is dominant over that of Ser616, whose phosphorylation status is controlled by cyclin-dependent-kinase 1 driving mitochondrial fission during the process of cell division. The stabilization of Drp1 on the mitochondrial surface is achieved by SUMOylation, a process that protects molecules from degradation by the ubiquitin-proteasome system (Taguchi et al., 2007; Harder et al., 2004; Wasiak et al., 2007).

The binding of Drp1 on the outer mitochondrial membrane occurs thanks to adaptor proteins such as Fis1. Fis1 is a membrane protein located in the outer mitochondrial membrane. It is bound to the membrane via its C-terminal transmembrane domain, and a small part of the protein protrudes to the intermembrane space. The protein region facing the cytoplasm is

composed of six alpha helices, where α2, α3, α4, α5 form TPR (tetratricopeptide-repeat like) domains, which enable protein-protein interactions (Suzuki et al., 2003). Fis1 mainly serves as an anchoring protein for effector molecules on the mitochondria, a conclusion coming from the fact that its overexpression leads to mitochondrial fragmentation, but the protein itself doesn't possess any enzymatic activity. Moreover, fragmentation caused by Fis1 overexpression can be blocked by a Drp1 dominant-negative mutant. In order for fission to be carried out in a proper way, the Drp1-Fis1 complex must dissociate suggesting that the interaction between these two proteins is actually transient (Yu et al., 2005). Apart from Fis1, other Drp1 receptors have been discovered, like the mitochondrial fission factor (Mff), and mitochondrial division factors (MiD, MiD49 and MiD51) also involved in Drp1 recruitment to the mitochondria and processes of mitochondrial fission (Otera et al., 2010; Gandre-Babbe and van der Bliek, 2008; Palmer et al., 2011).

3.1.3. Mechanisms of mitochondrial fusion

Fusion of the outer mitochondrial membrane depends on the activity of Mitofusin 1 (Mfn1) and Mitofusin 2 (Mfn2). These proteins are dynamin related GTPases that share a high degree of homology, and in terms of structure they possess an N-terminal GTPase domain, two hydrophobic heptad repeats (HR) and two transmembrane domains through which they insert into the outer mitochondrial membrane. Despite sharing a high degree of homology, they are functionally different. Mfn1 displays a higher GTPase activity, while the affinity for GTP itself is much lower compared to Mfn2, illustrating the fact that they have different roles in fusion (Rojo et al., 2002). Mfn1 governs mitochondrial tethering of two mitochondria which interact through their antiparalel HR2 repeats (a *trans* interaction) (Koshiba et al., 2004). The role of Mfn2 is still

not completely clear, but it has been shown that this protein is responsible for later steps in mitochondrial fusion, and it also plays a role in tethering mitochondria to the endoplasmatic reticulum (de Brito and Scorrano, 2008). However, in fibroblasts Mfn2 doesn't play a role, but the process of mitochondrial fusion in these cells is triggered by the inner membrane dynamin-related protein optic atrophy 1 (Opa1) working together with Mfn1 (Cipolat et al., 2004).

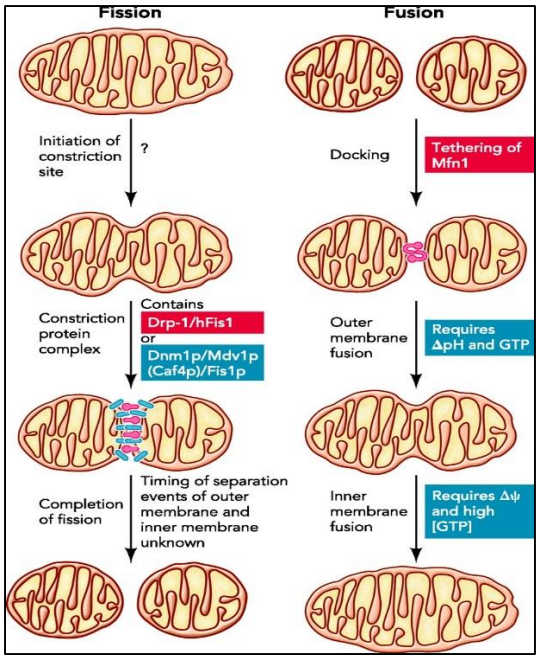

Figure 02. Steps of mitochondrial fission and fusion. Schematic representation of the mechanisms of fission and fusion in yeast (blue) and mammalian cells (red). Adapted from (Dimmer and Scorrano, 2006).

3.2. Opa1: A multifunctional protein

Mitochondria shaping protein Optic atrophy 1 (Opa1) is a dynamin related GTPase located in the internal mitochondrial membrane. Opa1 is a multifunctional protein: it has been discovered and confirmed, by our lab and others, that Opa1 (I) participates in promoting mitochondrial fusion; (II) has a role in apoptosis by keeping in check the cristae remodeling pathway; (III) regulates

mitochondrial metabolism by favoring the assembly and stability of respiratory chain supercomplexes; (IV) has a protective role in vivo against tissue damage, and as we will see later down the line, can play a role in cancer (Scorrano et al., 2002; Frezza et al., 2006; Cogliati et al., 2013; Varanita et al., 2015).

3.2.1. Opa1: From the gene to the protein

Following the discoveries of *OPA1* homologs in yeast (Mgm1p of *Saccharomyces cerevisiae* (Jones and Fangman, 1992) and Msp1p of *Schizosaccharomyces pombe* (Pelloquin et al., 1999)), human *OPA1* was identified in the year 2000 by two independent research groups (Delettre et al., 2000; Alexander et al., 2000), and its name derives from its implication in autosomal dominant optic atrophy, a hereditary optic neuropathy where *OPA1* is mutated. The homology between human and mouse *Opa1* gene is high, resulting in approximatively 90 % of similarity (Delettre et al., 2000). *OPA1* gene is located on chromosome 3q28-q29, taking up more than 90kb of genomic DNA. Open reading frame of human *OPA1* gene is composed of 30 exons (31 exons in mice), where three of these exons (4, 4b and 5b), are subjected to alternative splicing, giving rise to eight different mRNA molecules. Interestingly, exons 4b and 5b are only specific for vertebrates, while exon 4 is conserved throughout evolution (Olichon et al., 2007a). *OPA1* is ubiquitously expressed, while particularly high mRNA levels are present in the retina, brain, liver, heart and pancreas. In general all 8 splice forms are expressed, but the amount levels of individual transcripts are tissue specific (Delettre et al., 2001; Olichon et al., 2007a). On the other hand, in mice alternative splicing involves only exons 4a and 4b, giving rise to only 4 splice variants (Akepati et al., 2008), while in invertebrates there is no alternative splicing of *OPA1* orthologues (Olichon et al., 2007a).

Opa1 protein belongs to the family of dynamins, since it contains 3 conserved regions typical for the dynamin family: a GTPase domain, a middle domain and a coiled coil GTPase effector domain (GED) located at the carboxy terminus. The mentioned coiled-coil domain (CC2), and another downstream coiled-coil domain (CC1) might participate in oligomerization and activation of the dynamins. The amino terminal region contains the mitochondrial import sequence (MIS), followed by an evolutionary conserved transmembrane helix (TM1), necessary for anchoring Opa1 to the internal mitochondrial membrane. TM1 is followed by a coiled coil region (CC1). The described arrangement is found in every Opa1 splice variant, with the exception that in cases of 4b and 5b exon splicing Opa1 can contain the two additional hydrophobic domains TM2a and TM2b (encoded by the 4b and 5b spliced exons) together with another coiled-coil region (CC-0), (Figure 3) (Belenguer and Pellegrini, 2013).

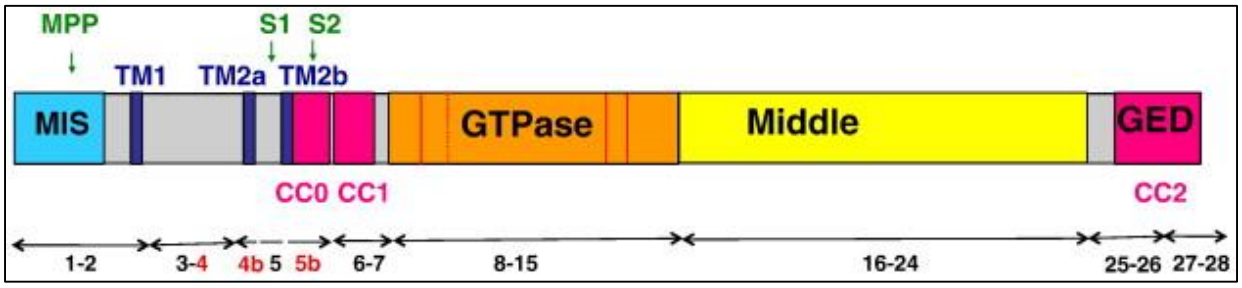

Figure 03. Schematic illustration of Opa1 gene structure. Opa1 shares several structural features with the dynamins: GTPase domain, middle domain and GTPase effector domain (GED) containing a coiled-coil region (CCII). Before the GTPase domain, Opa1 displays a mitochondrial import sequence (MIS), followed by a transmembrane region (TM1), and a coiled coil region (CCI). These domains are found in all Opa1 splice variants, while TM2a, TM2b and CC-0 are only found in splice exons 4b and 5b. Opa1 exons are numerated and indicated by double arrows. Intra-mitochondrial proteolytic cleavage sites are indicated, for mitochondrial processing peptidatse (MPP), paraplegin (S1), and Yme1L (S2). Adapted from (Belenguer and Pellegrini, 2013)

3.2.2. Opa1 proteolytic processing

Opa1 and its yeast orthologue Mgm1 are both subjected to proteolytic processing. In case of Mgm1, the protein precursor is produced with a mitochondrial leader sequence which subsequently gets cleaved by the mitochondrial processing peptidase (MPP), giving rise to the long isoform L-Mgm1. The mitochondrial rhomboid Pcp1/Rbd1 produces short S-Mgm1 (Herlan et al., 2003; McQuibban et al., 2003; Sesaki et al., 2003). Contrary to the relatively simple picture of yeast, Opa1 is subjected to a more complex process of proteolytic cleavage in vertebrates. The Opa1 protein precursors translated from the eight alternatively spliced mRNA molecules contain a mitochondria targeting sequence, which gets cleaved by the mitochondria processing peptidase (MPP) upon import into mitochondria, giving rise to long Opa1 forms (L-Opa1) (Olichon et al., 2002; Satoh et al., 2003). These long Opa1 forms are now subjected to further processing in order to give rise to short forms. Apart from the MPP processing site, each of the alternatively spliced mRNA encoded polypeptides, contain two specific cleavage sites, termed S1 and S2. Cleavage of the MPP site alone gives rise to long forms of Opa1, but further processing of these long forms at S1 or S2 cleavage sites, gives rise to one or more short forms (Figure 4.) (Song et al., 2007). However, the events behind this subsequent processing for short forms are still not completely understood. A model is proposed which includes the activity of m-AAA protease paraplegin or AFG3L2, or the i-AAA protease Yme1L that are acting on these sites and are responsible for generation of Opa1 short forms, which are then subjected to the activity of the rhomboid protease PARL, to release these forms now from the internal mitochondrial membrane, to the intermembrane space (Tatsuta and Langer, 2008; Ishihara et al., 2006; Griparic et al., 2007). Interestingly, under mitochondrial stress, like dissipation of the mitochondrial

membrane potential, presence of apoptotic signals, or low mitochondrial ATP levels, another protease, called OMA1, gets activated. OMA1 is an ATP-independent protease that is responsible for L-Opa1 cleavage under stressful conditions (Ehses et al., 2009).

In humans, Opa1 forms are experimentally retrieved as 5 different bands on a Western blot. The two higher molecular weight forms represent the long forms, and the 3 lower molecular weight bands represent the short forms. According to the current knowledge, both long and short forms are in association with the mitochondrial membrane, with the difference that the long form is anchored to the IMM, while the short form is peripherally attached to the IMM having a possibility to diffuse to the intermembrane space, and to associate with the OMM (Olichon et al., 2002; Cipolat et al., 2006; Ishihara et al., 2006). In order for fusion to be carried out in the proper way, the presence of both long, and short forms is required (DeVay et al., 2009).

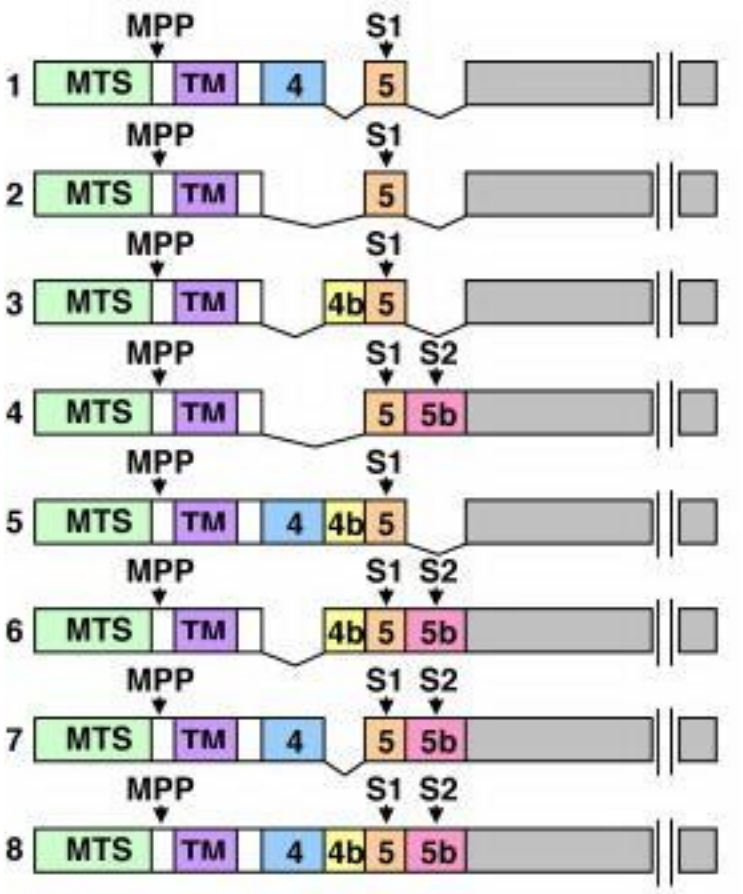

Figure 04. Schematic representation of 8 different OPA1 mRNA splice forms. The mRNA splice forms differ in the presence or absence of exons 4, 4b and 5b. Cleavage of the mitochondrial targeting sequence (MTS) by MPP, leads to the long isoforms. Additional cleavage at sites S1 (exon 5) or S2 (exon 5b), leads to the short isoforms. Adapted from (Song et al., 2007)

3.2.3. Opa1 and mitochondrial fusion

The role of Opa1 in mitochondrial fusion has initially been suggested through the studies carried out in yeast, where it has been demonstrated that yeast orthologues of Opa1 take part in the process of mitochondrial tubulation (Guan et al., 1993; Pelloquin et al., 1999). The initial attempt in deciphering what was the actual role of Opa1 in regulation of mitochondrial shape, came from

the pioneer works carried out in our lab, with an approach that involved a combination of genetics and imaging (Cipolat et al., 2004), and was further confirmed by others.

Overexpression of *Opa1* in mouse embryonic fibroblasts (MEFs), where mitochondria were punctuated, lead to tubulation and elongation of mitochondria, but in cells with already elongated mitochondria like HeLa or where *Opa1* overexpression was very high, it lead to fragmentation (Cipolat et al., 2004). On the other hand, gene knock out or silencing of *Opa1* variants by RNAi, lead to fragmentation of the otherwise tubular mitochondrial network (Cipolat et al., 2004; Griparic et al., 2004). Further evidence about the role of Opa1 in this process was acquired by assays of mitochondrial fusion, and confirmed by real-time imaging, that indeed Opa1 is responsible for mitochondrial fusion and not mitochondrial docking. Opa1 requires an intact GTPase domain and C-terminal coiled-coil domain in order to carry out its function properly. Its pro-fusion activity depends on Mfn1 and not Mfn2, since in cells deficient for Mfn1, Opa1 wasn't able to promote fusion, and reintroduction of Mfn1 restored this function, a phenomenon which didn't occur in case of Mfn2. Also, Mfn1 on its own wasn't able to promote fusion in cases where *Opa1* was ablated (Cipolat et al., 2004). Moreover, long and short forms of Opa1 are necessary for mitochondrial fusion, since these forms individually have little or no activity (Song et al., 2007). Opa1 is responsible for the fusion of the inner mitochondrial membrane, which is consistent with its localization, because Opa1 depletion doesn't affect the fusion of the outer mitochondrial membrane, in vitro or ex vivo (Song et al., 2009; Meeusen et al., 2006).

Depending on the levels of Opa1, two types of fusion can occur – a transient fusion ("kiss and run"), which leads to a fast exchange of soluble components between mitochondria, being

responsible for mitochondria quality control, but doesn't affect the mitochondrial morphology, and complete fusion, that leads both to mitochondria component exchange and has an effect on morphology (Liu et al., 2009).

3.2.4. Opa1 and apoptosis

Mitochondria are the main organelles that take part in the regulation of apoptosis caused by intrinsic stimuli. They are responsible for the release of cytochrome c, and other cofactors which participate in the cell death pathway and lead to the activation of effector caspases. Together with the release of these factors, mitochondria undergo structural changes, which involve mitochondrial fragmentation and activation of the cristae remodeling pathway, processes that are depending on the activity of mitochondria shaping proteins (Frank et al., 2001) (Scorrano et al., 2002).

The process of cristae remodeling occurs upon administration of apoptotic stimuli to the cell, and involves changes in the cristae shape, which are followed by complete release of cytochrome c. These changes involve inversion of the cristae curvature and widening of the cristae junctions, processes which ultimately lead to a redistribution of cytochrome c from the inside of the cristae, where it usually resides, to the intermembrane space, and from there across the outer membrane, and into the cytoplasm, to take its part in the cell death pathway. Frezza and colleagues (Frezza et al., 2006) demonstrated that Opa1 is involved in the regulation of the cristae shape and in the regulation of the size of cristae junctions during apoptosis, independently from its role in mitochondrial fusion. Opa1 forms multimeric complexes involving both the integral and soluble form of Opa1, where the production of the latter depends on the activity of the protease

Parl. Indeed, a genetic analysis demonstrated the importance of Parl in the process of apoptosis, where both Opa1 and Parl lie on the same apoptotic pathway, with Opa1 being downstream. Thus, a concentrated action of Opa1 and Parl is necessary for keeping the size of cristae junctions in check (Frezza et al., 2006; Cipolat et al., 2006).

Overexpression of Opa1 and inhibition of the cytochrome c release protects the cell from apoptosis induced by intrinsic stimuli (Frezza et al., 2006), whereas Opa1 downregulation has an opposite effect and increases the susceptibility of the cell to spontaneous and induced apoptosis (Olichon et al., 2003; Lee et al., 2004; Olichon et al., 2007b; Frezza et al., 2006). When mitochondria are incubated with BH3-only pro-apoptotic proteins, this leads to dissociation of Opa1 complexes and release of cytochrome c. On the other hand, overexpression of Opa1 or overexpression of disassembly-resistant mutants of the dynamin, has a stabilizing effect on Opa1 complexes, inhibiting mobilization of cytochrome c and further apoptosis despite the presence of apoptotic stimuli (Belenguer and Pellegrini, 2013). Experiments that involved knockdown of certain Opa1 slice variants revealed that isoforms containing exon 4 are involved in processes of fusion, while isoforms containing either exon 4b or 5b take part in the regulation of cytochrome c release (Olichon et al., 2007a).

Observations of the role of Opa1 in the cristae remodeling pathway, impinge on the fact that Opa1 can be considered as an anti-apoptotic protein, a very attractive feature that can be further exploited in cancer studies.

3.2.5. Opa1 and energy metabolism

Mitochondria are considered as metabolic power plants of the cell, since they are responsible for the generation of the energy molecule ATP, in the process of oxidative phosphorylation. The finely regulated process of energy conversion takes place in the internal mitochondrial membrane and takes advantage of the morphological features of the organelle. Immunoelectron microscopy studies gave proof that respiratory chain complexes accumulate inside the cristae membrane (Vogel et al., 2006), while respirometric experiments further expanded the picture, by revealing that these complexes organize into functional quaternary structures called respiratory chain supercomplexes (RCS) (Acin-Perez et al., 2008), thus increasing the efficiency of oxidative phosphorylation. Recent work carried out by our lab explored the relationship between mitochondrial ultrastructure and respiratory function, and found that the assembly and stability of RCS, and hens the efficiency of mitochondrial respiration, depends on cristae shape, revealing an important role for Op1 in this process (Cogliati et al., 2013).

Acute Opa1 ablation, apart from causing cristae alterations, leads to a reduced assembly of respiratory chain supercomplexes, thus leading to a less efficient respiration rate of complex-I. These findings have been further supported with the use of mouse models. A mouse model of conditional *Opa1* ablation confirmed the previous statement, providing evidence that in the absence of *Opa1*, respiratory chain complexes are less prone to organize into RCS, despite their starting levels. On the other hand, a transgenic mouse model of mild *Opa1* overexpression demonstrated that increased Opa1 levels have beneficial effects for mitochondrial respiration, leading to tighter cristae, and favoring the assembly of RCC into supercomplexes. Another interesting observation that came out from this study was the discovered correlation between

cristae shape and mitochondria-dependent cell growth. The ablation of *Opa1* (but not of *Mfn1* or *Mfn2*) lead to a slower cell proliferation rate in media that contained galactose instead of glucose, a mean to stimulate mitochondrial respiration. Conversely, the growth rate was faster, in cells overexpressing Opa1 compared to their wild type controls in galactose enriched media (Cogliati et al., 2013).

3.2.6. Opa1 protective effects in vivo

With the increasing accumulation of knowledge concerning the Opa1-dependent cristae remodeling pathway, obtained through many in vitro studies, efforts have been made to understand whether this pathway plays a role in vivo and if so, what role that might be.

In order to address this question, our lab took advantage of the already generated mouse transgenic model with a controlled overexpression of *Opa1* (Cogliati et al., 2013), and discovered that mild overexpression of *Opa1* has a protective effect in vivo. Mice overexpressing *Opa1* were viable, fertile and grew normally, displaying no obvious major phenotypes, an indication that the mild overexpression of this protein was compatible with life. Further analysis demonstrated that OPA1 had a protective effect from muscle atrophy. In experiments where atrophy was induced by muscle denervation, *Opa1* transgenic mice displayed less loss of glycolytic or oxidative fibers. The OPA1 protective effect was evident both for chronic and acute muscle atrophy, and was achieved by minimizing the dysfunction of mitochondria without changing the autophagic program or stimulating biogenesis of mitochondria. OPA1 also had a protective effect in the heart and in the brain, protecting these organs from ischemic damage. The overexpression of *Opa1* inhibits also mitochondria dependent liver apoptosis induced by activation of the Fas receptor in

the liver through administration of anti-Fas activating antibodies via tail-vein injection. Mechanistically, OPA1 reduced the production of reactive oxygen species and cytochrome c release, in primary tissues (Varanita et al., 2015). Furthermore, the mild *Opa1* overexpression corrects mouse models of primary mitochondrial dysfunction caused by defects in the respiratory chain. In this study, two mouse models for mitochondrial dysfunction have been used – the Ndufs4$^{-/-}$ mouse (a constitutive knockout for the structural complex I component Ndufs4), and Cox15$^{sm/sm}$ (a muscle specific conditional knockout for the complex IV assembly factor Cox15). These mice have been crossed with the *Opa1* overexpressing mouse. The progeny deriving from this cross demonstrated improved motor skills and activity of the respiratory chain with a correction of cristae ultrastructure and mitochondrial respiration, compared to the controls where *Opa1* was not overexpressed (Civiletto et al., 2015).

In conclusion, mild overexpression of *Opa1* has a beneficial effect. Its mild overexpression has a genetically distinguishable function in mitochondrial morphology, apoptosis, and mitochondrial physiology displaying an overall positive effect in these processes. All these functions concur to determine also a beneficial outcome of *Opa1* mild overexpression in vivo, protecting from chronic and acute tissue insults, and correcting mouse models of primary mitochondrial dysfunction. However, all these beneficial effects come with a counterpart, since *OPA1* is overexpressed in several human cancers, as it will be discussed in the following chapter.

3.3. Mitochondria and cancer

The notion that mitochondria might play a role in cancer was suggested for the first time at the beginning of the 20th century by Otto Warburg who suggested that cancer cells are able to acquire

metabolic imbalances, which allow them to constitutively upregulate the metabolism of glucose, even in the presence of oxygen. The observed phenomenon was symbolically named the "Warburg effect", also known as aerobic glycolysis (Kroemer, 2006). Since then, as both the field of mitochondria and cancer research expanded, new avenues about the possible links between the organelle and tumorigenesis opened. Since evasion of cell death represents one of the major hallmarks of cancer (Hanahan and Weinberg, 2000), and mitochondria play a key role in this process, considerable attention mounted in the cancer research field towards a better understanding of the role of mitochondria in tumorigenesis and progression.

Mitochondrial pathways of apoptosis involves the release of cytochrome c and other apoptogenic factors from the intermembrane space to the cytosol, upon their exposure to intrinsic apoptotic stimuli. Once in the cytosol, cytochrome c associates with Apaf1, which further leads to the activation of caspase-9 and other downstream caspases, finally resulting in cell demise (Li et al., 1997). As mentioned in previous chapters, in order to ensure a complete release of cytochrome c, mitochondria undergo structural changes at the early stages of apoptosis, through the process of cristae remodeling, a process which is under tight control by Opa1.

Studies have shown that cancer cells manage to evade apoptosis in numerous ways. One of the common methods includes failure to respond to apoptotic stimuli, for example though the loss of p53 when a cell becomes more resistant to apoptosis induced by DNA damage. Another also very common way, found in diverse tumors, includes upregulation of anti-apoptotic proteins of the Bcl2 protein family. With that in mind, reports are starting to emerge about the potential anti-apoptotic role of Opa1 in cancer: indeed, *OPA1* expression was found upregulated in several different cancers.

3.3.1. Opa1 and cancer

One of the key features of cancer cells is that they require very high levels of cytochrome c in their cytoplasm in order for apoptosis to take place (Zhivotovsky et al., 1998). Cytochrome c is the main killer molecule released from the mitochondria, responsible for enabling apoptosis in the cancer cell. Since the release of cytochrome c is under tight control of Opa1, this protein is emerging as an interesting target in cancer studies. Overexpression of *OPA1* has anti-apoptotic features, since it leads to tightening of the cristae and it enables maintenance of cytochrome c inside these compartments, thus preventing its translocation to the cytoplasm, and preventing further steps required for apoptosis.

A handful of studies demonstrated a role for Opa1 in human cancer. In lung adenocarcinoma it has been found that *OPA1* is overexpressed and high levels of Opa1 correlate with a worst prognosis and an impaired response to therapy. *OPA1* overexpression was detected in 76.6% of lung adenocarcinoma patients and this overexpression was associated with an increased resistance to anticancer drug cisplatin, through inactivation of caspase-dependent apoptosis in lung adenocarcinoma cells (Fang et al., 2012). On the other hand, downregulation of *OPA1* enabled sorafenib-induced apoptosis in hepatocellular carcinoma (Zhao et al., 2013). In another study aimed at deciphering the role of anticancer drug cisplatin in ovarian and cervical cancer, it has been shown that this drug induced processing of L-Opa1 in a process mediated by p53 and metallopeptidase Oma1, leading to mitochondrial fragmentation and apoptosis (Kong et al., 2014). Finally, in a study that was aimed at examining the role of CTMP protein in the context of mitochondria mediated apoptosis in human lung carcinoma cells, it has been found that CTMP changes mitochondrial morphology, and leads to cytochrome c release by inhibiting the

expression of *OPA1* in these cells (Hwang et al., 2012). These data indicate that Opa1 displays a role in cancer and is emerging as a significant target, since blocking its expression is associated with an induction of the mitochondria - associated apoptotic pathway in the cancer cell and a better clinical outcome.

The role of upregulated *OPA1* in cancer is also confirmed by the analysis of publically available databases. "Oncomine" is a cancer microarray database available also as a web-based data mining platform, with the aim to make all accumulated cancer microarray data from various genome-wide expression analyses public and available for data-mining and discovery (Rhodes et al., 2004). An Oncomine analysis performed by our lab (Scorrano L. unpublished observations), revealed that *OPA1* is overexpressed in several different cancers. From the cancers analyzed, *OPA1* is overexpressed 4-fold in cervical cancer, 2-fold in breast cancer, leukemia, and lung cancer, 1-fold in lymphoma, melanoma and pancreatic cancer, while in bladder cancer, brain and CNS cancers, colorectal, esophageal, gastric, ovarian, prostate, head and neck cancer, myeloma and sarcoma its overexpression wasn't detected using this approach (Figure 5). Another publicly available database, called "The human protein atlas" (HPA), also provided information on *OPA1* overexpression in certain cancers. The HPA is a platform based on antibody tissue profiling, and it contains publicly available information about protein expression and localization profiles in 48 normal human tissues and 20 different cancers (Uhlen et al., 2005). According to this database platform, *OPA1* is particularly overexpressed in colorectal cancer, thyroid cancer, liver cancer, endometrial cancer, ovarian cancer and melanoma (Figures 6 & 7). In conclusion, analysis of these publically available databases indicated that *OPA1* overexpression represents a strong feature of many different cancers.

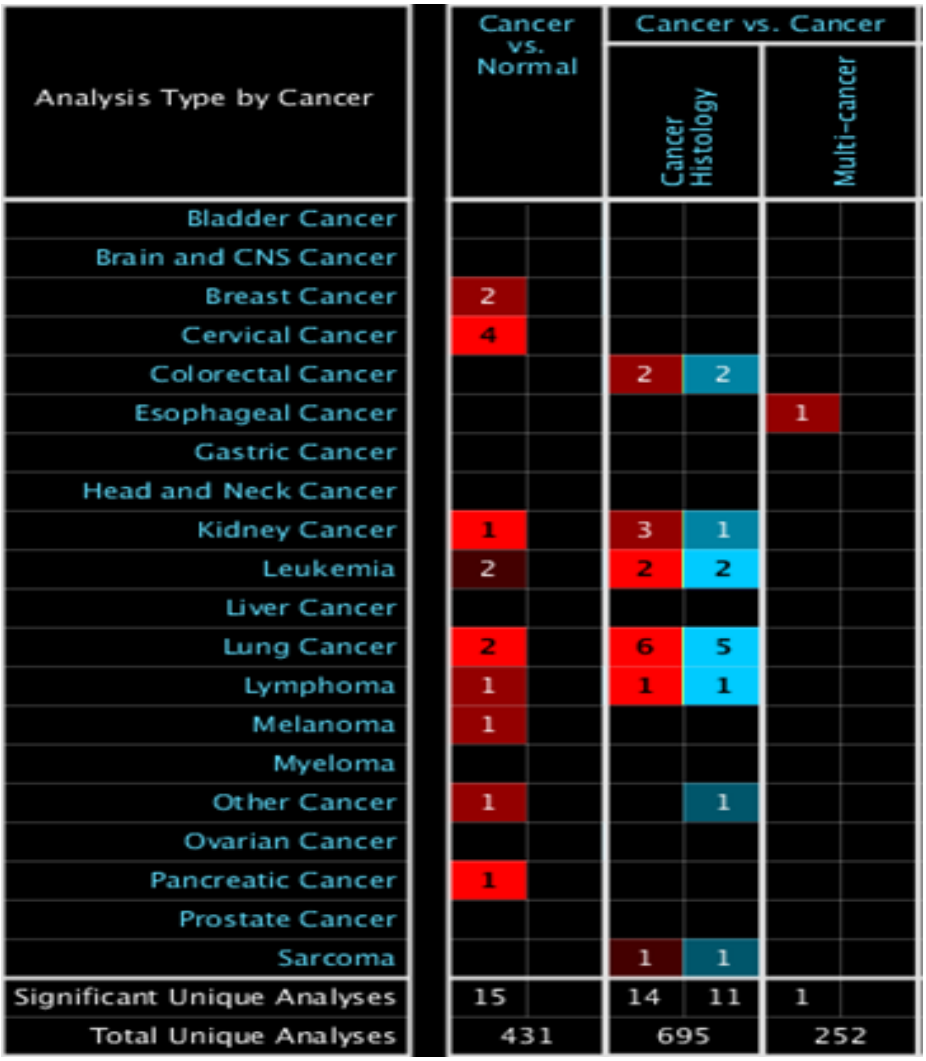

Figure 05. Oncomine analysis. Illustration of the results of OPA1 expression levels in several different cancers. First column: Types of analyzed cancers. Second column: OPA1 expression level as a ratio of Cancer vs. Normal cell. Third column: OPA1 expression levels as a ratio of Cancer vs. Cancer. Red: more than 2-fold overexpression (Scorrano L, unpublished observations).

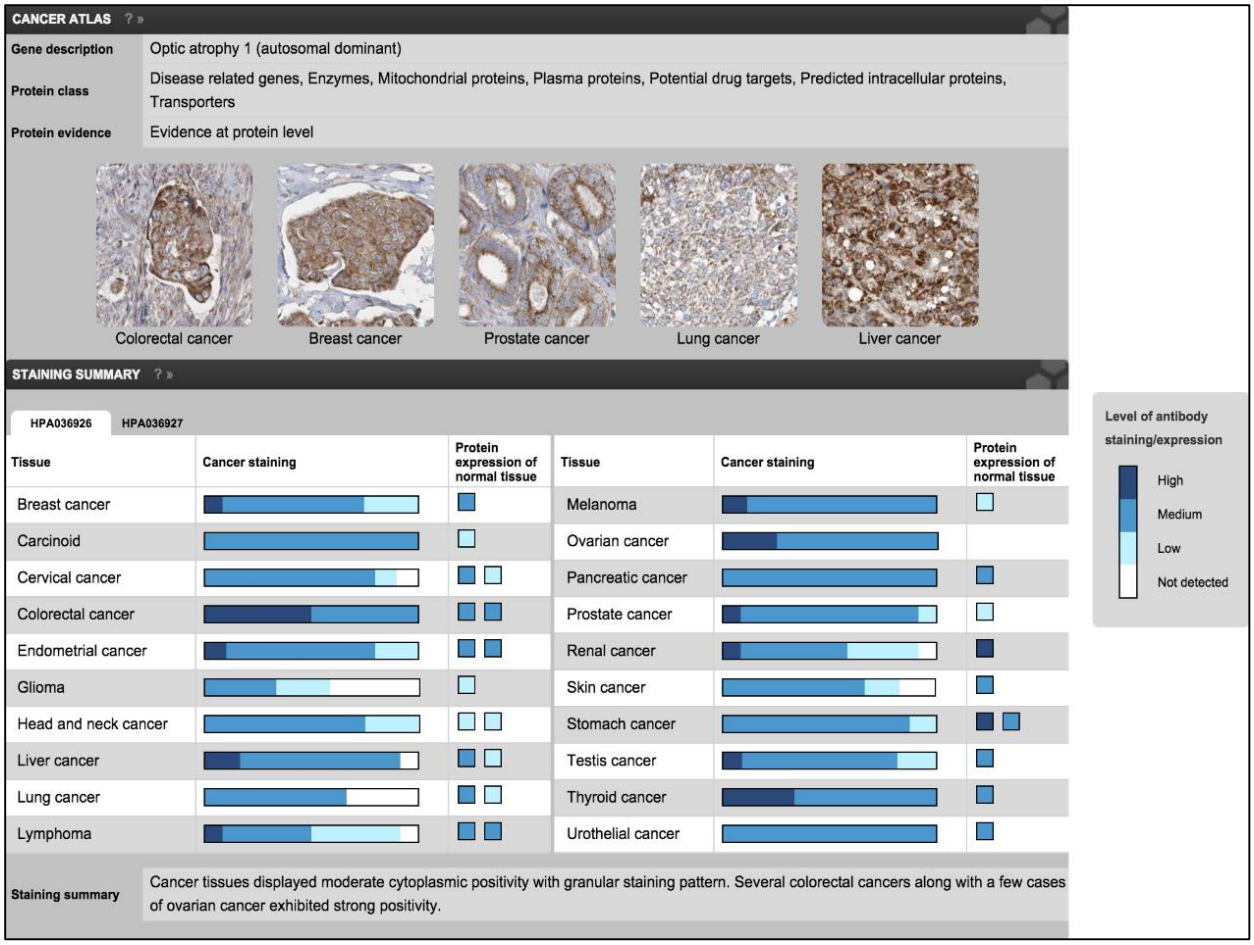

Figure 06. Human protein atlas for Opa1 overexpression in cancer tissue. Antibody used: HPA036926. For each cancer, the fraction of samples with antibody staining/protein expression level high, medium, low, or not detected are provided by the blue-scale color-coding (as described by the color-coding scale in the box to the right). The length of the bar represents the number of patient samples analyzed (max=12 patients). Next to the cancer staining data, the protein expression data of normal tissues or specific cell types corresponding to each cancer are shown and protein expression levels are indicated by the blue-scale color coding. At the bottom of the page, a summary of the overall protein expression pattern across the analyzed cancer tissues. Adapted from (Uhlen et al., 2005)

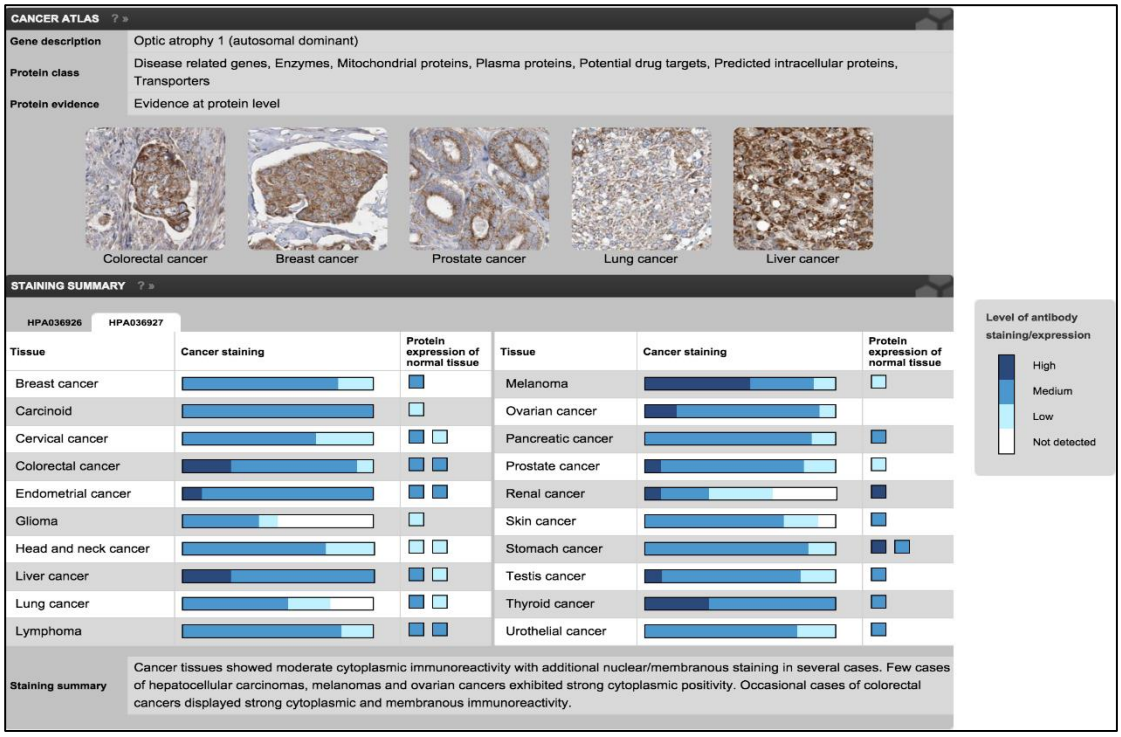

Figure 07. Human protein atlas for Opa1 overexpression in cancer tissue. Antibody used: HPA036927. For each cancer, the fraction of samples with antibody staining/protein expression level high, medium, low, or not detected are provided by the blue-scale color-coding (as described by the color-coding scale in the box to the right). The length of the bar represents the number of patient samples analyzed (max=12 patients). Next to the cancer staining data, the protein expression data of normal tissues or specific cell types corresponding to each cancer are shown and protein expression levels are indicated by the blue-scale color coding. At the bottom of the page, a summary of the overall protein expression pattern across the analyzed cancer tissues. Adapted from (Uhlen et al., 2005)

3.4. B cells and lymphoma

B lymphocytes represent a population of white blood cells which express clonally diverse cell surface Immunoglobulin receptors that enable recognition of specific antigens. B cells and their antibodies are key mediators of humoral immunity and, acting as part of the adaptive immune system, provide protection against a large variety of pathogens (Pieper et al., 2013). However, B

cells are exceptionally prone to malignant transformation, since the process of B cell maturation and strategies for antibody diversification are very complex and include many steps, all quite subjected to different chromosomal translocations and oncogenic mutations. In B cell malignancies normal signaling pathways are often disrupted and redirected towards a constitutive activation of prosurvival signaling (Shaffer, III et al., 2012). Since the mechanisms of B cell development, differentiation and B cell signaling are important for understanding the lymphoma onset, these processes will be discussed here in more detail.

3.4.1. B cell biology and development

B cell development is a complex process that occurs through several different stages (Table 1). All of these stages are represented by a change of the genome content in the antibody loci, therefore the specific assembly of B cell antigen receptor (BCR) components defines each stage. The development of the B cell lineage starts in the primary lymphoid tissue (fetal liver and bone marrow). During embryogenesis, hematopoietic stem cells develop in the fetal liver, from where they migrate to the bone marrow, and there they get committed to develop into B lineage cells (Pieper et al., 2013). The first B cell developmental stage in the so-called pro B stage. It is characterized by a rearrangement of the immunoglobulin heavy chain (μH). On the cell surface of a pro B cell, of Igα (CD79a) and Igβ (CD79b) are expressed together with associated chaperon proteins. As soon as the heavy chain gets properly rearranged it gets associated with the mentioned proteins, together with a surrogate light chains lambda5 and VpreB. This association generates a form of a pre-BCR like IgM, which marks the transition into the next developmental stage – the pre B cell stage. The V to DJ rearrangements of the pro B stage are governed by interleukin 7 (IL-7), a cytokine produced by bone marrow stromal cells. If the heavy chain

rearrangements are not properly executed or the components of the pre-BCR receptor are not properly assembled, the transition to the next stage is blocked and the cell undergoes apoptosis. The pre B cell stage is characterized by the recombination of the V and J light chain fragments, whose proper assembly will allow transition to the next stage – the immature B cell (Kurosaki, 2010; Melchers et al., 2000; Perez-Vera et al., 2011).

Apart from the VDJ rearrangement patterns, the aforementioned B cell stages are also characterized by specific cell surface markers and proliferation state. Since VDJ rearrangements occur through the process of non-homologous recombination and replication of DNA during proliferation is governed by homologous recombination, there is a need of a tight control of these processes in order to avoid high mutation rates. Indeed, the fine regulation of these processes is achieved by the action of *RAG1* and *RAG2* genes which are active in the G0 and then get degraded before entrance to the S phase of the cell cycle. In this way the cell avoids that non-homologous recombination events happen during proliferation, therefore minimizing the chances of mutations (Perez-Vera et al., 2011).

When the immature B cell leaves the bone marrow and sets off to the periphery, it is now called naïve B lymphocyte. At this stage processes of alternative splicing of the heavy chain mRNA occur, leading to the generation of membrane bound IgD and IgM. If after several days of circulating through the bone marrow and the periphery, the naïve B lymphocyte doesn't encounter a recognizable antigen, the cell becomes a mature B lymphocyte. However, if the cell gets exposed to a proper antigen, it will develop into a memory B lymphocyte or a plasma cell (Table 1). All these events are occurring in the so-called germinal centers within secondary lymphoid organs

where mature B cells proliferate, differentiate, undergo somatic mutations and antibody class switching, as a normal immune response to infection (Levine et al., 2000; Kurosaki, 2010).

Stages in B Cell Development							
	Stem cell	**Early pro B cell**	**Late pro B cell**	**Large pre B cell**	**Small pre B cell**	**Immature B cell**	**Mature B cell**
H chain genes	germline	D-J joining	V-DJ joining	VDJ rearranged	VDJ rearranged	VDJ rearranged	VDJ rearranged
L chain genes	germline	germline	germline	germline	V-J joining	VJ rearranged	VJ rearranged
Surface Ig	none	none	none	m chain in pre-B receptor	m chain in cytoplasm and on surface	membrane IgM	membrane IgM and IgD
Membrane markers	CD34	CD34 CD45 (B220) Class II	CD45R Class II CD19 CD40	CD45R Class II pre-B-R CD19 CD40	CD45R Class II pre-B-R CD19 CD40	CD45R Class II IgM CD19 CD40	CD45R Class II IgM IgD CD19 CD21 CD40

Table 1. Stages of B cell development: Depiction of various stages of B cell development, from the stem cell to the mature B cell, with a classification of heavy and light chain gene rearrangements, presence or absence of the surface immunoglobulin, and surface markers characteristic for a particular stage. Adapted from "The immune system" P. Parham, Garland Science 2009, 3rd edition

3.4.2. Antibody production

The key feature of B cells are immunoglobulin (Ig) molecules which are either expressed on the B cell surface, or secreted extracellularly. When an immunoglobulin molecule gets secreted into the extracellular space it is knows as an antibody. Antibodies are the mediators of immunity. The

effector function of antibodies lies in their ability to bind microbial antigens with high specificity and affinity, leading to their neutralization by activating other elements of the immune system like the complement, or stimulating phagocytosis (Kurosaki, 2010). In order to fulfil the requirements of the immune system, and to provide a strong defense against various different pathogens, antibodies are characterized by extreme diversity. The diversification process is achieved through and antigen independent, and an antigen dependent way.

Diversification of antibodies happening in an antigen-independent way is a process taking place in the bone marrow, during B cell differentiation. Through processes of V(D)J recombination, each antibody is assigned to a heavy and a light chain. Recombination of variable (VH), diversity (DH), and joining (JH) gene segments give rise to different variants of heavy chains, while recombination of only variable (VH), and joining (JH) gene segments, generates light chains. Humans possess only two light chain loci, kappa and lambda, and only one of these loci is expressed per cell, so each produced antibody by that cell can have either a kappa or a lambda light chain. Just by this process of V(D)J recombination, a diversity greater than 3 million antibodies is guaranteed (Schatz and Swanson, 2011).

Diversity that is depending on exposure to antigens is a process happening at the periphery. Once exposed to antigens, the immunoglobulin molecules of B cells undergo somatic hypermutations, which leads to accumulation of mutations in the immunoglobulin genes. Only those B cells that acquired mutations in their Ig genes which give them a higher affinity to foreign antigens are selected to survive, which further leads to affinity maturation during the humoral immune response (Teng and Papavasiliou, 2007).

3.4.3. B cell receptor signaling

The development and maturation of normal B cells largely depends on the proper function and signaling from the B cell receptor, which is present on all B cells. Regulated activity from this receptor enables proliferation of selected B cells, or leads to cell death of the unwanted ones. However, studies on many B cell malignancies have demonstrated that the BCR signaling pathway is largely implicated in tumorigenesis, where cancer cells find various ways of activating the BCR signaling pathway in order to promote their cancerous phenotype (Niemann and Wiestner, 2013).

The B cell antigen receptor (BCR) is a multiprotein structure composed of an antigen binding subunit and a signaling subunit. The antigen binding subunit is composed of membrane immunoglobulin molecules (IgM) each consisting of two immunoglobulin light (IgL) and two immunoglobulin heavy chains (IgH) covalently associated. The signaling subunit consist of an Igα/Igβ (CD79A/CD79B) heterodimer, not in covalent association. The membrane immunoglobulin molecules serve as docking sites for antigens, which leads to receptor aggregation, while Igα/Igβ (CD79A/CD79B) transfer signals inside the cell. The aggregation of the BCR receptor quickly activates the Scr family of kinases (Lyn, Fyn, Blk) that phosphorylate the so-called ITAM motifs (immunoreceptor tyrosine-based activation motif) on Igα/Igβ. The phosphorylation of Igα/Igβ leads to recruitment of the Syk kinase from the cytoplasm to the perimembrane space. Syk then undergoes two rounds of phosphorylation: first it gets phosphorylated by Src, and then it gets auto-phosphorylated, which leads to its full activation. Activated Syk now catalyzes phosphorylation of other signaling molecules such as PLCγ2 (a lipase), BTK (a protein tyrosine kinase that also activates PLCγ2), and BLNK (an adaptor molecule).

Once activated, PLCγ2 is able to cleave phosphatidylinositol 4,5–bisphosphate, giving rise to diacylglycerol and inositol triphosphate (Figure 8). This leads to mobilization of calcium from the intracellular and extracellular stores, and an activation of downstream pathways like the AKT, MAP kinase, RAS and NF-kB pathway. These pathways then activate several transcription factors which modify cell metabolism, promoting cell survival, proliferation, B cell differentiation into memory or plasma cells, and also production of antibodies (Cheng et al., 2011; Dal Porto et al., 2004; Kurosaki, 2010).

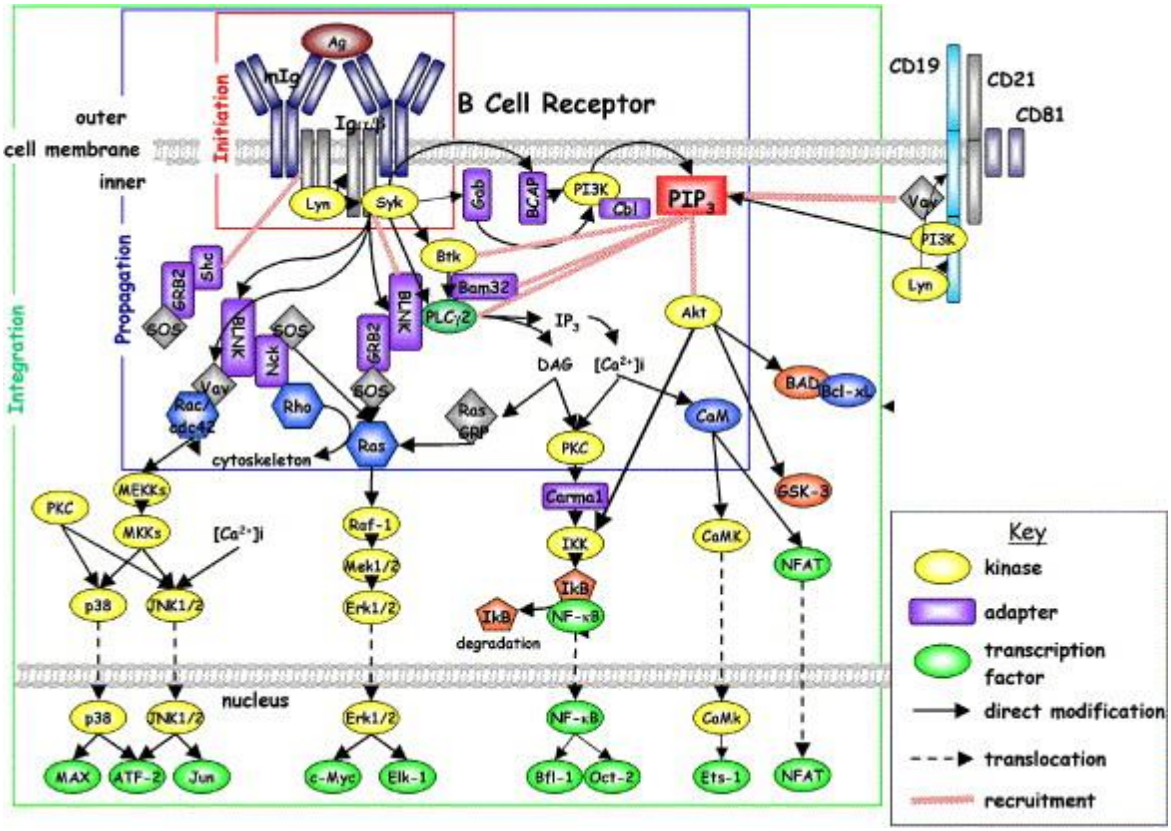

Figure 08. BCR signaling: The signaling cascade starts with the antigen binding to the mIg on the cell surface, leading to receptor agregation, formation of the signalosome composed of the BCR, tyrosine kinases, adaptor proteins, and signaling enzymes. Signals coming from the signalosome activate downstream signaling cascades,

with an end result in changes in the cell metabolism, gene expression, cytoskeletal organization, proliferation and diferentiation of the cell. Adapted from (Dal Porto et al., 2004)

3.4.4. B cell malignant transformation

B cell differentiation and activation are tightly regulated processes , but due to their complex nature they are also highly prone to dysregulation that can lead to B cell malignancies (Shaffer et al., 2002).

Classification of different lymphoma subtypes involves use of various genetic, pathological, and clinical methods. Every lymphoma subtype has a phenotype resembling a certain stage of B cell differentiation, as determined by gene expression profiling, and presence or absence of mutations in the variable immunoglobulin region. The normal B cell and its differentiation status from which other malignant B cells derived is termed the “cell of origin”. However, in the field, there are still some debates about the differentiation status of the actual cell of origin, since some B cells acquire mutations that promote the cancerous phenotype, but still allow the cell to differentiate and move onto the next differentiation stage, so the actual cell of origin in a lymphoma could be a B cell that is on an earlier stage of differentiation in respect to its normal B cell counterpart (Shaffer, III et al., 2012).

During B cell differentiation the first potential pitfall is the process of B cell receptor generation taking place in the bone marrow. This process, called V(D)J recombination, as previously mentioned, involves immunoglobulin gene rearrangements by mechanisms of non-homologous recombination. If the generated double-stranded DNA breaks don’t get properly resolved, this can lead to chromosomal translocations which put in association one of the immunoglobulin loci

with a cellular proto-oncogene, a typical feature of many B cell malignancies. These rearrangements lead to constitutive expression of the proto-oncogene, a feature found in many lymphomas. Some of the examples of these translocations include the follicular lymphoma with an overexpression of the *BCL 2* due to t(14;18) translocation where *BCL 2* is now under the control of IgH; Burkitt's lymphoma with the most common translocation t(8;14) where the *c-MYC* oncogene gets translocated to IgH; mantle cell lymphoma with the t(11;14), where cyclin D is also under the IgH control. Another opportunity for chromosomal translocations occurs through mechanisms of immunoglobulin class switching recombination (CSR) and immunoglobulin somatic recombination (SHM) happening in germinal centers of secondary lymphoid organs, which also generate DNA strand breaks and it too can lead to translocations (Shaffer et al., 2002).

B cells acquire their malignant phenotype through these various chromosomal rearrangements, mutations, and deletions since these processes either block B cell differentiation, block apoptosis or promote cell proliferation and cell growth. Translocations and somatic mutations of *c-MYC* promote cell growth and proliferation. Activation of the Nf-kB pathway through CD40 and BCR signaling, and subsequent overexpression of anti-apoptotic factors such as Bcl-XL and Bcl-2 are mechanisms that block apoptosis (Liu et al., 1991; Craxton et al., 2000). Most common genetic modifications that lead to the blockage of B cell differentiation include mutations in the *BCL6* gene, whose transcription gives rise to a transcriptional regulator of germinal center B cell proliferation and differentiation (Dalla-Favera et al., 1999).

Another way through which B lineage cells promote their malignant phenotype is through B cell receptor signaling. Apart from the fact that a malignant B cell acquires mutations in the immunoglobulin locus, in many cases it still expresses the BCR receptor on its outer surface,

which implies that these cells can use signaling coming from the BCR receptor to activate downstream pathways which can promote proliferation and cell survival (Kuppers, 2005).

Studies of the BCR signaling pathway went on to discover two ways of signaling from the BCR receptor – the "tonic signaling" and "chronic active signaling".

Experiments involving ablation of IgM (Lam et al., 1997) or Igα (Bedard and Krause, 2007) in mice demonstrated that after several weeks, in the spleen and in the lymph nodes, all mature B cells are abolished, and a substitution of Igα with a truncated version that doesn't contain ITAMs, does indeed reconstitute the BCR but doesn't allow survival od mature B cells, highlighting the importance of B cell signaling for survival (Kraus et al., 2004). Signaling, coming from the BCR receptor but without antigen binding is called tonic BCR signaling. This type of BCR signaling depends on AKT activation through PI3K, and one of the best examples of this phenomenon is Burkitt's lymphoma (BL), whose cells die upon knock down of Syk or Igα (Bojarczuk et al., 2015).

Chronic active B cell signaling is a phenomenon that was widely studied in activated B-cell-like diffuse large B-cell lymphoma (ABC-DLBCL). Most cases of ABC-DLBC are known to carry mutations in Igβ and *CARD11* gene, which results in a constitutive activation of the NF-kB pathway. During normal antigen stimulation in lymphocytes, Card11 protein (caspase recruitment domain-containing protein 11) get phosphorylated and activated, acting as a signaling scaffold which coordinates the activation of IkB kinase β (IKK), which is a positive regulator of the NF-kB pathway. However, mutations in the *CARD11* gene are a gain-of-function mutations, and they lead to a constitutive activation of IKK, leading to an enhanced response of the NF-kB pathway to exogenous stimuli. Also, *CARD11* mutations may also allow lymphoma cells

to activate the NF-kB pathway even in the absence of antigen receptor signals. In the cases of ABC-DLBCL where *CARD11* was not mutated, RNA interference genetic screens revealed the importance of BTK (Burton's tyrosine kinase) for promoting survival of these cell lines. Overall, the functional consequence of increased NF-kB signaling in ABC-DLBC is to allow propagation of the malignant cell to the plasma cell stage (Davis et al., 2010; Lenz et al., 2008).

The differences between tonic and chronic active B cell signaling can clearly be distinguished. Tonic signaling doesn't require Card11 and downstream components following its activation like Bcl-10 and MALT1, since mice which were deficient for these components still had a relatively normal number of follicular B cells, contrary to mice that had tonic signaling blocked (Thome, 2004). On the other hand, activation of *CARD11* and its downstream components proved essential for chronic active B cell signaling. Another distinguishable characteristic between tonic and chronic signaling is that tonic signaling acts in direction of maintaining resting B cells, that have their BCRs unclustered. Contrary, in ABC-DLBCL, their B cell receptors are clustered, gravitating towards an antigen stimulated cell, and not so much to a resting B cell (Staudt, 2010).

Another way that lymphoma cells managed to use in their advantage, in order to promote their survival and proliferation, is though antigen binding. For example, in cases of B-cell chronic lymphocytic leukaemia (B-CLL), the BCR receptor is often autoreactive and has a high affinity to bind autoantigens (Borche et al., 1990), whereas in other cases, B-CLL cells have an affinity to bind foreign antigens, like viral proteins (Sthoeger et al., 1989).

3.4.5. Diffuse Large B Cell Lymphoma

Diffuse large B cell lymphoma represent one of the most common adult non-Hodgkin lymphoid malignancies today, with 30 000 newly reported cases each year (Lohr et al., 2012). The cause of many DLBCL lymphomas remains largely unknown, but there are some factors that might predispose to the disease including different congenital and acquired immunodeficiency states, often connected with dysregulation in apoptosis or defects in DNA repair (Hartge and Devesa, 1992). The name of DLBCL lymphoma comes from the fact that transformed B lymphocytes represent large cells that exit the lymph node or the extranodal site in a diffuse way. They are deriving from normal B cells already exposed to an antigen, which migrated through germinal centers of lymph nodes or secondary lymphoid organs. The cells express typical B cell markers such as CD20, CD19, CD22, and CD79a, and in most cases the surface immunoglobulin is present. Based on their morphology, these cells have been classified as centroblastic, immunoblastic, anaplastic and T cell /histiocyte rich (Harris et al., 1994). Based on their clinical features, these malignancies are classified as primary mediastinal, intravascular or primary effusion lymphomas (Harris et al., 1994).

Many genetic abnormalities have been reported in these lymphomas. These abnormalities mostly include chromosomal translocations that abolish normal functions of genes such as *BCL 6, BCL 2* and *c-MYC*, where due to translocations these genes fall under the control of immunoglobulin regulatory elements in an improper fashion, leading to their overexpression. The transcription repressor *BCL 6* is a gene whose expression is limited to the GC B cell pool, and in normal conditions downregulation of this gene is required for further differentiation of normal GC B cells into memory and plasma cells. Since in cases of DLBC this gene is largely overexpressed,

this feature gives a proliferative advantage and stops maturation of GC cells (Ye et al., 1993). In the GC centers apoptosis plays a pivotal role in the process of negative selection and in the normal GC B cell expression of *BCL 2* is downregulated. Similarly, in many cases of DLBCL, *BCL 2* is overexpressed, which leads to apoptosis inhibition, to a proliferative advantage and contributing to lymphomagenesis (Gascoyne et al., 1997). Overexpression of *c-MYC* in these lymphomas also confers a proliferative advantages (Kramer et al., 1998). Mutations in the FAS ligand have also been reported in cases of DLBCL, that act in a dominant-negative manner and destabilize trimeric FAS receptors, disabling apoptosis and negative selection of B cells within germinal centers (Davidson et al., 1998).

The one common denominator for these lymphoid malignancies is that DLBCLs are a very heterogeneous group of tumors. This heterogeneity can be appreciated both on the genetic, biological and clinical level. Therefore, classification of these tumors in order to capture all their features in a coherent way, proved to be very challenging. Classification based on their morphology proved not to be very reproducible, since it led to a lot of diagnostic discrepancies between patients. However, the biggest breakthrough in attempting to classify these malignancies came from gene expression profiling experiments. The pioneer work by Alizadeh and Staudt in the year 2000, using gene expression profiling, managed to give a classification scheme for these tumors based on their cell of origin, since distinct forms of DLBCL displayed gene expression patterns that could be correlated to different stages of B cell differentiation (Alizadeh et al., 2000).

With the use of a specialized microarray chip, the so-called Lymphochip, that captured genes preferentially expressed in lymphoid cells and genes that had a role in immunology and cancer,

they managed to analyze gene expression patterns in diffuse large B cell lymphoma snap frozen tissue samples. This analysis lead to the Cell Of Origin (COO) DLBCL classification system, which distinguishes three groups of DLBCLs according to the gene expression patterns resembling to the normal B cell in a certain stage of its development:

Germinal Center B-cell like (GCB) group – a DLBCL group that has a gene expression signature of germinal center B cells, with a high expression of genes like *BCL 6* and *LMO2*.

Activated B-cell like (ABC) group – a group with a similar but not absolutely identical signature of activated B cells in the peripheral blood, expressing genes that are usually upregulated in the cells where the BCR signaling is activated, like *NF-kB* and *IRF4*.

"Other" goup of DLBCLs that remained undefined according to the cell of origin gene expression parameters.

The initial gene expression profile included 375 analyzed genes, then this signature was further refined, to include only 100 genes in the analysis, and then even more refined including only 27 genes. However, all these approaches again distinguished only GC and ABC tumor groups without being able to give more clarification to the third unspecified group, and this was very important since around 40% of tumors belonged to this group (Alizadeh et al., 2000) (Abramson and Shipp, 2005).

Since DLBCLs is not a homogeneous malignancy, differing only in terms of its cell of origin or a clinical outcome, it was necessary to deepen the initial gene expression profiling studies. Thanks to the work of Monti et al, efforts have been made in order to capture this unrecognized biological heterogeneity within DLBCLs, with the use of genome wide arrays and algorithms of

consensus clustering (Monti et al., 2005; Caro et al., 2012). Their approach was based on using three different clustering algorithms – hierarchical clustering, self-organizing maps and probabilistic clustering, together with a consensus clustering method (resampling based method), that would select in an automatic fashion the most stable cluster groups with each of these algorithms. Their method of classification, termed Consensus Cluster Classification (CCC), managed to distinguish three separate and reproducible clusters: OxPhos cluster, BCR cluster and Host Response (HR) cluster. Signature analysis of these clusters revealed that the OxPhos cluster was highly enriched in genes involved in mitochondrial function, oxidative phosphorylation, electron transport, regulation of apoptosis and proteasomal degradation. The BCR (B cell receptor)/proliferation cluster, on the other hand, was enriched in genes involved in the B cell signaling pathway, (*CD19, CD79a, BLK, SYK, PLCγ2, MAP4K*), B cell specific transcription factors like *MYC, BCL-6, STAT6* and DNA repair genes. The third, Host Response (HR) cluster, contrary to the OxPhos and BCR, contained an elevated signature of genes characteristic for the host response and not the tumor itself – overexpression of genes for T cell receptor components, *CD2*, molecules connected with T/NK cell activation, activators for monocytes and macrophages, components of the complement, TNF related proteins, adhesion molecules and cytokine receptors (Monti et al., 2005). Cross-comparison of DLBCL tumors classified either by COO or CCC revealed that these two classification frameworks capture different features of diffuse large B cell lymphoma biology. It was shown that 46% of the tumors classified as OxPhos, and 53% of tumors classified as BCR, fell under the GC group, and the rest was either ABC or Other, and the major part of HR group fell under the COO unspecified group Other. All of this pinpointed how

these classification frameworks provide non-overlapping information about these lymphomas, highlighting again their complex nature (Monti et al., 2005).

In order to find rational targets that can be used for treatment within subsets of diffuse large B cell lymphomas, extensive research has been performed, focusing on different aspects of DLBCL biology. One of these studies, important for this Thesis, focused on understanding the metabolic profiles of DLBCL groups classified by consensus clustering – OxPhos and BCR, in order to reveal whether metabolic differences exist between these tumor subsets, and whether some of these metabolic features might confer a proliferative advantage for a certain subtype, and hence can be used as a therapeutic target.

Considering that a large variety of DLBCLs use B cell signaling for their survival it was interesting to discover that the OxPhos subset didn't possess a functional BCR signaling network (Chen et al., 2008), which implied that there might be other mechanisms that these tumors use for promoting their survival. Considering that the OxPhos signature involved upregulation of genes implicated in mitochondrial metabolism, it was compelling to redirect the research focus to the metabolic component of this disease – energy metabolism and fuel utilization. The study went on to show that in the OxPhos subset there was an enhanced energy transduction in the mitochondria, that these tumors were incorporating carbons coming from nutrients into the TCA cycle with a much higher efficiency, and that their levels of glutathione were increased, compared to the BCR. The survival limiting feature for this DLBCL subset proved to be the glutathione synthesis and oxidation of fatty acids, since the perturbation of either of the two turned out to be selectively toxic for this tumor group. The metabolic profiling of these DLBCL tumor subsets was carried out in a highly integrative manner that involved metabolomics, mitochondrial respirometry and

proteomics (Caro et al., 2012). A proteomic approach, based on DIGE (two dimensional differential gel electrophoresis), mass spectrometry and the ITRAQ (Isobaric Tag for Relative and Absolute Quantitation) analysis, was used to carefully dissect components of the mitochondrial proteome in the BCR versus OxPhos subsets. Interestingly, this analysis identified additional components of the mitochondrial signature, that weren't detected before with previously used methods by other groups. Indeed, levels of Opa1 were higher in the OxPhos subset compared to BCR (Danial N, 2012 unpublished data), thus implicating Opa1 in the cancer profile.

3.5. Murine models of B cell lymphoma

Human B cell lymphomas are one of the most common hematologic malignancies today, currently holding the fourth place in its occurrence, with a very strong research focus directed towards them. The most striking feature of these lymphomas, as mentioned previously, is that they are very heterogeneous. They differ both in the tumor location and in the type of malignant cell. Strong heterogeneity of these tumors makes research very difficult. Discriminative parameters necessary for a proper classification of collected human samples are often not very clear, there is a limited availability of biopsies, together with existing differences among patients and differences in subtypes of lymphomas, making cancer studies very challenging. In order to overcome these research obstacles there was a high need for developing good animal models for lymphoma studies. The positive aspect of developing good animal models is that they provide homogenous material to work with, thus allowing a more standardized investigation of tumor

characteristics, tumor microenvironment and performance of preclinical studies (Donnou et al., 2012).

Murine models for B cell lymphomas can be classified as either spontaneous or induced. Spontaneous models refer to the ones when the lymphoma develops spontaneously in a genetically engineered mouse, whereas the induced model is the one when a tumorigenic cell line gets implanted into a mouse. Depending on the type of the study in which these murine models will be used, it is possible to further classify them in three large groups (Donnou et al., 2012):

1. Murine models for studying lymphomagenesis

2. Murine models for studying lymphoma microenvironment

3. Murine models for analyzing the efficacy of new therapies

Since in this Thesis the emphasis is on studying the role of Opa1 overexpression in a lymphoma background, the murine models for studying lymphomagenesis will be described in more detail, with a special focus on the Emu-myc mouse.

3.5.1. Murine models for studying lymphomagenesis

One of the key questions in all cancer studies refers to understanding the origin and the mechanism of tumor development. In order to understand how B cell lymphomas arise and how they mature in different tumor environments, many spontaneous murine tumor models have been created (Table 2).

NAME	LYMPHOMA SUBTYPE/ORIGIN	STRAIN (HAPLOTYPE)
B10 H-2a H-4bp/Wts	CLL	C57Bl/10 (H-2b)
SL/KH	Pre-B lymphoma	SL/KH (H-211)
Eμ-N-myc	Indolent B-NHL	C57Bl/6 x DBA/2 (H-2b/d)
NFS.V+	Marginal zone lymphoma	NFS.V+ (H-2sq4)
NMRI/RFB-MuLV	n.d.	NMRI (H-2q)
B6-l-MYC	Burkitt-like lymphoma	C57Bl/6 (H-2b)
VavP-Bcl2	Follicular lymphoma	C57Bl/6 (H-2b)
Lig4/p53 KO	Pro/Pre-B lymphoma	C57Bl/6 × sv129
Eμ-BRD2	DLBCL	FVB (H-2q)
Bcl6 Knock in	Germinal center, DLBCL	C57Bl/6 × sv129
Bcl6/Myc transgenic	Post germinal center, DLBCL	C57Bl/6 × sv129
IL-14aTGxc-Myc TG (DTG)	Blastoid variant of mantle-cell lymphoma	C57Bl/6 (H-2b)
Myc/BCRHEL/HEL	Burkitt-like lymphoma	C57Bl/6 (H-2b)
Eμ-myc	From follicular to DLBCL (time dependant)	C57Bl/6 × sv129
RzCD19Cre	NHL, hepatitis C induced	129/Sv (H-2bc); BALB/c (H-2d); C57Bl/6 (H-2b)
UVB induced	Mature B-cell lymphoma	C57Bl/6 p53+/– (H-2b)

Table 02. Spontaneous models of B cell lymphoma. B-NHL: non – Hodgkin B cell lymphoma; CLL: chronic lymphocytic leukemia; DLBCL: diffuse large B cell lymphoma; DTG: double transgenic mice; n.d.: not determined. Adapted from (Donnou et al., 2012)

Thanks to the advances in genetic engineering it became possible to generate transgenic mouse models which contain known modifications of the human genome responsible for B lymphoma development (Harris et al., 1988). When a gene is inserted in to a fertilized ovum it usually integrates into a host chromosome within few cell divisions, and in this way all the tissues of the transgenic mouse acquire the gene, but the regulatory elements associated with the gene are the ones that are responsible for tissue specific expression. When immunoglobulin genes are introduces they are only expressed in the lymphoid cells of the transgenic mouse (Adams et al., 1985). One of the most frequent modifications of the human genome that is found in almost

every case of Burkitt's B cell lymphoma is the translocation of the *c-MYC* proto-oncogene into or close to the one of the immunoglobulin loci. This rearrangement of the cellular genome releases the *c-MYC* gene from its normal sensitivity to negative regulation, making the gene constitutively active in cells that express immunoglobulin genes (Harris et al., 1988). The involvement of such a translocation in lymphomagenesis is studied in the Eμ-myc mouse model, the most common mouse model for lymphoma studies (Donnou et al., 2012).

3.5.1.1. Eμ-myc mouse: A model for high-incidence spontaneous lymphoma and leukemia of B cell

Eμ-Myc mice are transgenic mice carrying a fusion gene of the otherwise normal *Myc* oncogene (*c-Myc*) which is put in association with the Eμ immunoglobulin heavy chain enhancer and myc promoter. Expression of the *Myc* transgene is restricted to the B cell lineage and tumors that arise are all lymphoblastic lymphomas (Adams et al., 1985). The Eμ-myc mouse was originally created through a collaborative project between R.L. Brinster, R.D. Palmiter and J. Adams and S. Corey back in 1985, as a way to test the hypothesis whether a chromosomal translocation leading to juxtaposition of immunoglobulin and *Myc* genes can further lead to cancer. By generating transgenic mice which possess different forms of the *c-Myc* gene, they have proven that association of this proto-oncogene with the immunoglobulin enhancer converts it into a potent leukemogenic agent for the B lymphocyte lineage (Adams et al., 1985). They have developed seven constructs that have been introduced into mice. These constructs included an intact murine c-gene, a truncated form bearing the coding region (exons 2 and 3), and 5 versions with *c-Myc* coupled to other regulatory regions. In order to generate a transgenic *Myc* mouse, (C57BL

x SJL)F2 eggs were injected with a construct, implanted into pseudopregnant females, where after the transgenic pups got detected by hybridization to tail DNA.

The *Eμ-myc* gene proved to be very potent, where 13 of 15 primary transgenic animals developed lymphoma. Both u and k enhancer constructs lead to tumor development, which all involved lymphoid tissue whereas the non-immunoglobulin constructs gave few tumors. No tumors developed in mice that were carrying the tagged normal *Myc* gene or the truncated form characteristic for most murine plasmacytomas over the observation period of 10 months. This was implying that the efficacy and specificity of these constructs was connected with the presence of immunoglobulin enhancers. The overall conclusion from the initial work with the Eμ-myc mice is that these animals develop pre B cell and mature B cell lymphomas (Adams et al., 1985). However, further characterization of these mice went on to show that most young Eμ-myc mice actually don't contain malignant clones and that there is a noticeable pre-malignant faze before the malignancy onset. The Eμ - driven *c-Myc* overexpression in these animals favors proliferation of B cells, and not their maturation. In the prelymphomatous bone marrow there is a strong presence of large pre B cells, and this cell population is polyclonal. The spleens of young Eμ-myc animals are enlarged and contain an abnormally expanded populations of pre B cells, which is a cell type not usually found in the spleen. In the prelymphomatous state, pre B cells do not infiltrate other lymphoid organs like the thymus and lymph nodes, even though these organs actually represent the primary sites of tumor formation in these animals. Studies on fetal livers and postnatal bone marrows went on to show that a higher production of pre B cells starts even before birth, and that the pre B cell amount ratios at that stage are much higher compared to their wild type littermates. At 21 days of age the B cell amount ratios in these animals are much

lower compared to their wild type littermates, implying that the enforced *c-Myc* overexpression rewires the program of B cell differentiation favoring higher proliferation of pre B cells and a delayed and slowed maturation into B cell (Langdon et al., 1986).

After a variable period during which there is a benign overerproliferation of pre B cells, all Eμ-myc transgenic mice eventually develop malignant lymphomas of the B cell lineage, with associated leukemia. Transplantation experiments further confirmed that the lymphoblast masses that were evident in enlarged lymphoid tissues were indeed malignant. The disease phenotype of these mice includes massively enlarged lymph nodes, easily detected by palpation. The enlargement usually occurs between 3 and 18 weeks of age, starting with the enlargement of the inguinal lymph nodes. A couple of weeks later mice develop the so-called "water-wings" represented as prominent lumps on both shoulders and neck, which reflects enlargement of brachial and cervical lymph nodes. Eμ-myc mice also display a modest enlargement of the spleen and the thymus. Liver and lungs are often quite enlarged, and it has been also reported that some animals develop tumor masses inside the skull. Lymphoblasts are present in all enlarged lymphoid organs and in the blood, and there is also a variable invasion of lymphoblasts to other tissues too. When mice become terminally ill, they manifest hunched posture, slow movement, ruffled fur and tachypnea (Adams et al., 1985; Harris et al., 1988).

The discovery that *c-Myc* overexpression favors proliferation over maturation, and that the proliferating cells weren't tumorigenic also highlighted the fact that the mere overexpression of the *c-Myc* oncogene wasn't sufficient to dictate the lymphoma phenotype, suggesting that tumorigenesis requires additional events to occur (Langdon et al., 1986; Harris et al., 1988; Alexander et al., 1989). It has been shown that these additional events could include a somatic

activation of a cellular oncogene that has the ability to cooperate with *Myc*, such as *Ras*. Mutations in *N-Ras* and *K-Ras* oncogenes were reported in two independent Emu-myc lymphomas, together with the fact that the mutated *N-Ras* has the ability to cooperate with *c-Myc* and lead to transformation of B cells in vitro, implying that spontaneous mutations of *Ras* genes are one of the pathways leading to lymphoid malignancy in Emu-myc mice (Alexander et al., 1989).

Works by (Vaux et al., 1988) and (Strasser et al., 1990) went on to demonstrate that one of the key hallmarks of cancer was indeed a suppression of apoptosis. Co-expression of *c-Myc* together with the well-known inhibitor of apoptosis *Bcl 2* resulted in an increased rate of lymphoma development highlighting the important role for the blockage of the mitochondrial death pathway in tumor progression. Constitutive *BCL 2* expression, achieved by juxtaposition of the *BCL 2* gene to the immunoglobulin heavy chain locus, is an event found in human follicular B cell lymphoma. This translocation doesn't change the gene product itself but it just leads to its constitutive overexpression. This overexpression of *BCL 2* leads to an increase in cell survival, and it also has a protective role for human B and T lymphoblasts under stress (Tsujimoto, 1989; Reed et al., 1990) providing a growth advantage. Transgenic mice which possess this translocation accumulate small non-cycling B cells that have strong survival capabilities in vitro, but don't develop spontaneous tumors. Pioneer in vitro experiments suggested that *BCL 2* can indeed cooperate with an overexpressing *MYC*, improving growth of pre B and B cells in vitro (Vaux et al., 1988). Further confirmation about the *Bcl 2 / Myc* synergy, important for tumorigenesis, came from studies of doubly transgenic mice, which contained both overexpressed Bcl 2 and *c-Myc*. These doubly transgenic mice demonstrated a hyperproliferation of pre B and B cells, and they

were developing tumors much faster than their Eμ-myc mouse counterparts (Strasser et al., 1990)

Since tumorigenesis in Eμ-myc mice is a multistep process, efforts have been made to understand cellular events underlying tumorigenesis. This has been achieved by quantifying B cell populations at various stages of this process, staining the cells from the peripheral blood with different monoclonal antibody combinations, all of which was followed by a flow cytometric analysis. Eμ-myc mice can be distinguished at weaning from their non-transgenic littermates based on the size of lymphocytes in the peripheral blood. This measure can also be used for following the lymphocyte proliferation status in individual animals. According to this it is possible to distinguish three distinct phases of the tumorigenic process:

(1) Early stage – an initial period of B cell lineage polyclonal proliferation. The cell surface antigen phenotype of this stage corresponds to a mixture of IgM-positive and IgM- negative cells, weak B220 positive, weak Mac-1 positive and CD4, CD8 and CD5 negative cells.

(2) Intermediate stage – a prolonged remission phase that has a variable duration from mouse to mouse, where peripheral B lymphocytes are non-proliferative and not large in numbers. Their immunophenotype corresponds to a typical B cell – IgM positive, B220 positive, CD5 negative and Mac-1 negative B cell populations.

(3) Late stage (ending with the death of the animal) – at this point there is again an active B cell proliferation in the blood, with a similar immunophenotype of the early stage – IgM positive and IgM negative, weak B220 positive, weak Mac-1 positive and CD5 negative cell populations.

Based on this immunophenotypic analysis, the late stage monoclonal B cells present in tumors have a phenotype corresponding to an early polyclonal proliferating B cell. Since in the intermediate stage there is a high level of cell death in the bone marrow, the entry into the terminal stage depends on a clone of cells which was able to avoid normal processes of cell death, that normally regulate the exit of B cells from the bone marrow to the periphery, again highlighting the importance of apoptosis suppression for acquiring a cancer phenotype (Sidman et al., 1993). However, with the availability of large Eμ-myc cohorts, with the use of gene expression profiling, and especially analysis of signatures of cell signaling pathway activation, it became possible to distinguish several different forms of B cell lymphomas in Eμ-myc mice depending on the time of the tumor onset. Some of these tumor types indeed did not get detected with the classical immunophenotyping approaches. Two main tumor categories discovered with the gene expression profiling approach include an early stage tumor composed mainly of pre - B cells, with a strong resemblance to Burkitt's lymphoma; whereas the other tumor category is detected in the late stage (after 400 days of age), and the tumor is mainly composed of differentiated (mature) B cells, thus resembling to human diffuse large B cell lymphoma (Mori et al., 2008).

4. RESULTS

The mitochondria-shaping protein Opa1 participates in lymphoma progression

Dijana Samardzic[1,2], Nika Danial[3], and Luca Scorrano[1,2]

[1] Dulbecco Telethon Institute, Venetian Institute of Molecular Medicine, Via Orus 2, 35129 Padova, Italy

[2] Department of Biology, University of Padova, Via Ugo Bassi 58 B, 35131 Padova, Italy

[3] Department of Cancer Biology, Dana-Farber Cancer institute, 450 Brookline Ave, Boston, MA 02115, United States

Address correspondence to:

Luca Scorrano. Email: luca.scorrano@unipd.it

Character count:

SUMMARY

Mitochondria are key organelles that amplify apoptosis through the release of cytochrome c and other cofactors that activate downstream caspases. Cytochrome c release is accompanied by mitochondrial cristae remodeling controlled by the inner mitochondrial membrane shaping protein Opa1. While levels of Opa1 are increased in certain cancers, the direct relationship between Opa1 and tumor generation, maintenance and severity was never explored. Here we show that increased Opa1 levels aggravate a mouse model of lymphoma. Proteomic profiling identified upregulated Opa1 in the Oxidative phosphorylation (OxPhos) subset of diffuse large B cell lymphoma. Morphological and functional analysis revealed that increased Opa1 levels impacted on mitochondrial morphology, metabolism and ultrastructure of the OxPhos lymphoma cells, ultimately conferring a proliferative advantage when cells were forced to rely on mitochondria for energy generation. Accordingly, Opa1 overexpression aggravated the clinical features of disseminated lymphoma and decreased survival rates of an in vivo Eμ-Myc lymphoma mouse model. Thus, Opa1 displays oncogenic features and can be considered as a novel therapeutic target for cancer treatment.

INTRODUCTION

Mitochondria are double membrane–enclosed organelles that play a key role in energy conversion, metabolism, regulation of cellular signaling and amplification of programmed cell death (Wasilewski and Scorrano, 2009). During apoptosis mitochondria release cytochrome c and other cofactors that are required to amplify cell death (Li et al., 1997). The complete release of cytochrome c depends on the changes in the shape and in the ultrastructure of the organelle: during these processes mitochondrial network undergoes fragmentation accompanied by cristae remodeling and widening of cristae junctions (Frank et al., 2001; Scorrano et al., 2002). Of note, deregulation of apoptosis represents a typical hallmark of cancer, since cancer cells exploit the inhibition of the mitochondrial arm of apoptosis to acquire the malignant phenotype (Thompson, 1995).

Mitochondrial shape in the steady state is the result of the balanced action of fission and fusion events (Griparic and van der Bliek, 2001). The process of mitochondrial fission is controlled by a synchronized action of the cytosolic Dynamin – related protein 1 protein (Drp1) (Cereghetti et al., 2008) that is recruited to the outer mitochondrial membrane where it binds its adaptors Fission – 1 (Fis1), Mitochondrial fission factor (MFF), Mitochondrial division (Mid) 49 and 51, and participates in the division of mitochondria (Palmer et al., 2011). Mitochondrial fusion, on the other hand, is controlled by Mitofusins (Mfn) 1 and 2, large GTPases located in the outer mitochondrial membrane, together with the inner membrane GTPase Optic Atrophy 1 (Opa1) (Santel and Fuller, 2001; Chen et al., 2003; Cipolat et al., 2004). In humans, alternative splicing of Opa1 gives rise to 8 mRNA splice variants which further get processed by proteolytic proteases giving rise to 2 long and 3 short forms of Opa1 (Olichon et al., 2007; Duvezin-Caubet et al., 2007).

Opa1 is a multifunctional protein: apart from its function in promoting mitochondrial fusion (Cipolat et al., 2004), it also plays a key role in the control of apoptosis by keeping in check the cristae remodeling pathway, by forming multimeric complexes that control the size of the cristae junctions during apoptosis (Frezza et al., 2006; Cipolat et al., 2006). Moreover, Opa1 controls mitochondrial metabolism, by favoring the assembly of respiratory chain complexes into supercomplexes, increasing the efficiency of oxidative phosphorylation (Cogliati et al., 2013). All these functions concur to determine the beneficial outcome of its mild overexpression in vivo, which protects from heart and brain ischemia, denervation-induced muscular atrophy and fulminant hepatitis (Varanita et al., 2015). Furthermore, it corrects mouse models of primary mitochondrial dysfunction caused by defects in components of the respiratory chain (Civiletto et al., 2015).

The beneficial effects of Opa1 overexpression apparently come with a counterpart, since a handful of studies reported that Opa1 is overexpressed in several human cancers where high levels of Opa1 correlated with a worst prognosis and an impaired response to therapy (Fang et al., 2012), while its downregulation in cancer cells engages the mitochondrial apoptotic pathway and improves the sensitivity to classical chemotherapeutic agents (Zhao et al., 2013). However, whether Opa1 has a role in the acquisition and maintenance of the cancer phenotype is unclear, especially in the context of cancers where mitochondria have been reported to play a role. In addition to their role as regulators of apoptosis, mitochondria seem to play a role in cancer due to their role in metabolism: not only OxPhos is switched off during oncogenesis (the well known Warburg effect), but also these organelles represent the source of a group of metabolites (the so called oncometabolites) that act in the cytoplasm to stabilize hypoxia inducible factor (HIF) and

therefore to promote tumor survival and proliferation (Yang et al., 2013). In addition, several recent omics studies indicated previously unappreciated changes in mitochondrial profiles as a hallmark of different subsets of cancers. This is the case of diffuse large B cell lymphoma (DLBCL), one of the most common adult non-Hodgkin lymphoid malignancies (Lohr et al., 2012). DLBCLs are a genetically heterogeneous group of tumors that can be further divided in several subsets, identified by their distinct molecular signatures (Alizadeh et al., 2000). Genome wide arrays and multiple clustering algorithms defined a B cell receptor (BCR)/proliferation cluster (BCR–DLBCL), which displays upregulation of genes encoding BCR signaling components, and an OxPhos cluster (OxPhos–DLBCL) which is enriched in genes involved in mitochondrial oxidative phosphorylation. The OxPhos subset lacks an intact BCR signaling network, suggesting dependence on alternative survival mechanisms, which are not yet defined (Monti et al., 2005; Caro et al., 2012). Notably, a proteomic approach aimed at carefully dissecting components of the mitochondrial proteome in the BCR versus OxPhos cell group, identified increased levels of Opa1 in the OxPhos (Danial N, manuscript in preparation).

Here we show that Opa1 is increasingly processed in the BCR DLBCL subset and that mitochondrial morphology and ultrastructure are different between the BCR and the OxPhos DLBCL subsets that display different levels of Opa1. Furthermore, *Opa1* and *c-Myc* synergize in doubly transgenic mouse models, where Opa1 overexpression contributes to the development of, and aggravates cancer in Eμ-Myc transgenic animals. Our data indicate a role for Opa1 in DLBCL features, and tumor progression in vivo.

RESULTS

Opa1 is cleaved in the BCR subset of DLBCL

In order to verify the proteomic result that Opa1 is upregulated in the Oxphos DLBCL subset, we capitalized on 8 established DLBCL cell lines, 4 of which (D4, D6, Ly7 and Ly1) belonging to the BCR subset, and other 4 (Pfeiffer, Toledo, Ly4 and K422) to the OxPhos subset, in accordance with their metabolic signature based on the Consensus Cluster Classification system (Monti et al., 2005; Caro et al., 2012). In humans, the 8 Opa1 molecules generated by alternative splicing further undergo proteolytic processing giving rise to two long Opa1 forms of higher molecular weight, and 3 short forms of lower molecular weight, which can be seen as 5 distinguishable bands on a Western blot (Olichon et al., 2007; Duvezin-Caubet et al., 2007). Western blot analysis followed by densitometry quantification performed on these 8 DLBCL cell lines revealed that levels of the mitochondria-shaping protein Fis1 were generally higher in the BCR subset, whereas besides variability among the different cell lines, levels of Drp1, Mfn1 and Mfn2 were comparable. Conversely, levels of Opa1 were higher in the Oxphos subset, and strikingly, in the BCR subset short Opa1 forms accumulated (Figure 1A and quantification in C), especially in the D6, Ly7 and Ly1 cell lines, whereas in the cell line D4 long forms were still retrieved. Of note, the balance between long and short Opa1 forms was maintained in both B lymphocytes isolated from spleens of healthy C57/Bl6J male mice and B lymphocytes from buffy coats of healthy adult male subjects, suggesting that the unbalance observed in the BCR cells was specific for this cancer cell subset (Figure 1B).

In order to clarify the mechanism of increased Opa1 cleavage in the BCR DLBCL subset, we focused our attention on B cell receptor signaling that is increased in the BCR subset (Chen et al., 2008), as well as on known mitochondrial factors responsible for Opa1 cleavage such as changes in mitochondrial membrane potential and activation of Opa1 processing proteases (McBride and Soubannier, 2010). Increasing signaling from the BCR leads to cellular calcium accumulation (Sugawara et al., 1997), but chelation of intracellular calcium did not interfere with Opa1 cleavage (Figure S1A). Similarly, fostamatinib (R406) - a commercially available SYK inhibitor (Chen et al., 2008), ibrutinib – BTK inhibitor (Goldstein et al., 2015), and Cal 101 – a PI3K inhibitor (Lannutti et al., 2011), all known to abolish signaling from the BCR, had no effect on Opa1 cleavage (Figure S1B). Finally, levels of OMA1, an ATP-independent protease responsible for Opa1 cleavage (Ehses et al., 2009), were unchanged in all the 8 cell lines tested, and also mitochondrial membrane potential was not varying between these two cell subsets (results not shown). In sum, the increased Opa1 cleavage observed in the BCR DLBCL subset cells cannot be explained in the framework of the known signaling pathways downstream of the BCR.

Different levels of Opa1 are mirrored by changes in mitochondrial ultrastructure

Irrespective of the fine mechanism responsible for the increased Opa1 cleavage in the BCR DLBCL subset, we decided to investigate whether the observed differences in Opa1 levels and cleavage were reflected by changes in mitochondrial architecture. Confocal microscopy analysis of DLBCL cell lines stained using the Tom20 mitochondrial marker was followed by reconstruction of the confocal Z stacks and segmentation-based digital analysis using Squassh (segmentation and quantification of subcellular shapes), an ImageJ plugin specifically designed for detecting and delineating the observed morphologies (Rizk et al., 2014). This automated analysis did not reveal

major changes in mitochondrial morphology among the different 8 cell lines tested here, suggesting that the balance between long and short forms of Opa1 does not affect mitochondrial length in DLBCL cells (Figure 2A and quantification in B).

Given the fundamental role of Opa1 in mitochondrial cristae shape, we decided to analyze mitochondrial ultrasctucture of DLBCL cell lines by electron microscopy. In glucose rich media, cristae of OxPhos mitochondria appear slightly tighter, compared to their BCR counterparts (Fig. 3A – B, and quantification in C). Cristae shape transitions from orthodox to condensed, where cristae are wider, when mitochondrial respiration is stimulated (Hackenbrock, 1966), in an Opa1 dependent process (Patten et al., 2014). When cells were cultivated for 48 hours in galactose rich media, where ATP production relies on mitochondrial metabolism, cristae were wider in all DLBCL cell lines, but more so in BCR cells compared to the Oxphos counterparts (Fig. 3A – B and quantification in C). This tighter cristae morphology correlates with the pre-existing balance between Opa1 long and short forms, since we could not find any significant difference in this ratio upon shifting the two subsets of DLBCL cell lines to galactose enriched media (Figure 3D and Figure 3 E). In conclusion, the altered ratio between long and short Opa1 forms correlates with wider cristae when cells are forced to rely on mitochondria for ATP production.

OxPhos DLBCL cell lines display a growth advantage when they rely on mitochondria for energy supply

Since Opa1-dependent cristae shape affects mitochondrial-dependent cell growth (Cogliati et al., 2013), we verified whether observed differences in Opa1 levels and cristae shape affected proliferation rates of DLBCL cell lines when they are forced to use mitochondria for energy supply.

While proliferation of BCR DLBCL cell lines in galactose rich media was slower than when they were cultivated in galactose (Figure 4A), OxPhos DLBCL cells grew comparably irrespective of whether they had to rely on mitochondria for energy supply (Figure 4B). Thus, maintenance of long/short Opa1 ratio in the OxPhos DLBCL cells confers a proliferative advantage when cells rely on mitochondria for energy supply and could explain at least partially why the OxPhos DLBCL are more aggressive.

Generation of an Opa1 overexpressing Eμ-myc lymphoma mouse model

Our in vitro data correlate increased Opa1 levels and maintained Opa1 long/short form ratio to a proliferative advantage for DLBCL cells. However, they fail to address the issue of whether increased Opa1 levels act as a lymphoma modifier in vivo. The intrinsic susceptibility of individual mouse strains to different types of cancer can be greatly increased by the expression of specific oncogenes, such as c-myc (leukemias/lymphomas, liver tumors), or mutated H-Ras (lung cancer, liver cancer) (Strasser et al., 1996; Maronpot et al., 1991; Sandgren et al., 1989). Co-expression of c-myc together with the well-known inhibitor of apoptosis bcl 2 increases the rate of lymphoma development, highlighting the role of the mitochondrial death pathway in tumor progression (Strasser et al., 1996). With this in mind, we decided to generate an Opa1 overexpressing lymphoma mouse model. We first crossed $Opa1^{flx/flx}$ with $Opa1^{tg}$ mice (Cogliati et al., 2013) to generate $Opa1^{flx/flx}$::$Opa1^{tg}$ animals that were then further crossed to Eμ-myc mice, a well characterized mouse model of lymphoma studies. Eμ-Myc mice carry a fusion gene of the otherwise normal Myc oncogene (c-myc) under Eμ immunoglobulin heavy chain enhancer and Myc promoter. Expression of the Myc transgene is restricted to the B cell lineage and tumors that arise are all lymphoblastic lymphomas (Adams et al., 1985; Harris et al., 1988). By standard

breeding strategies we obtained Eμ-myc::Opa1$^{flx/+}$::Opa1^{tg} triple mutants (hereby referred to as Eμ-myc::Opa1^{tg} mice, Figure 5 A and Figure 5 B). Western blot analysis revealed that as expected levels of Opa1 were higher in Eμ-myc::Opa1^{tg} spleen, thymus, lung and kidneys compared to their Eμ-myc control littermates (Figure 5 C).

Lymphomas are more severe and aggressive in Eμ-myc::Opa1^{tg} mice.

Follow up of a large colony of single Eμ-myc and double Eμ-myc::Opa1^{tg} transgenic animals highlighted the emergence of lymphomas, clinically evident as palpable lymph nodes associated later in the progression of the disease with a deterioration of the general physical status of the mice that were euthanized when their clinical status appeared poor. These palpable masses and the decline in the general health status appeared earlier in the double Eμ-myc::Opa1^{tg} mice, prompting us to statistically follow survival rates in a cohort of 95 single Eμ-myc and double Eμ-myc::Opa1^{tg} transgenic animals in total, for 20 months. Censorial Kaplan Meier analysis demonstrated that Eμ-myc::Opa1^{tg} doubly transgenic animals become terminally ill at a faster rate and more synchronously then their littermates bearing only the Eμ-myc transgene, especially in the case of male subjects (Figure 6A).

Gross anatomy inspection of representative 3 month old mice revealed a significant enlargement of the lymphoid organs such as spleen, thymus and lymph nodes in the doubly transgenic Eμ-myc::Opa1^{tg} mouse models, compared to the heathy controls (wt and Opa1$^{flx::tg}$), and Eμ-myc littermates (Figure 6B). Necropsy analysis was performed by skilled independent mouse pathologists on selected single transgenic Eμ-myc, and doubly transgenic Eμ-myc::Opa1^{tg} animals of different age, ranging from pre-symptomatic two months old mice, up to 5 and 6 month old

mice where lymphoma was completely developed. Disseminated malignant lymphoma was more severe in the Eμ-myc::Opa1^{tg} animals with enlargement and massive lymphoid infiltrations in spleen and thymus, as well as with cancer foci in lungs, liver and kidney already in the pre-symptomatic animals (Table 1). Even in 5 and 6 months old symptomatic mice the clinical picture was more severe in the doubly transgenic animals, characterized by massive enlargement of spleen, thymus and lymph nodes (Figure S4 A - B). Overall, any inspected organ at any analyzed age appeared more infiltrated by tumor in the Eμ-myc::Opa1^{tg} animals (Table 1), indicating that Opa1 overexpression aggravates Eμ-myc driven lymphomas.

We next inspected lymphoid and infiltrated tissues by histology. The normal architecture of 3 months old Eμ-myc and Eμ-myc::Opa1^{tg} spleens was disrupted, with loss of the clear distinction between the red and white pulp; however, the severity of lymphoblast dissemination was stronger in the doubly transgenic mouse, with a severe and diffuse neoplastic lymphoid infiltration of cells characterized by a scant amount of amphophilic cytoplasm and round central nuclei with finely stippled chromatin and multiple basophilic nucleoli. The mitotic activity was also higher in the Eμ-myc::Opa1^{tg} characterized by 8-10 mitosis per high-power field (HPF) compared to the 6-7 mitosis per HPF in the Eμ-myc, whereas the healthy control littermates displayed a moderate mitotic activity of 2-3 mitoses per HPF (Figure 7A). Albeit both Eμ-myc and Eμ-myc::Opa1^{tg} 3 months old thymi displayed multifocal and sometimes coalescing infiltrates of lymphoid cells characterized by a scant amount of amphophylic cytoplasm and round, central nuclei with finely stippled chromatin and multiple basophilic nucleoli, architecture of the thymus (with the clear distinction between the cortex and the medulla) was preserved in Eμ-myc but not in Eμ-myc::Opa1^{tg} mice. Also in the thymus mitotic activity was increased in Eμ-myc::Opa1^{tg} mice

reaching 7-8 mitosis per HPF compared to the 5-6 mitosis per HPF of single Eμ-myc transgenics (Figure 7B). While intrasinusoidal neoplastic lymphoid cell infiltrations in the liver (Figure 7C) and multifocal perivascular infiltrations of the interstitium and the adipose tissue in the kidney (Figure 7D) were comparable between 3 months old Eμ-myc and Eμ-myc::Opa1^{tg}, the interstitial neoplastic infiltration was severe in the Eμ-myc::Opa1^{tg} mouse but only moderate in the Eμ-myc (Figure 7E). In conclusion, very mild Opa1 overexpression worsens Eμ-myc driven lymphomas.

We next wanted to address if the worsened clinical phenotype of the Eμ-myc::Opa1^{tg} mice was a consequence of a specific effect of Opa1 on the program of B cell differentiation. Flow cytometric analysis using antibodies for the cell surface markers defining characteristic stages of the B cell development revealed that bone marrow levels of pro B cells (CD19+cKit+) as well as of pre-B cells (CD19+cKit-) were higher in Eμ-myc::Opa1^{tg} mice compared to their Eμ-myc counterparts at all analyzed time points (Figure 8A). As a matter of fact, in the Eμ-myc::Opa1^{tg} mice cells positive for the pan-B cell marker B220 were more in all primary and secondary lymphoid organs at all analyzed time points (Figure 8B,C), suggesting increased B cell proliferation or reduced B cell apoptosis in these mice. We also excluded that the ubiquitous Opa1 expression affected T cell development (figure S5 A) or monocyte/macrophage (Mac1+Gr1-) and granulocyte lineages (Mac1+Gr1+) (figure S5 B). In conclusion, moderate Opa1 overexpression worsens Eμ-myc driven lymphomas by favoring bone marrow accumulation of pre and pro B cells as well as B cell infiltration in peripheral lymphoid organs.

DISCUSSION

One of the main strategies exploited during tumor development is to evade apoptosis, and alterations that prevent cells from undergoing cell death can be considered as oncogenic (Cory et al., 1999). While the role of mitochondrial apoptosis in oncogenesis is clear, the contribution of mitochondrial dynamics to cancer development and progression is much less defined. Here we demonstrate that higher levels of Opa1 are responsible for certain features of diffuse large B cell lymphoma cell subsets and we formally prove that Opa1 overexpression leads to a more severe cancer phenotype in a mouse lymphoma model.

The link between impaired apoptosis and the process of tumorigenesis started to become widely appreciated with the discovery that Bcl 2 promotes cell survival (Vaux et al., 1988) and acts synergistically with Myc in promoting lymphomagenesis in mice (Strasser et al., 1990). These discoveries set the stage to explore the role in cancer formation for other genes and proteins reported to participate in the regulation of cell death. The discovery that Opa1 regulates the mitochondrial apoptotic pathway, through the process of cristae remodeling and of cytochrome c release (Scorrano et al., 2002; Frezza et al., 2006), together with the discovery that it is upregulated in certain cancers (Fang et al., 2012), suggested that also this inner membrane protein might play a role in cancer. However, whether Opa1 is directly involved in cancer generation was never explored. We therefore set out to explore if the observed upregulated levels of Opa1 in the Oxphos subset of DLBCL (Danial N, Manuscript in preparation) played any role in the cellular and in vivo features of lymphoma.

In vitro, we observed that not only Opa1 was upregulated in the OxPhos subset of DLBCL, but also the ratio between long and short Opa1 forms was reduced in the BCR subset. While this change did not impact on mitochondrial morphology, it affected cristae that appeared wider in the BCR subsets especially when these cells were forced to rely on mitochondria for energy production. Along the same line, OxPhos cells grew faster in media supplemented with galactose, a maneuver that forces mitochondrial ATP generation. This is in line with what was observed in other cell types and might reflect an increased efficiency of mitochondrial respiration due to supercomplex assembly of the respiratory chain complexes (Cogliati et al., 2013). Alternatively, the increased Opa1 levels might protect Oxphos DLBCL cells from spontaneous apoptosis, but we conversely found that the mitochondrial apoptotic machinery is inhibited due to Bcl 2 upregulation and Bax downregulation in the BCR subset. These changes might reflect the adaptation of BCR cells to reduced Opa1 levels and suggest that the observed decreased proliferation in galactose rich media is not due to increased cell death.

In vivo, Opa1 overexpression contributed to cancer development in Eμ-myc transgenic mice, shortening their life span and leading to a more severe clinical picture of disseminated lymphoma. Necroscopic, pathology and immunophenotypic analysis performed on these mice further corroborated that Opa1 overexpression allowed immature as well as mature B cells to survive in primary as well secondary lymphoid organs and to invade e.g. lungs. Our results indicate that Opa1 levels can directly aggravate oncogenesis by Myc and in this respect can phenocopy what already observed with Bcl 2 (Strasser et al., 1990; Strasser et al., 1996). Historically, the double Eμ-myc Bcl 2 transgenic mouse model established a firm role for Bcl 2 as an oncogene that acts in a separate pathway from cellular proliferation, i.e. by blocking

apoptosis. Our results indicate that also the mitochondria shaping protein Opa1 is found to be upregulated in DLBCL patients and aggravates the phenotype of a mouse model of lymphoma, thereby placing mitochondrial ultrastructure in the arena of cancer formation and progression.

Our work unravels a role for Opa1 in cancer features and in the development and progression of the disease, identifying Opa1 as a novel oncogene candidate. Targeting Opa1 - dependent cristae remodeling pathway emerges as an appealing strategy to increase apoptosis of cancer cells. Development of new therapies which would specifically target Opa1 function, with the aim of increasing the recruitment of the mitochondrial apoptotic pathway, represent a potential strategy to combat cancer.

EXPERIMENTAL PROCEDURES

Cell culture

DLBCL cell lines were cultured in RPMI 1640 medium (GIBCO Life Technologies), supplemented with 10 % FCS, 2mM L-glutamine, 100 U/ml penicillin and 100 µg/ml streptomycin. Cells were maintained in culture for maximum 20 passages.

Proliferation assay

Cells were cultured in RPMI 1640 complete media (GIBCO Life Technologies) and RPMI 1640 media without glucose (GIBCO life Technologies) supplemented with 0.9 mg/ml galactose, together with 10 % FCS, 2mM L-glutamine, 100 U/ml penicillin and 100 µg/ml streptomycin. 50000 cells / ml have been washed with PBS 1x, and resuspended in the indicated media in a total volume of 15 ml. Cell growth was monitored for 5 days and was determined by Trypan Blue exclusion with the use of Burker cell counting chamber.

B lymphocyte isolation

Mouse B lymphocytes were isolated from 3 months old BL6 wild type mouse spleens. Spleen cell suspension was obtained by smashing the spleens through a 70 µm cell strainer (BD Falcon) and the obtained cell suspension was further treated following the EasySep Stem Cell Technologies protocol for isolation of mouse B lymphocytes based on negative selection.

Human B lymphocytes were isolated from buffy coats of heathy patients, received from the University Hospital Padova. Human B lymphocytes were isolated following the RosetteSep Stem Cell Technologies protocol based on negative selection.

The purity of isolation was checked by FACS where the obtained B lymphocyte cell suspension was stained with the CD19 antibody.

Immunoblotting

Cell pellets were lysed in RIPA lysis buffer 1x (20 mM Tris-HCl (pH 7.5), 150 mM NaCl, 1 mM Na_2EDTA, 1 mM EGTA, 1% NP-40, 1% sodium deoxycholate, 2.5 mM sodium pyrophosphate, 1 mM β-glycerophosphate, 1 mM Na_3VO_4, 1 µg/ml leupeptin) supplemented with PIC. Equal amounts of extracted protein were separated by SDS-PAGE (NuPage, Invitrogen), transferred onto polyvinylidene fluoride membranes (Millipore) and immunoblotted with indicated antibodies. Antibodies used include: anti – Opa1 (BD Transduction, 1:1000), anti – Mfn2 (Abnova, 1:1000), anti – Mfn1 (Milipore, 1:2000), anti – Drp1 (BD Transduction, 1:2000), anti – Fis1 (Alexis, 1:1000), anti – Grp75 (Santa Cruz, 1:4000), anti – Actin (Chemicon, 1:10 000). Isotype-matched, horseradish peroxidase-conjugated secondary antibodies (Sigma) were used, followed by detection by chemiluminescence (Pierce). Densitometry quantification of Western blot bands was performed using the Gel Pro Analyzer software.

Immunofluorescent staining and confocal microscopy

60000 cells were seeded on top of a poly – L– lysine pre-coated microscope diagnostic slide (Menzel Thermoscientific). Cells were fixed with cold 4 % FA for 20 minutes on RT, and immunofluorescent blotting was achieved using anti – Tom20 antibody (Santa Cruz, 1:100), followed by secondary fluorescent blotting with FITC (1:200).

For confocal imaging, microscope slides were placed on the stage of Zeiss LSM 700 confocal microscope using a Plan Apochromat 63x 1.4 Oil DIC objective. Digital images were processed

using the National Institute of Health Image J software, and further analysis of mitochondrial morphology was performed with the use of the "Squassh" plugin for the ImageJ software.

Transmission electron microscopy

Cells were fixed for 20 minutes at room temperature using glutaraldehyde at final concentration of 2.5 % (v/v) in PBS 1x. Embedding and staining was performed as described in (Scorrano et al., 2002). Thin sections were imaged on a Tecnai-20 electron microscope (Philips-FEI). Cristae width was measured with the use of the National Institute of Health Image J software.

Generation of Opa1$^{flx/flx}$, Opa1^{tg}, Eμ-myc::Opa1$^{flx/+}$::Opa1^{tg} mice

The experimental approach used for the generation of Opa1$^{flx/flx}$ and Opa1^{tg} mice was previously described in detail in (Cogliati et al., 2013). The Eμ-myc (B6.Cg-Tg(IghMyc)22Bri/J) mouse was purchased from Jackson laboratory. The TgN(IghMyc)22Bri transgenic strain was made in the laboratory of Dr Ralph Brinster, University of Pennsylvania in collaboration with Dr. Alan Harris, currently of the Walter and Eliza Hall Institute of Medical Research, Melbourne, Australia. The transgene construct consists of the *Myc* oncogene (c-*myc*) in association with the Emu immunoglobulin heavy chain enhancer and *Myc* promoter. Expression of the mouse *Myc* transgene is restricted to the B cell lineage. We generated a stable colony of genetically modified animals carrying a floxed Opa1 allele (Opa1$^{flx/flx}$) and the targeted Opa1 overexpression on the X chromosome (Opa1^{tg}). The generated females Opa1$^{flx/flx}$::Opa1^{tg} (carrying the transgene in homozygosity on the X chromosome) were then crossed with Eμ-myc males, giving rise to a triple mutant Eμ-myc::Opa1$^{flx/+}$::Opa1^{tg} mouse model used in our study. All experimental procedures performed on mice have been authorized by the CEASA of the University of Padova.

Genotyping

DNA from mouse tails was extracted following the DNeasy blood & tissue kit protocol (Qiagen). The mice with the correct genotype were selected on the basis of PCR genotyping on tail DNA with the use of the following primers: primer for $Opa1^{flx}$ detection (F: 5'- CAG TGT TGA TGA CAG CTC AG - 3', R: 5' - CAT CAC ACA CTA GCT TAC ATT TGC - 3') primers for $Opa1^{tg}$ detection (F: 5'- GCA ATG ACG TGG TCC TGT TTTG - 3', R: 5'- GAT AGG TCA GGT AAG CAA GCA AC - 3'), primers for $Opa1^{wt}$ detection (F: 5' - GAG GGA GAA AAA TGC GGA GTG - 3', R: 5'- CTC CGG AAA GCA GTG AGG TAA G -3'), primers for Eμ-myc detection (F: 5' - TTA GAC GTC AGG TGG CAC TT - 3', R: 5' - TGA GCA AAA ACA GGA AGG CA - 3').

Gross pathology and histology

Selected mice were sent for necropsy analysis to the Istituto Zooprofilattico Sperimentale delle Venezie pathology department in Padova, Italy. Hematoxylin and eosin staining was performed on paraffin embedded sections by the pathology department of the aforementioned institute. The h&e stained tissue section microscopic slides were placed on the stage of the Trinocular Brightfield / Fluorescence w/ 4 Position FL Cube Turret Olympus BX60 Microscope and the images were acquired using the Olympus UPlanApo 4x Infinity Corrected Objective.

Immunophenotyping

Mouse organs have were harvested, washed in PBS 1x enriched with 2% FCS, and smashed through a 100 μm cell strainer (BD Falcon). The obtained cell suspension was treated with an RBC lysis solution, to lyse the erythrocytes. Single – cell suspensions from thymus, spleen, inguinal lymph nodes, liver, lung, kidney and bone marrow were surface stained with monoclonal

antibodies, in 200 µl of PBS enriched with 2% FCS, together with the antibodies diluted in 1:200, and incubated for at least 30 minutes on ice in the dark. The following monoclonal antibodies were used: Gk1.5 (anti-CD4) Biolegend, 53-6.7 (anti-CD8) eBioscience, RB6-8C5 (anti-Gr1) Biolegend, M1/70 (anti-Mac1) eBioscience, 11/6c (anti-IgD) eBioscience, IL/41 (anti-IgM) eBioscience, Ra3-6B2 (anti-B220) eBioscience, MB19-1 (anti-CD19) eBioscience, 2B8 (anti-cKit) eBioscience, 3C7 (anti-CD25) Biolegend. Flow cytometric analysis was performed using a FACSCalibur cell analyzer (BD Biosciences) and 100 000 – 200 000 events were acquired for the analysis.

Acknowledgements

L.S. is a Senior Telethon Scientist at the Dulbecco-Telethon Institute. Research in his lab is supported by Telethon Italy (GGP12162 and GGP14187A), by the AIRC (the Italian Association for Research on Cancer), by the European Research Council (FP7-282280, FP7 CIG PCIG13-GA-2013-618697), and by the Italian Ministry of Research (FIRB RBAP11Z3YA_005).

FIGURE LEGENDS

Figure 1. Levels of Opa1 differ between BCR versus OxPhos DLBCL cell subsets

(A) Equal amounts of protein (10 µg) from the indicated DLBCL cell lines were separated by SDS – PAGE and immunoblotted with the indicated antibodies.

(B) B lymphocytes from adult mouse spleens (Mouse) and B lymphocytes from buffy coats of heathy adults (Human) were isolated as described. Equal amount of protein (10 µg) extracted from B lymphocyte cell pellets, and from DLBCL cell lines were separate by SDS – PAGE, and immunoblotted with the indicated antibodies.

(C) Densitometry quantification of the ratio between long and short Opa1 forms. Data represent average ±SEM, n = 4 for each cell line.

Figure 2. Mitochondrial morphology in DLBCL cell lines

(A) Representative 2D Z - project reconstructions of confocal Z – stacks. Cells were fixed and immunostained with the mitochondrial marker Tom20, followed by fluorescent labeling with FITC. Scale bar 5 µm.

(B) Morphometric analysis of the mitochondrial morphology using Squassh plugin for the ImageJ software. Data represent mean of ±SEM of 3 independent experiments (n=20 cells per cell type, per each experiment), histogram bars represent the average mitochondrial length, measured per cell type.

Figure 3. DLBCL cell line cristae ultrastructure in glucose vs. galactose: OxPhos cristae are more organized compared to their BCR DLBCL counterparts

(A) Representative electron micrographs of BCR DLBCL cell lines in glucose vs galactose media. **(B)** Representative electron micrographs of OxPhos DLBCL cell lines in glucose vs galactose media. DLBCL cell lines were previously cultivated for 48h hours in complete RPMI 1640 media containing glucose, or complete RPMI 1640 media containing galactose 0.9 mg/ml, fixed and processed for electron microscopy. Scale bar 200 nm.

(C) Morphometric analysis of mitochondrial cristae electron micrographs. Quantification of cristae width corresponding to DLBCL cell lines previously cultivated in glucose enriched complete RPMI 1640 media for 48h, or galactose enriched complete RPMI 1640 media for 48h, using ImageJ software. Data represent mean ±SEM of 3 independent experiments (n=180 mitochondria per cell type, per each experiment), histogram bars represent the average cristae width, measured per cell type.

(D) DLBCL cell lines were previously cultivated in complete RPMI 1640 media enriched with glucose (GLU) or galactose (GAL), for 48h. Following this treatment equal amounts of proteins (10 µg) from the indicated cell lines were separated by SDS – PAGE and immunoblotted with Opa1 **a)** Representative Western blot for the BCR DLBCL cell subset **b)** Representative Western blot for the OxPhos DLBCL cell subset.

(E) Densitometry quantification of the ratio between long and short Opa1 forms. Data represent average ±SEM, n = 4 for each cell line **a)** Densitometric analysis of the BCR DLBCL cell subset **b)** Densitometric analysis of the OxPhos DLBCL subset.

Figure 4. Mitochondrial dependent cell growth is facilitated in cell lines expressing higher levels of Opa1

(A) Growth curves of representative BCR DLBCL cell lines, grown in RPMI 1640 complete media enriched with glucose (GLU) or galactose (GAL). Data represent mean ±SEM of 6 independent experiments.

(B) Growth curves of representative OxPhos DLBCL cell lines, grown in RPMI 1640 complete media enriched with glucose (GLU) or galactose (GAL). Data represent mean ±SEM of 6 independent experiments.

Figure 5. Generation of the Eμ-myc::Opa1^{tg} mouse

(A) Schematic representation of the mouse crossing strategy.

A stable colony of genetically modified animals was generated by crossing in the parental generation Opa1 $^{flx/flx}$ males with Opa1^{tg} (double transgenic) females. In the case of Opa1$^{flx/flx}$ animals, the targeting vector contained loxP elements between exons 1-2 and 3-4, and a neomycin resistance cassette was introduced downstream of the first LoxP site. The targeting vector was then introduced into ES cells by electroporation, where G-418-resistence ES cells were tested for homologous recombination. Three positive clones C57BL6ES were microinjected into C57BL6 blastocytes and implanted into host mice in order to obtain chimeric mice. The crossbreeding of chimera with wildtype mice resulted in heterozygous genetically engineered mice, where the further crossing of the heterozygotes gave rise to homozygous Opa1$^{flx/flx}$ mice.

Opa1^{tg} mice were generated by a gene targeting approach where a transgene carrying mouse variant 1 of Opa1 was put in association with the human beta-actin promoter, and the transgene has been targeted by homologous recombination into the HPRT region of the murine X chromosome, resulting in one copy of the transgene.

Male mice of the Opa1$^{flx/flx}$::Opa1^{tg} stable colony were further crossed with Eμ-myc female mice. The original Eμ-myc construct contains 2.3 kb of immunoglobulin DNA (open bar), spanning the H-chain enhancer (diamond), inserted 361 base pairs (bp) 5' to c-myc exon. The schematic illustration of this Eμ-myc construct is the representation of the linear fragment that was isolated from plasmid constructs before injection. The solid bar represents c-myc sequences with exons raised, untranslated regions stripped, ϕx174 marker DNA as a triangle, and vector sequence as a thin line.

The result of this cross gave rise to Eμ-myc::Opa1$^{flx/+}$::Opa1^{tg} male and female test mice (further referred to as the Eμ-myc::Opa1^{tg} mouse). In the second generation as the result of the cross between Opa1$^{flx/flx::tg}$ males and Eμ-myc::Opa1$^{flx/+}$::Opa1^{tg} females, we got Eμ-myc::Opa1$^{flx/flx}$::Opa1^{tg} mice (this cross not shown).

(B) PCR analysis of genomic DNA extracted from mouse tails. Depiction of representative bands corresponding to: Opa1 conditional knockout heterozygous (flx/+) or homozygous (flx/flx), or wild type; Opa1 transgenic homozygous (tg/tg), transgenic heterozygous (tg/+), or wild type; Wild type non-existing (-/-), wild type heterozygous (-/+), wild type homozygous (+/+); Eμ-myc heterozygous or wild type.

(C) Equal amounts of protein (20 μg) from tissues of the indicated genotypes were separated by SDS-PAGE and immunoblotted with the indicated antibodies.

Figure 6. Eμ-myc::Opa1^{tg} mice die faster and develop a more severe clinical picture of malignant disseminated lymphoma compared to their Eμ-myc littermates and healthy controls

(A) Kaplan - Meier survival curve of Eμ-myc and Eμ-myc::Opa1^{tg} mice. Total mice (n = 95 total, n= 62 Eμ-myc::Opa1^{tg} n = 33 Eμ-myc). Male mice (n = 45, n = 32 Eμ-myc::Opa1^{tg} , n = 13 Eμ-myc). Female mice (n = 50, n = 30 Eμ-myc::Opa1^{tg}, n = Eμ-myc).

(B) Gross anatomy of 3 months old male mice: Images of lymphoid organs – spleen, thymus and lymph nodes, corresponding to indicated genotypes. Scale bar in millimeters.

Table 1. Clinical phenotype of representative mice belonging to age groups of 2 months, 3 months, 4 months, 5 months and 6 months

Table legend: Neoplastic lymphoid infiltration: + rare, ++ mild, +++ moderate, ++++ severe. N = 3 mice per age group.

Figure 7. Histopathological representation of the clinical picture corresponding to disseminated lymphoma

Bright field microscopy images of hematoxylin and eosin stained histopathological tissue sections, of representative organs for the indicated mouse genotypes. **(A)** spleen **(B)** thymus **(C)** liver **(D)** kidney **(E)** lung

Figure 8. Immunophenotypic analysis of the B cell differentiation stages in Wild Type, Opa1$^{flx/flx::tg}$, Eμ-myc and Eμ-myc::Opa1^{tg} mice

(A) Single cell suspensions from bone marrow of 2 month (2M), 3 month (3M) and 6 month (6M) old mice were stained with fluorochrome labeled antibodies for cell surface markers identifying pro B cells (CD19+cKit+) in the first graphs in line, and pre B cells (CD25+) in the second graphs in line; entire B cell population (B220+) in the third graphs in line; and subpopulations within the

entire (previously gated) B cell population in the fourth graphs in line: IgM+IgD- immature B cells, IgM^{low}IgD+ recirculating B cells. Data represent averages of n=2 animals per genotype, DN – double negative.

(B) Single cell suspensions from inguinal lymph nodes of 2 month (2M), 3 month (3M) and 6 month (6M) old mice were stained with fluorochrome labeled antibodies for cell surface markers identifying the entire B cell population (B220+) in the first graph in line, and subpopulations within the entire (previously gated) B cell population in the second graphs in line: IgM+IgD- immature B cells, IgM^{low}IgD+ recirculating B cells. Data represent averages of n=2 animals per genotype, DN – double negative.

(C) Single cell suspensions from the spleen of 2 month (2M), 3 month (3M) and 6 month (6M) old mice were stained with fluorochrome labeled antibodies for cell surface markers identifying the entire B cell population (B220+) in the first graphs in line, and subpopulations within the entire (previously gated) B cell population in the second graphs in line: IgM+IgD- transitional type 1 (T1), IgM^{low}IgD+ follicular B cells (FO), and IgM+IgD+ transitional type 2 (T2). Data represent averages of n=2 animals per genotype, DN – double negative.

Supplemental information

The mitochondria-shaping protein Opa1 participates in lymphoma progression

Dijana Samardzic, Nika Danial, and Luca Scorrano

Inventory of Supplemental Information

EXPERIMENTAL PROCEDURES

Calcium chelation

Selected DLBCL cell lines were cultivated in complete RPMI 1640 medium, and treated with the calcium chelator BAPTA – AM (Calbiochem) at the final concentration 40 μM, at different incubation times ranging from 30, 60 and 90 minutes. Cells were washed with PBS 1x, pelleted down, lysed and prepared for SDS-PAGE / Western blot.

Inhibition of B cell signaling kinases

Selected DBCL cell lines were cultivated in complete RPMI 1640 medium, and treated with different kinase inhibitors, at varying concentrations. Inhibitors used were: Fostamatinib Disodium (Selleck Chemicals) at final concentrations of 2 μM, 4 μM and 6 μM, for a 24h and 48h treatment; Ibrutinib (Selleck Chemicals) at final concentration of 5 μM for 30 min, 2h and 24h incubation; Cal-101 (Selleck Chemicals) at final concentration of 5 μM for 30 min, 2h and 24h incubation. Cells were washed with PBS, pelleted down, lysed and prepared for SDS-PAGE / Western blot.

Cell death analysis

Selected DLBCL cell lines were cultivated in complete RPMI 1640 medium (two million cells / ml, in a total media volume of 1 ml), and treated with staurosporine at the final concentration 2 μM. At given time points (0h, 8h, 24h and 32h) cells were collected and incubated with Annexin-V-FITC and propidium iodide (PI) (Bender MedSystem) according to the manufacturer's protocol.

Cell viability was measured by flow cytometry (FACSCanto) as the percentage of Annexin-V-negative, PI-negative cells.

Selected DLBCL cell lines were cultivated in either complete RPMI 1640 medium, or in RPMI 1640 medium (deprived from glucose) enriched with galactose instead, at the concentration of 0.9 mg/ml. 50 000 cells / ml were cultivated in a total media volume of 4 ml. At given time points (Day 0 and Day 4) cells were collected and incubated with Annexin-V-FITC and propidium iodide (PI) (Bender MedSystem) according to the manufacturer's protocol. Cell viability was measured by flow cytometry (FACSCanto) as the percentage of Annexin-V-negative, PI-negative cells.

Immunoblotting

Cell pellets were lysed in RIPA lysis buffer 1x (20 mM Tris-HCl (pH 7.5), 150 mM NaCl, 1 mM Na_2EDTA, 1 mM EGTA, 1% NP-40, 1% sodium deoxycholate, 2.5 mM sodium pyrophosphate, 1 mM β-glycerophosphate, 1 mM Na_3VO_4, 1 µg/ml leupeptin) supplemented with PIC. Equal amounts of extracted protein were separated by SDS-PAGE (NuPage, Invitrogen), transferred onto polyvinylidene fluoride membranes (Millipore) and immunoblotted with indicated antibodies. Antibodies used include: anti – Bcl2 (Santa Cruz, 1:1000), anti – Bak (Milipore, 1:1000), anti – Bax (Upstate, 1:1000), anti – Actin (Chemicon, 1:10 000). Isotype-matched, horseradish peroxidase-conjugated secondary antibodies (Sigma) were used, followed by detection by chemiluminescence (Pierce).

SUPPLEMENTARY FIGURE LEGENDS

Supplementary Figure S1. Chelation of intercellular calcium and blockage of BCR signaling kinases by chemical inhibitors didn't affect the levels of Opa1 forms

(A) Equal amounts of protein (10 μg) from the indicated DLBCL cell lines, that were previously incubated with (B) / without (0) 40 μM BAPTA - AM for the indicated time points, were separated by SDS – PAGE and immunoblotted with the indicated antibodies.

(B) Equal amounts of protein (10 μg) from the indicated DLBCL cell lines, that were previously incubated with / without **a)** fostamatinib inhibitor at increasing μM concentrations as indicated, for the indicated incubation times **b)** ibrutinib inhibitor at indicated μM concentrations for the indicated incubation times **c)** Cal 101 inhibitor at indicated μM concentrations for the indicated incubation times were separated by SDS – PAGE and immunoblotted with the indicated antibodies.

Supplementary Figure S2. Resistance to apoptosis is reduced in the OxPhos DLBCL cell subset due to higher levels of pro-apoptotic proteins in these cell lines

(A) Apoptosis was triggered in D6 (BCR) and K422 (OxPhos) cell lines by 2μM staurosporine treatment, and viability is presented on the graph as a percentage of double negative cells population (Annexin-V-negative, PI-negative) obtained from the dot plot presented as a ratio between staurosporine treated and untreated cells. Data represents mean ±SEM of n=3 independent experiments.

(B) Equal amounts of protein (65 μg) from the indicated DLBCL cell lines were separated by SDS – PAGE and immunoblotted with the indicated antibodies.

Supplementary figure S3. K422 (OxPhos) cell line is more resistant to growth in galactose enriched media, displaying a lower death rate compared to D6 (BCR)

(A) Apoptosis was measured in the D6 (BCR) cell line cultivated in glucose or galactose enriched media, at indicated time points. Viability is presented as a percentage of Annexin-V-negative, PI-negative cells. Data represent mean ±SEM of n=3 independent experiments.

(B) Apoptosis was measured in the K422 (OxPhos) cell line cultivated in glucose or galactose enriched media, at indicated time points. Viability is presented as a percentage of Annexin-V-negative, PI-negative cells. Data represent mean ±SEM of n=3 independent experiments.

Supplementary figure S4. Enlargement of lymphoid organs and clinical picture of 6 months old mice, are more severe in the Eμ-myc::Opa1^{tg} compared to Eμ-myc mouse

(A) Gross anatomy of representative lymphoid organs in Eμ-myc and Eμ-myc::Opa1^{tg} mice.

(B) Bright field microscopy images of hematoxylin and eosin stained histopathological tissue sections of mouse organs from the indicated genotypes.

Supplementary figure S5. T cells are not affected in the periphery and there is a shift towards neutrophils in the Eμ-myc::Opa1^{tg} mice

(A) Single cell suspensions from thymus, spleen, lymph node and bone marrow of 2 months old (2M), 3 months old (3M) and 6 months old (6M) mice, were stained with fluorochrome labeled antibodies for cell surface markers specific for T cells identifying CD4+, CD8+ single positive or

CD4+CD8+ double positive cells deriving from the indicated organs of mice from the indicated genotypes. Data represent averages of n=2 animals per genotype, DN – double negative.

(B) Single cell suspension from bone marrow, lymph node, liver, lung and kidney of 2 months old (2M), 3 months old (3M) and 6 months old (6M) mice**,** were stained with fluorochrome labeled antibodies for cell surface markers specific for monocytes /granulocytes, identifying Gr1+, Mac1+, or double positive Gr1+Mac1+ cells deriving from the indicated organs of mice from the indicated genotypes. Data represent averages of n=2 animals per genotype, DN – double negative.

Reference List

Adams,J.M., Harris,A.W., Pinkert,C.A., Corcoran,L.M., Alexander,W.S., Cory,S., Palmiter,R.D., and Brinster,R.L. (1985). The c-myc oncogene driven by immunoglobulin enhancers induces lymphoid malignancy in transgenic mice. Nature *318*, 533-538.

Alizadeh,A.A., Eisen,M.B., Davis,R.E., Ma,C., Lossos,I.S., Rosenwald,A., Boldrick,J.C., Sabet,H., Tran,T., Yu,X., Powell,J.I., Yang,L., Marti,G.E., Moore,T., Hudson,J., Jr., Lu,L., Lewis,D.B., Tibshirani,R., Sherlock,G., Chan,W.C., Greiner,T.C., Weisenburger,D.D., Armitage,J.O., Warnke,R., Levy,R., Wilson,W., Grever,M.R., Byrd,J.C., Botstein,D., Brown,P.O., and Staudt,L.M. (2000). Distinct types of diffuse large B-cell lymphoma identified by gene expression profiling. Nature *403*, 503-511.

Caro,P., Kishan,A.U., Norberg,E., Stanley,I.A., Chapuy,B., Ficarro,S.B., Polak,K., Tondera,D., Gounarides,J., Yin,H., Zhou,F., Green,M.R., Chen,L., Monti,S., Marto,J.A., Shipp,M.A., and Danial,N.N. (2012). Metabolic signatures uncover distinct targets in molecular subsets of diffuse large B cell lymphoma. Cancer Cell *22*, 547-560.

Cereghetti,G.M., Stangherlin,A., Martins de,B.O., Chang,C.R., Blackstone,C., Bernardi,P., and Scorrano,L. (2008). Dephosphorylation by calcineurin regulates translocation of Drp1 to mitochondria. Proc. Natl. Acad. Sci. U. S. A *105*, 15803-15808.

Chen,H., Detmer,S.A., Ewald,A.J., Griffin,E.E., Fraser,S.E., and Chan,D.C. (2003). Mitofusins Mfn1 and Mfn2 coordinately regulate mitochondrial fusion and are essential for embryonic development. J. Cell Biol. *160*, 189-200.

Chen,L., Monti,S., Juszczynski,P., Daley,J., Chen,W., Witzig,T.E., Habermann,T.M., Kutok,J.L., and Shipp,M.A. (2008). SYK-dependent tonic B-cell receptor signaling is a rational treatment target in diffuse large B-cell lymphoma. Blood *111*, 2230-2237.

Cipolat,S., Martins de Brito O., Dal Zilio B., and Scorrano,L. (2004). OPA1 requires mitofusin 1 to promote mitochondrial fusion. Proc. Natl. Acad. Sci. U. S. A *101*, 15927-15932.

Cipolat,S., Rudka,T., Hartmann,D., Costa,V., Serneels,L., Craessaerts,K., Metzger,K., Frezza,C., Annaert,W., D'Adamio,L., Derks,C., Dejaegere,T., Pellegrini,L., D'Hooge,R., Scorrano,L., and De Strooper,B. (2006). Mitochondrial Rhomboid PARL Regulates Cytochrome c Release during Apoptosis via OPA1-Dependent Cristae Remodeling. Cell *126*, 163-175.

Civiletto,G., Varanita,T., Cerutti,R., Gorletta,T., Barbaro,S., Marchet,S., Lamperti,C., Viscomi,C., Scorrano,L., and Zeviani,M. (2015). Opa1 overexpression ameliorates the clinical phenotype of two mitochondrial disease mouse models. Cell Metabolism.

Cogliati,S., Frezza,C., Soriano,M.E., Varanita,T., Quintana-Cabrera,R., Corrado,M., Cipolat,S., Costa,V., Casarin,A., Gomes,L.C., Perales-Clemente,E., Salviati,L., Fernandez-Silva,P., Enriquez,J.A., and Scorrano,L. (2013). Mitochondrial cristae shape determines respiratory chain supercomplexes assembly and respiratory efficiency. Cell *155*, 160-171.

Cory,S., Vaux,D.L., Strasser,A., Harris,A.W., and Adams,J.M. (1999). Insights from Bcl-2 and Myc: malignancy involves abrogation of apoptosis as well as sustained proliferation. Cancer Res. *59*, 1685s-1692s.

Duvezin-Caubet,S., Koppen,M., Wagener,J., Zick,M., Israel,L., Bernacchia,A., Jagasia,R., Rugarli,E.I., Imhof,A., Neupert,W., Langer,T., and Reichert,A.S. (2007). OPA1 processing reconstituted in yeast depends on the subunit composition of the m-AAA protease in mitochondria. Mol. Biol. Cell *18*, 3582-3590.

Ehses,S., Raschke,I., Mancuso,G., Bernacchia,A., Geimer,S., Tondera,D., Martinou,J.C., Westermann,B., Rugarli,E.I., and Langer,T. (2009). Regulation of OPA1 processing and mitochondrial fusion by m-AAA protease isoenzymes and OMA1. J Cell Biol *187*, 1023-1036.

Fang,H.Y., Chen,C.Y., Chiou,S.H., Wang,Y.T., Lin,T.Y., Chang,H.W., Chiang,I.P., Lan,K.J., and Chow,K.C. (2012). Overexpression of optic atrophy 1 protein increases cisplatin resistance via inactivation of caspase-dependent apoptosis in lung adenocarcinoma cells. Hum. Pathol. *43*, 105-114.

Frank,S., Gaume,B., Bergmann-Leitner,E.S., Leitner,W.W., Robert,E.G., Catez,F., Smith,C.L., and Youle,R.J. (2001). The role of dynamin-related protein 1, a mediator of mitochondrial fission, in apoptosis. Dev. Cell *1*, 515-525.

Frezza,C., Cipolat,S., Martins,d.B., Micaroni,M., Beznoussenko,G.V., Rudka,T., Bartoli,D., Polishuck,R.S., Danial,N.N., De Strooper,B., and Scorrano,L. (2006). OPA1 Controls Apoptotic Cristae Remodeling Independently from Mitochondrial Fusion. Cell *126*, 177-189.

Goldstein,R.L., Yang,S.N., Taldone,T., Chang,B., Gerecitano,J., Elenitoba-Johnson,K., Shaknovich,R., Tam,W., Leonard,J.P., Chiosis,G., Cerchietti,L., and Melnick,A. (2015). Pharmacoproteomics identifies combinatorial therapy targets for diffuse large B cell lymphoma. J. Clin. Invest *2015*.

Griparic,L. and van der Bliek,A.M. (2001). The many shapes of mitochondrial membranes. Traffic *2*, 235-244.

Hackenbrock,C.R. (1966). Ultrastructural bases for metabolically linked mechanical activity in mitochondria. I. Reversible ultrastructural changes with change in metabolic steady state in isolated liver mitochondria. J. Cell Biol. *30*, 269-297.

Harris,A.W., Pinkert,C.A., Crawford,M., Langdon,W.Y., Brinster,R.L., and Adams,J.M. (1988). The E mu-myc transgenic mouse. A model for high-incidence spontaneous lymphoma and leukemia of early B cells. J. Exp. Med. *167*, 353-371.

Lannutti,B.J., Meadows,S.A., Herman,S.E., Kashishian,A., Steiner,B., Johnson,A.J., Byrd,J.C., Tyner,J.W., Loriaux,M.M., Deininger,M., Druker,B.J., Puri,K.D., Ulrich,R.G., and Giese,N.A. (2011). CAL-101, a p110delta selective phosphatidylinositol-3-kinase inhibitor for the treatment of B-cell malignancies, inhibits PI3K signaling and cellular viability. Blood *117*, 591-594.

Li,P., Nijhawan,D., Budihardjo,I., Srinivasula,S.M., Ahmad,M., Alnemri,E.S., and Wang,X. (1997). Cytochrome c and dATP-dependent formation of Apaf-1/caspase-9 complex initiates an apoptotic protease cascade. Cell *91*, 479-489.

Lohr,J.G., Stojanov,P., Lawrence,M.S., Auclair,D., Chapuy,B., Sougnez,C., Cruz-Gordillo,P., Knoechel,B., Asmann,Y.W., Slager,S.L., Novak,A.J., Dogan,A., Ansell,S.M., Link,B.K., Zou,L., Gould,J., Saksena,G., Stransky,N., Rangel-Escareno,C., Fernandez-Lopez,J.C., Hidalgo-Miranda,A., Melendez-Zajgla,J., Hernandez-Lemus,E., Schwarz,C., Imaz-Rosshandler,I., Ojesina,A.I., Jung,J., Pedamallu,C.S., Lander,E.S., Habermann,T.M., Cerhan,J.R., Shipp,M.A., Getz,G., and Golub,T.R. (2012). Discovery and prioritization of somatic mutations in diffuse large B-cell lymphoma (DLBCL) by whole-exome sequencing. Proc. Natl. Acad. Sci. U. S. A *109*, 3879-3884.

Maronpot,R.R., Palmiter,R.D., Brinster,R.L., and Sandgren,E.P. (1991). Pulmonary carcinogenesis in transgenic mice. Exp. Lung Res. *17*, 305-320.

McBride,H. and Soubannier,V. (2010). Mitochondrial function: OMA1 and OPA1, the grandmasters of mitochondrial health. Curr. Biol. *20*, R274-R276.

Monti,S., Savage,K.J., Kutok,J.L., Feuerhake,F., Kurtin,P., Mihm,M., Wu,B., Pasqualucci,L., Neuberg,D., Aguiar,R.C., Dal,C.P., Ladd,C., Pinkus,G.S., Salles,G., Harris,N.L., Dalla-Favera,R., Habermann,T.M., Aster,J.C., Golub,T.R., and Shipp,M.A. (2005). Molecular profiling of diffuse large B-cell lymphoma identifies robust subtypes including one characterized by host inflammatory response. Blood *105*, 1851-1861.

Olichon,A., Elachouri,G., Baricault,L., Delettre,C., Belenguer,P., and Lenaers,G. (2007). OPA1 alternate splicing uncouples an evolutionary conserved function in mitochondrial fusion from a vertebrate restricted function in apoptosis. Cell Death. Differ. *14*, 682-692.

Palmer,C.S., Osellame,L.D., Laine,D., Koutsopoulos,O.S., Frazier,A.E., and Ryan,M.T. (2011). MiD49 and MiD51, new components of the mitochondrial fission machinery. EMBO Rep. *12*, 565-573.

Patten,D.A., Wong,J., Khacho,M., Soubannier,V., Mailloux,R.J., Pilon-Larose,K., MacLaurin,J.G., Park,D.S., McBride,H.M., Trinkle-Mulcahy,L., Harper,M.E., Germain,M., and Slack,R.S. (2014). OPA1-dependent cristae modulation is essential for cellular adaptation to metabolic demand. EMBO J *33*, 2676-2691.

Rizk,A., Paul,G., Incardona,P., Bugarski,M., Mansouri,M., Niemann,A., Ziegler,U., Berger,P., and Sbalzarini,I.F. (2014). Segmentation and quantification of subcellular structures in fluorescence microscopy images using Squassh. Nat. Protoc. *9*, 586-596.

Sandgren,E.P., Quaife,C.J., Pinkert,C.A., Palmiter,R.D., and Brinster,R.L. (1989). Oncogene-induced liver neoplasia in transgenic mice. Oncogene *4*, 715-724.

Santel,A. and Fuller,M.T. (2001). Control of mitochondrial morphology by a human mitofusin. J. Cell Sci. *114*, 867-874.

Scorrano,L., Ashiya,M., Buttle,K., Weiler,S., Oakes,S.A., Mannella,C.A., and Korsmeyer,S.J. (2002). A distinct pathway remodels mitochondrial cristae and mobilizes cytochrome c during apoptosis. Dev. Cell *2*, 55-67.

Strasser,A., Elefanty,A.G., Harris,A.W., and Cory,S. (1996). Progenitor tumours from Emu-bcl-2-myc transgenic mice have lymphomyeloid differentiation potential and reveal developmental differences in cell survival. EMBO J. *15*, 3823-3834.

Strasser,A., Harris,A.W., Bath,M.L., and Cory,S. (1990). Novel primitive lymphoid tumours induced in transgenic mice by cooperation between myc and bcl-2. Nature *348*, 331-333.

Sugawara,H., Kurosaki,M., Takata,M., and Kurosaki,T. (1997). Genetic evidence for involvement of type 1, type 2 and type 3 inositol 1,4,5-trisphosphate receptors in signal transduction through the B-cell antigen receptor. EMBO J. *16*, 3078-3088.

Thompson,C.B. (1995). Apoptosis in the pathogenesis and treatment of disease. Science *267*, 1456-1462.

Varanita,T., Soriano,M.E., Romanello,V., Zaglia,T., Quintana-Cabrera,R., Semenzato,M., Menabò,R., Costa,V., Civiletto,G., Pesce,P., Viscomi,C., Zeviani,M., Di Lisa,F., Mongillo,M., Sandri,M., and Scorrano,L. (2015). The Opa1-Dependent Mitochondrial Cristae Remodeling Pathway Controls Atrophic, Apoptotic, and Ischemic Tissue Damage. Cell Metabolism *21*.

Vaux,D.L., Cory,S., and Adams,J.M. (1988). Bcl-2 gene promotes haemopoietic cell survival and cooperates with c-myc to immortalize pre-B cells. Nature *335*, 440-442.

Wasilewski,M. and Scorrano,L. (2009). The changing shape of mitochondrial apoptosis. Trends Endocrinol. Metab *20*, 287-294.

Yang,M., Soga,T., and Pollard,P.J. (2013). Oncometabolites: linking altered metabolism with cancer. J. Clin. Invest *123*, 3652-3658.

Zhao,X., Tian,C., Puszyk,W.M., Ogunwobi,O.O., Cao,M., Wang,T., Cabrera,R., Nelson,D.R., and Liu,C. (2013). OPA1 downregulation is involved in sorafenib-induced apoptosis in hepatocellular carcinoma. Lab Invest *93*, 8-19.

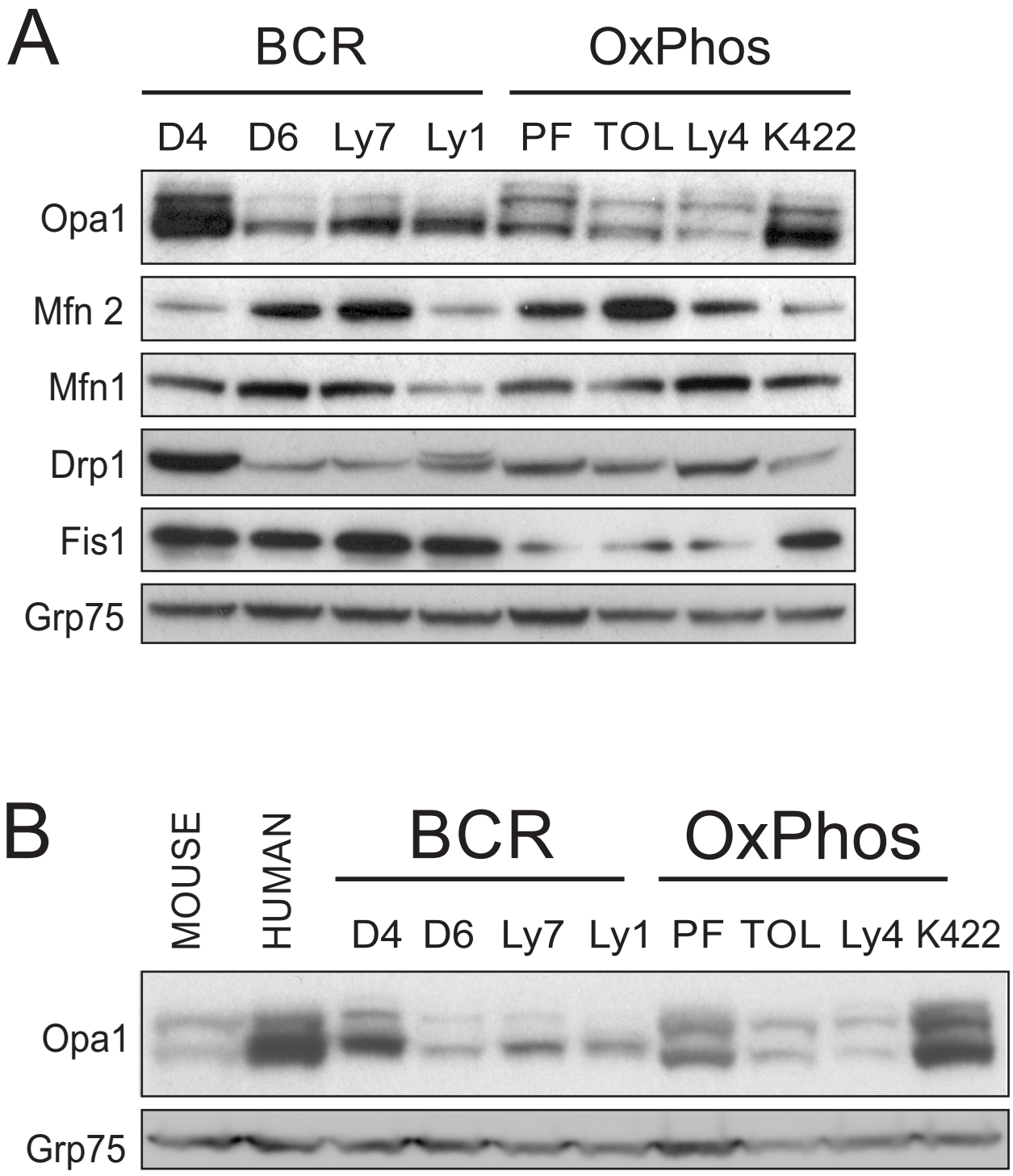
A
BCR
OxPhos
D4 D6 Ly7 Ly1 PF TOL Ly4 K422
Opa1
Mfn 2
Mfn1
Drp1
Fis1
Grp75
B
MOUSE
HUMAN
BCR
OxPhos
D4 D6 Ly7 Ly1 PF TOL Ly4 K422
Opa1
Grp75
C
Long/Short Opa1
1.4
1.2
1.0
0.8
0.6
0.4
0.2
0.0
D4
D6
Ly7
Ly1
Pfeiffer
Toledo
Ly4
K422

Figure 1.

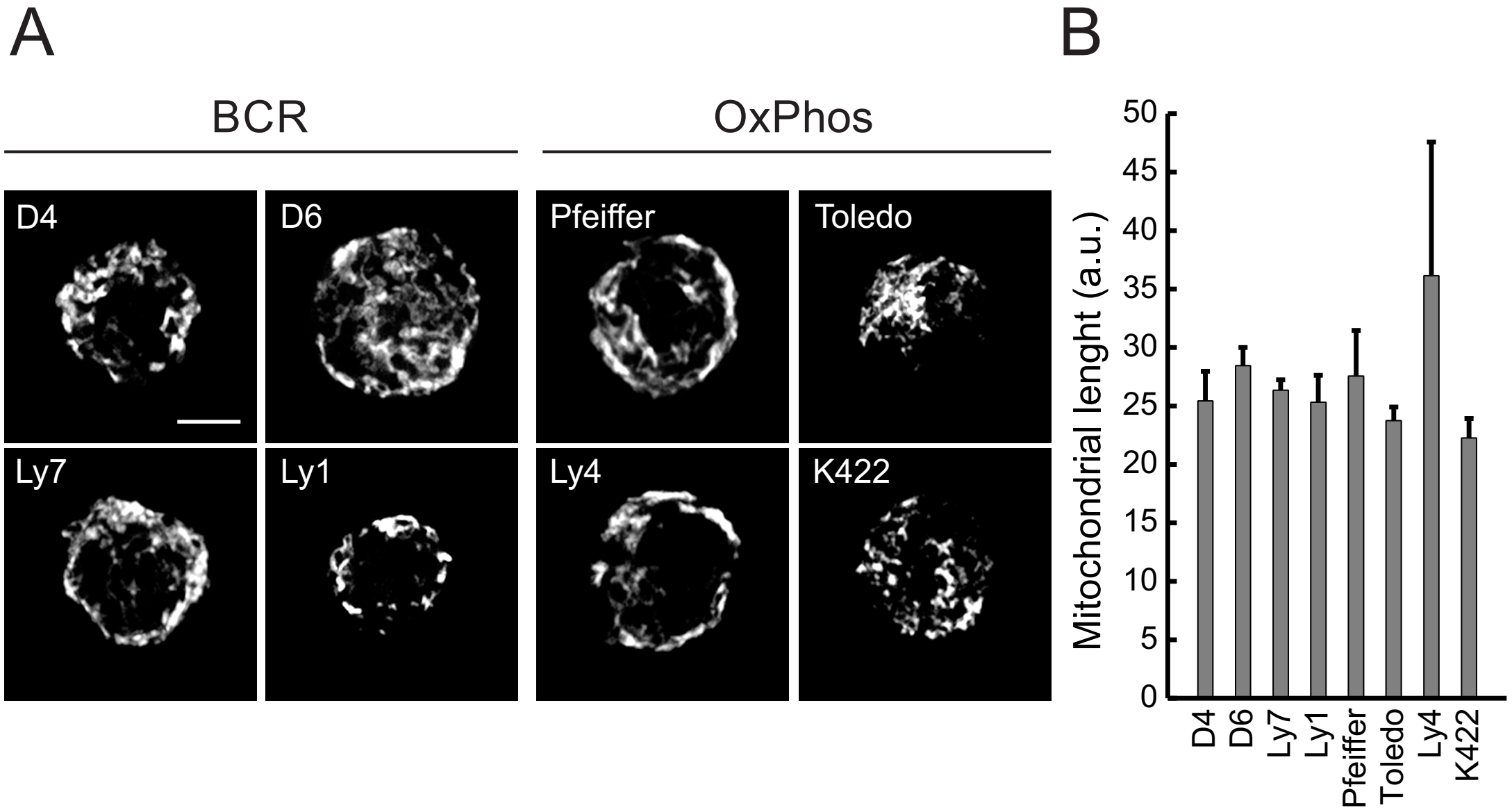
A
BCR
OxPhos
D4
D6
Pfeiffer
Toledo
Ly7
Ly1
Ly4
K422
B
Mitochondrial lenght (a.u.)
0
5
10
15
20
25
30
35
40
45
50
D4
D6
Ly7
Ly1
Pfeiffer
Toledo
Ly4
K422

Figure 2.

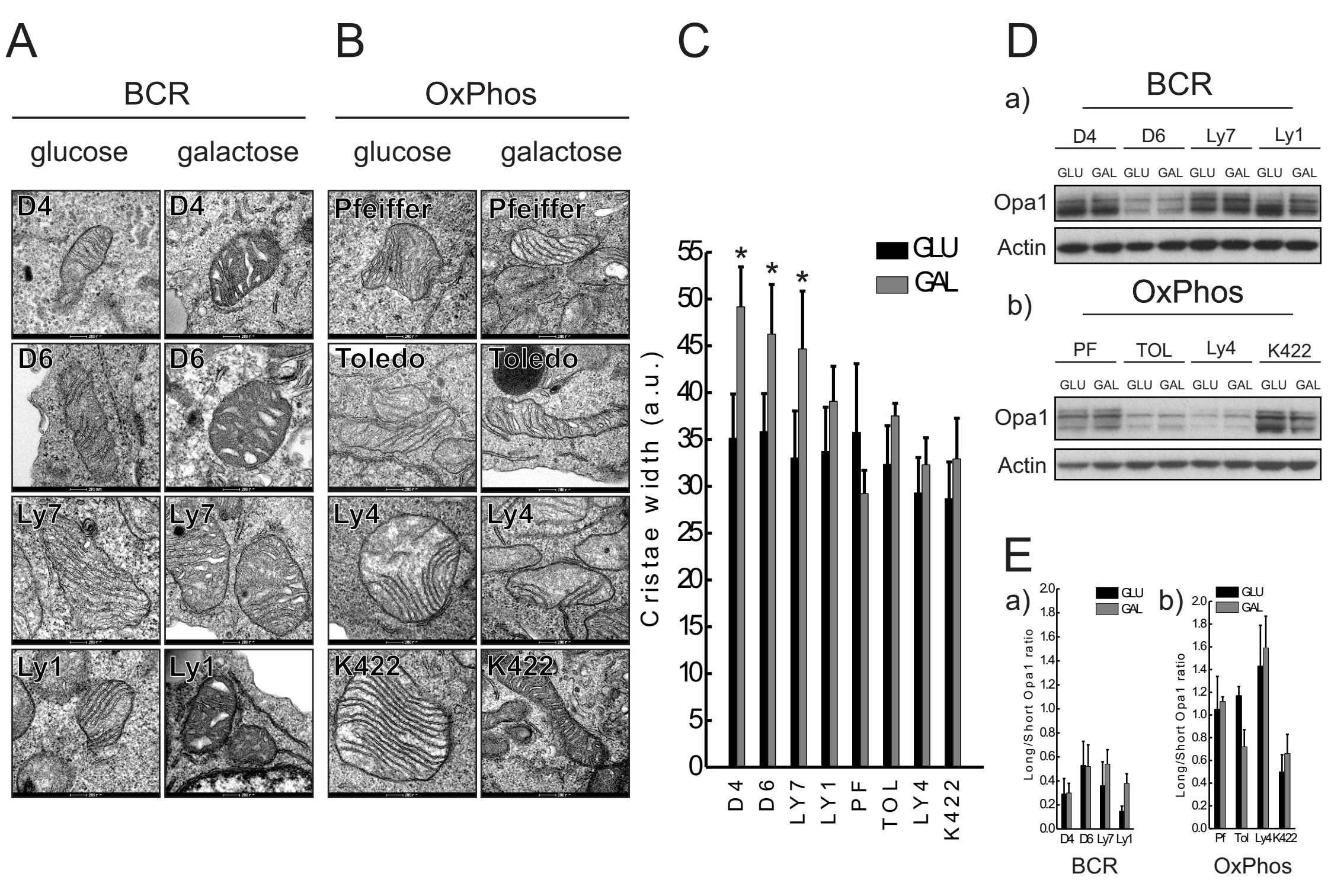
A
BCR
glucose
galactose
D4
D4
D6
D6
Ly7
Ly7
Ly1
Ly1
B
OxPhos
glucose
galactose
Pfeiffer
Pfeiffer
Toledo
Toledo
Ly4
Ly4
K422
K422
C
Cristae width (a.u.)
GLU
GAL
*
*
*
D4
D6
LY7
LY1
PF
TOL
LY4
K422
D
a)
BCR
D4
D6
Ly7
Ly1
GLU GAL GLU GAL GLU GAL GLU GAL
Opa1
Actin
b)
OxPhos
PF
TOL
Ly4
K422
GLU GAL GLU GAL GLU GAL GLU GAL
Opa1
Actin
E
a)
b)
GLU
GAL
Long/Short Opa1 ratio
D4 D6 Ly7 Ly1
BCR
Pf Tol Ly4 K422
OxPhos

Figure 3.

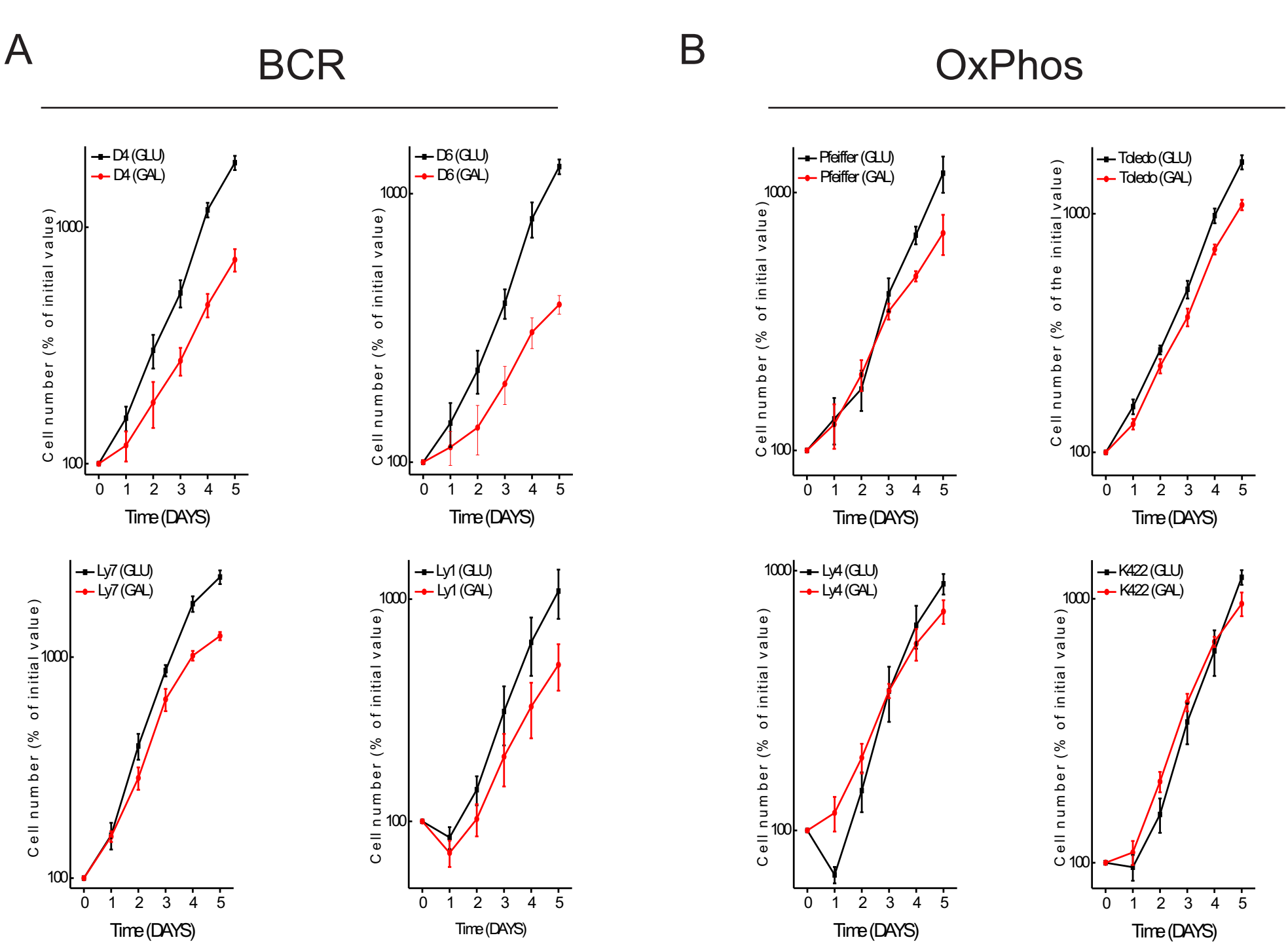
A
BCR
B
OxPhos
D4 (GLU)
D4 (GAL)
D6 (GLU)
D6 (GAL)
Pfeiffer (GLU)
Pfeiffer (GAL)
Toledo (GLU)
Toledo (GAL)
Ly7 (GLU)
Ly7 (GAL)
Ly1 (GLU)
Ly1 (GAL)
Ly4 (GLU)
Ly4 (GAL)
K422 (GLU)
K422 (GAL)
Cell number (% of initial value)
Cell number (% of the initial value)
Time (DAYS)
100
1000
0 1 2 3 4 5

Figure 4.

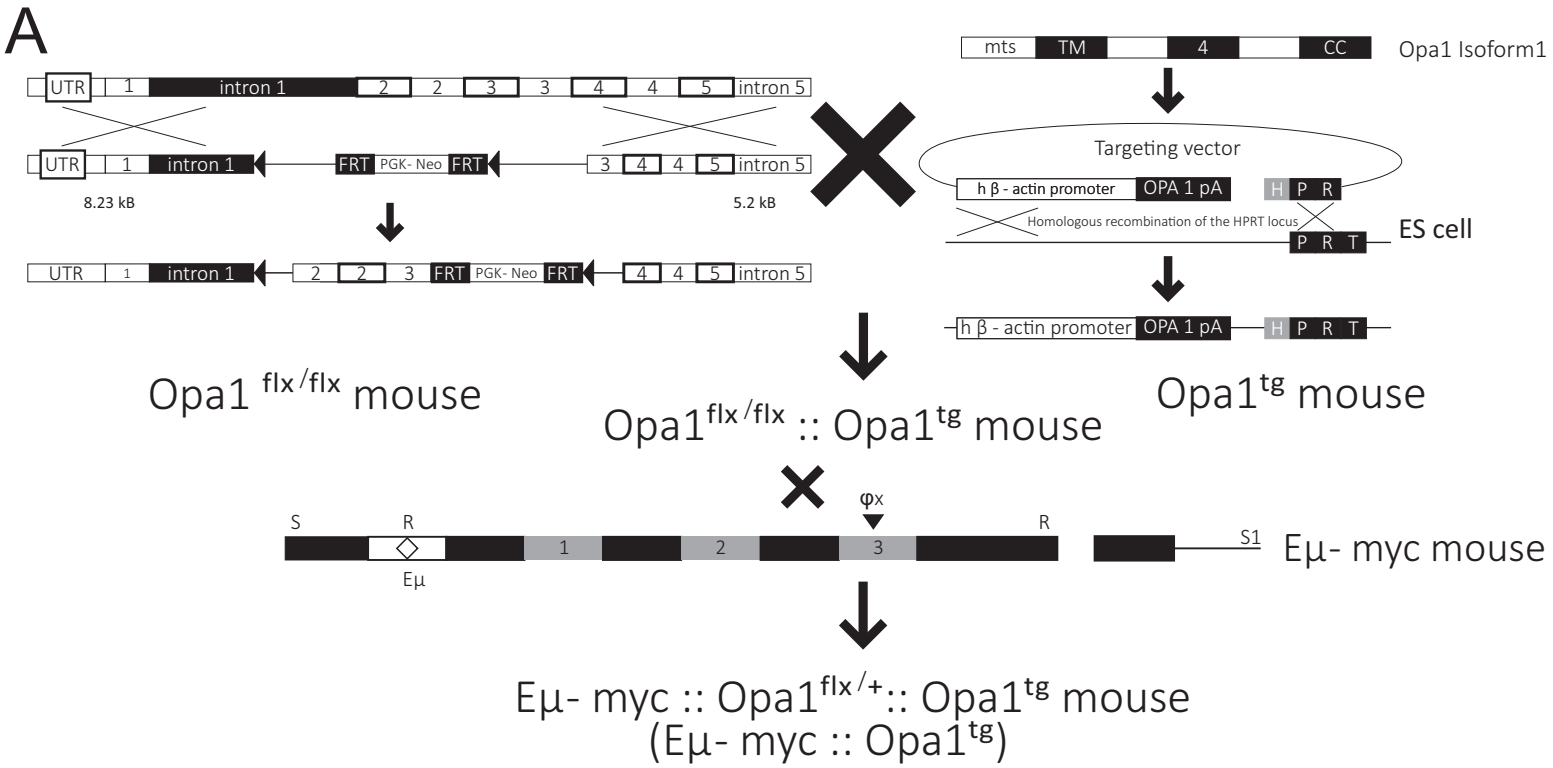
A
mts
TM
4
CC
Opa1 Isoform1
UTR
intron 1
intron 5
FRT
PGK- Neo
8.23 kB
5.2 kB
Targeting vector
h β - actin promoter
OPA 1 pA
H P R
Homologous recombination of the HPRT locus
P R T
ES cell
Opa1 flx/flx mouse
Opa1flx/flx :: Opa1tg mouse
Opa1tg mouse
S
R
φx
Eμ
S1
Eμ- myc mouse
Eμ- myc :: Opa1flx/+:: Opa1tg mouse
(Eμ- myc :: Opa1tg)

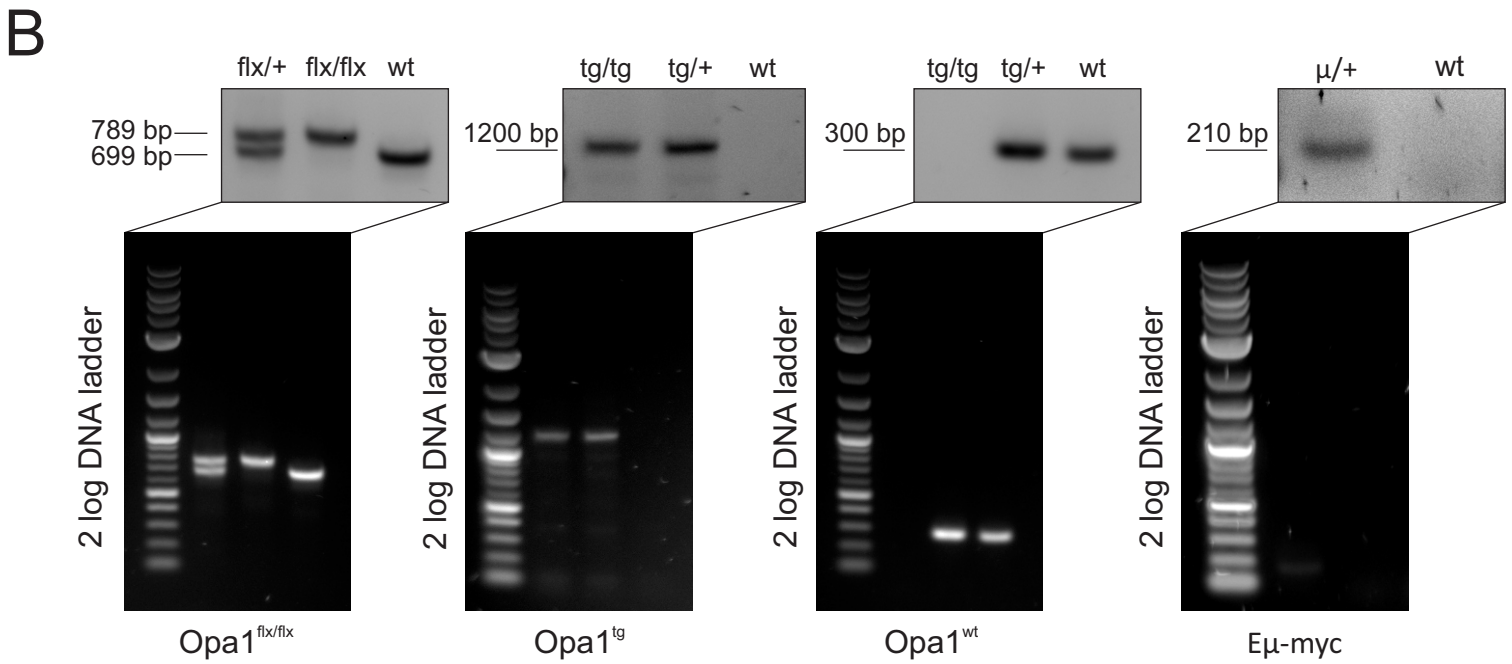
B
flx/+
flx/flx
wt
789 bp
699 bp
tg/tg
tg/+
1200 bp
300 bp
μ/+
210 bp
2 log DNA ladder
Opa1flx/flx
Opa1tg
Opa1wt
Eμ-myc

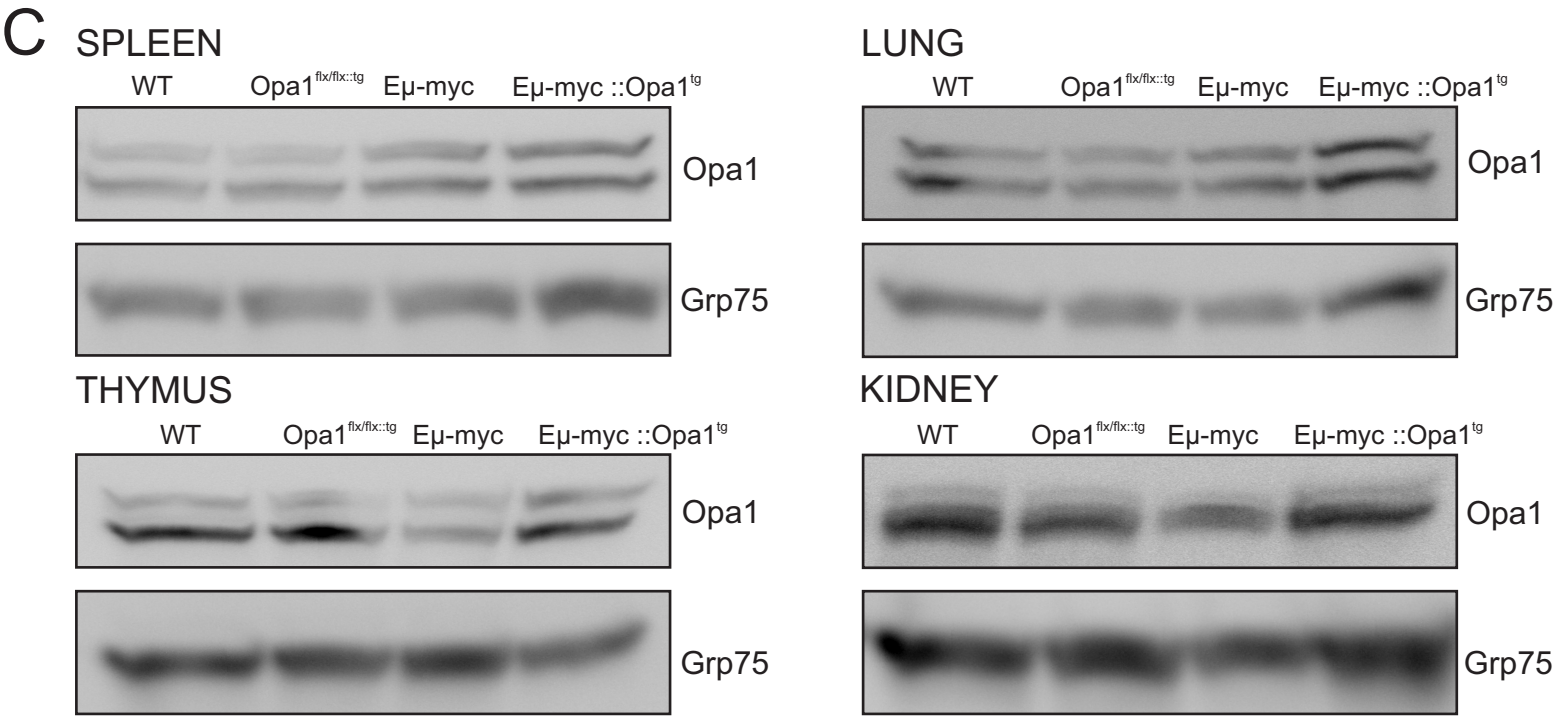
C
SPLEEN
WT
Opa1flx/flx::tg
Eμ-myc
Eμ-myc ::Opa1tg
Opa1
Grp75
LUNG
THYMUS
KIDNEY

Figure 5.

A

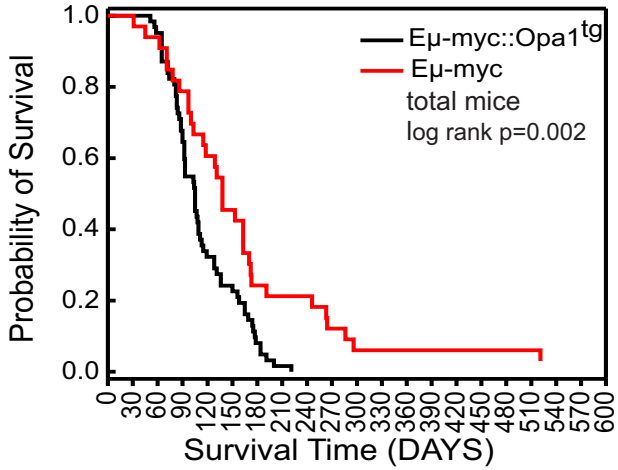
Eμ-myc::Opa1tg
Eμ-myc
total mice
log rank p=0.002
Probability of Survival
Survival Time (DAYS)

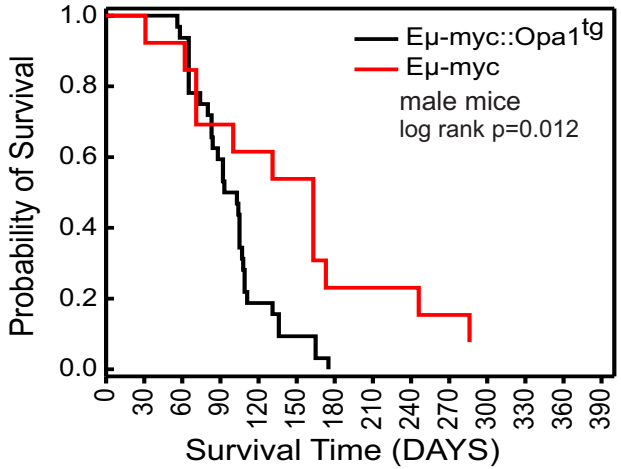
Eμ-myc::Opa1tg
Eμ-myc
male mice
log rank p=0.012
Probability of Survival
Survival Time (DAYS)

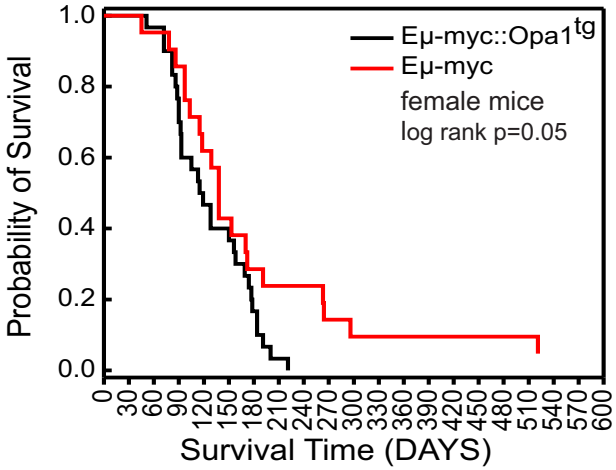
Eμ-myc::Opa1tg
Eμ-myc
female mice
log rank p=0.05
Probability of Survival
Survival Time (DAYS)

B

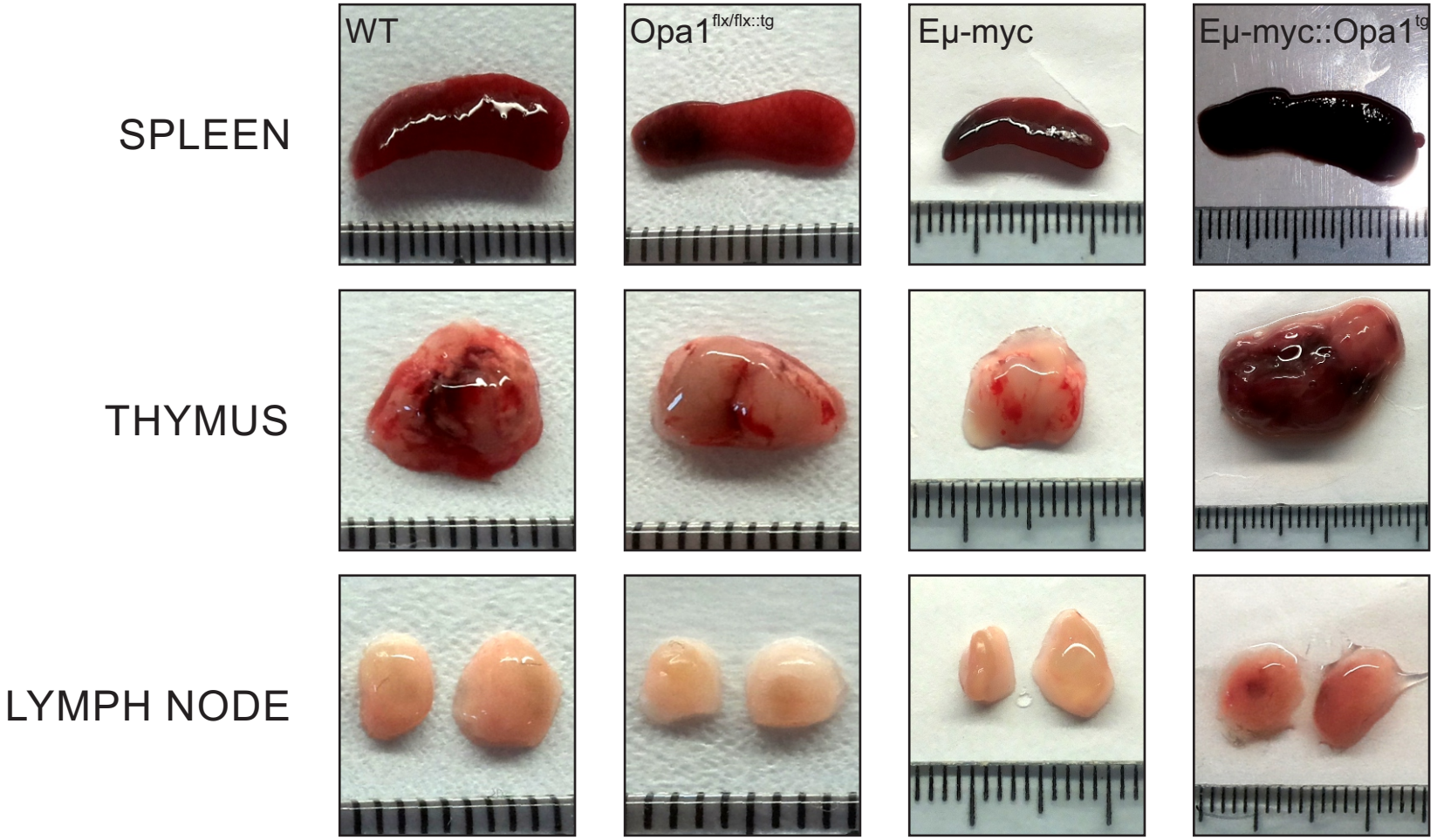
WT
Opa1flx/flx::tg
Eμ-myc
Eμ-myc::Opa1tg
SPLEEN
THYMUS
LYMPH NODE

Figure 6.

Table 1.

	2 months old		3 months old		4 months old		5 months old		6 months old	
MOUSE	Eμ-myc	Eμ-myc Opa1^{tg}	Eμ-myc	Eμ-myc Opa1^{tg}	Eμ-myc	Eμ-myc Opa1^{tg}	Eμ-myc	Eμ-myc Opa1^{tg}	Eμ-myc	Eμ-myc Opa1^{tg}
SPLEEN Neoplastic lymphoid infiltration	+ 2/3 ++ 1/3	+++ 1/3 ++ 1/3 + 1/3	++++ 1/3 ++ 1/3 0 1/3	++++ 3/3	+++ 1/3 ++ 1/3 0 1/3	++++ 2/3 ++ 1/3	++ 3/3	++++ 3/3	++++ 1/3 +++ 2/3	++++ 3/3
THYMUS Neoplastic lymphoid infiltration	+ 2/3 ++ 1/2	++++ 1/3 ++ 2/3	+/3 0 2/3	++++ 1/3 +++ 1/3 ++ 1/3	++++ 1/3 0 2/3	++++ 3/3	++ 3/3	++++ 3/3	++++ 1/3 +++ 2/3	++++ 3/3
LIVER Neoplastic lymphoid infiltration	0/3	+++ 1/3 + 2/3	+ 1/3 0 2/3	++ 3/3	++++ 1/3 0 2/3	+++ 1/3 ++ 2/3	+ 3/3	+++ 3/3	++++ 1/3 +++ 1/3 ++ 1/3	+++ 3/3
LUNG Neoplastic lymphoid infiltration	+ 3/3	+++ 1/3 + 2/3	+ 1/3 0 2/3	++++ 2/3 ++ 1/3	++ 1/3 0 2/3	+++ 1/3 ++ 2/3	+ 3/3	++++ 1/3 +++ 2/3	++++ 1/3 ++ 2/3	++++ 3/3
KIDNEY Neoplastic lymphoid infiltration	0/3	++ 1/3 0/2	0/3	++++ 1/3 ++ 2/3	+++ 1/3 0 2/3	++ 2/3 + 1/3	0/3	++++ 3/3	++++ 1/3 +++ 1/3 ++ 1/3	++++ 3/3

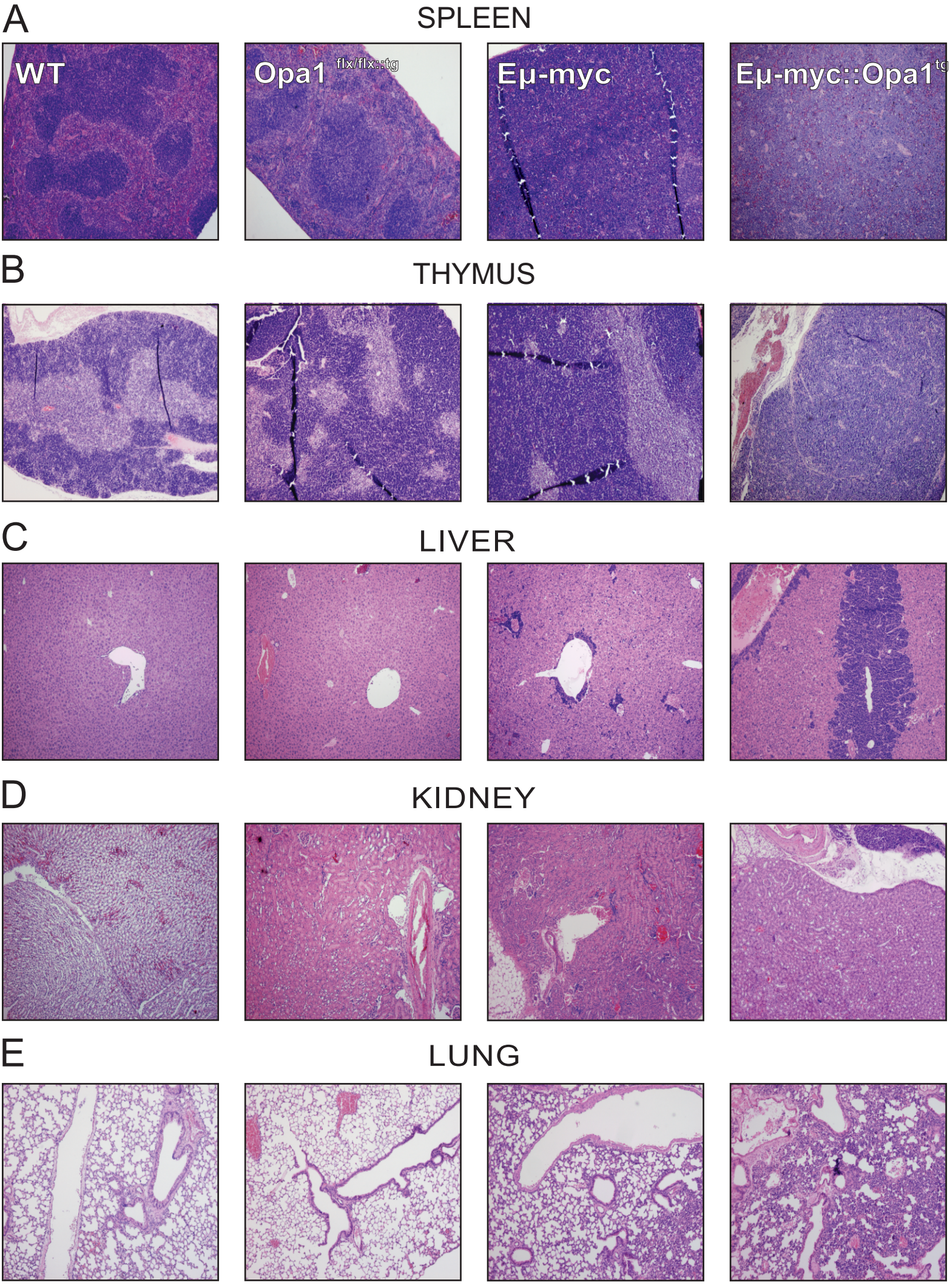
A
SPLEEN
WT
Opa1 flx/flx::tg
Eμ-myc
Eμ-myc::Opa1 tg
B
THYMUS
C
LIVER
D
KIDNEY
E
LUNG

Figure 7.

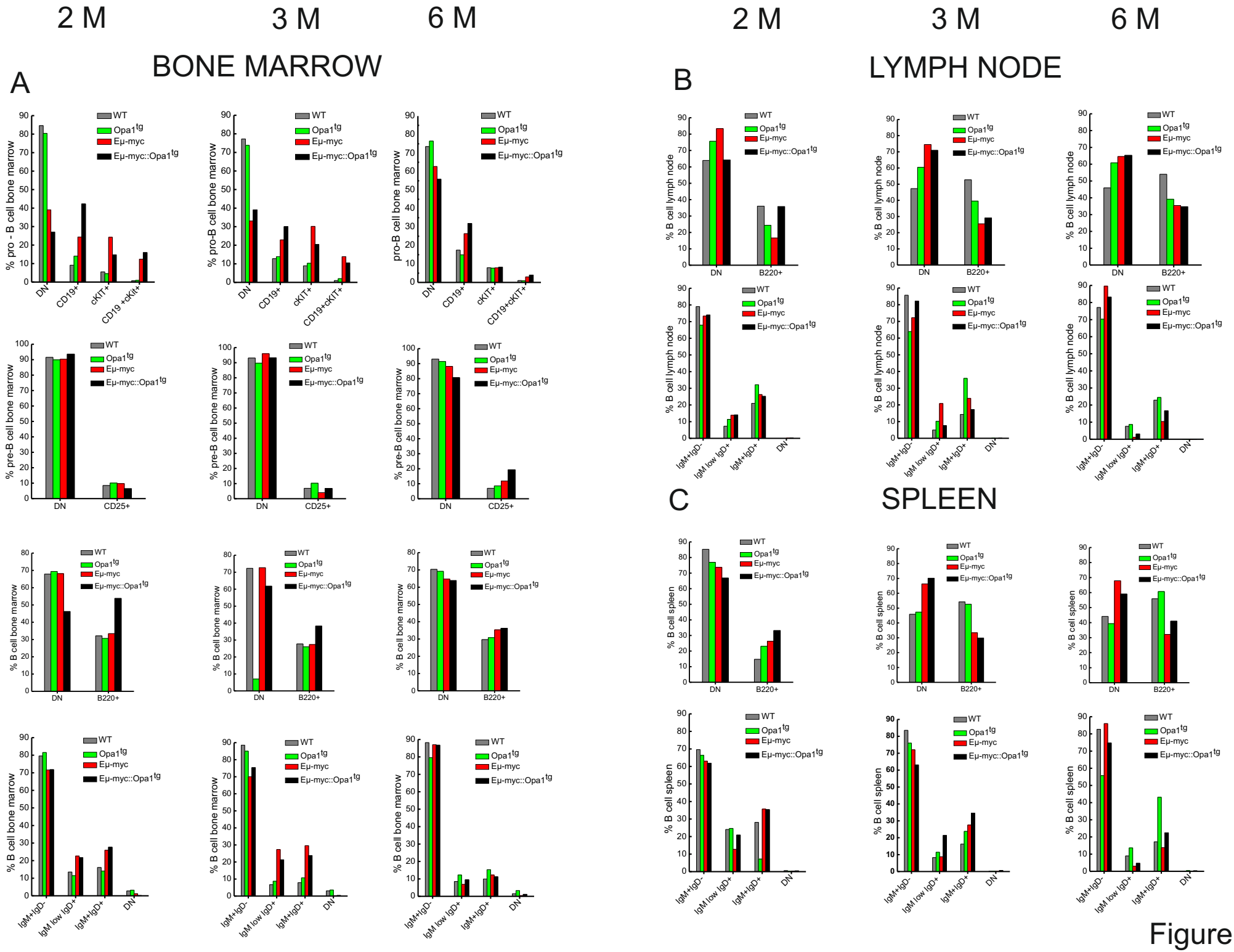
2 M
3 M
6 M
BONE MARROW
A
2 M
3 M
6 M
LYMPH NODE
B
SPLEEN
C
WT
Opa1tg
Eμ-myc
Eμ-myc::Opa1tg
% pro - B cell bone marrow
% pro-B cell bone marrow
pro-B cell bone marrow
% pre-B cell bone marrow
% B cell bone marrow
% B cell lymph node
% B cell spleen
DN
CD19+
cKIT+
CD19 +cKit+
CD19+cKIT+
CD25+
B220+
IgM+IgD-
IgM low IgD+
IgM+IgD+
DN'

Figure 8.

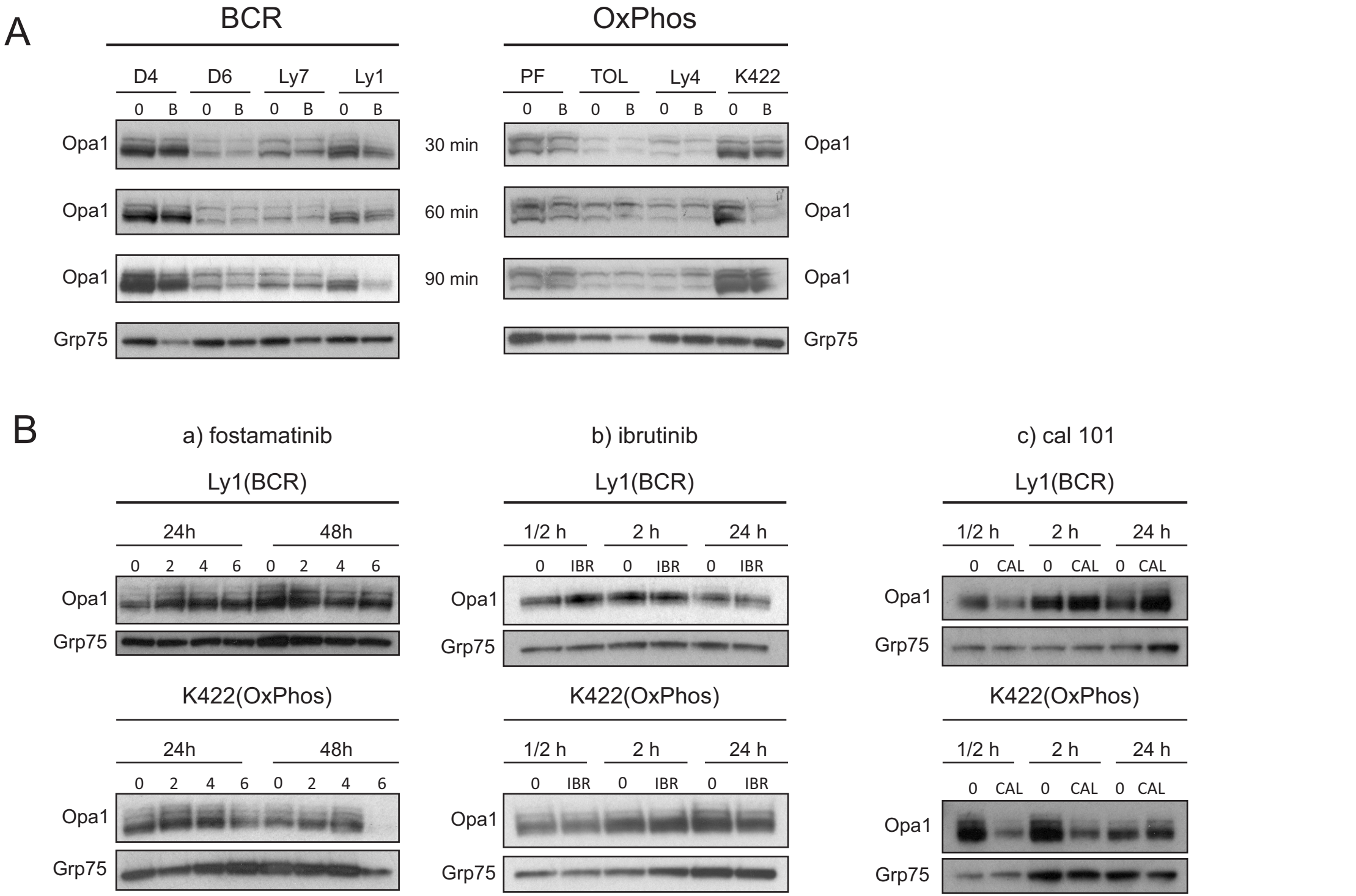
A
BCR
D4
D6
Ly7
Ly1
0 B 0 B 0 B 0 B
Opa1
Opa1
Opa1
Grp75
30 min
60 min
90 min
OxPhos
PF
TOL
Ly4
K422
0 B 0 B 0 B 0 B
Opa1
Opa1
Opa1
Grp75
B
a) fostamatinib
Ly1(BCR)
24h
48h
0 2 4 6 0 2 4 6
Opa1
Grp75
K422(OxPhos)
24h
48h
0 2 4 6 0 2 4 6
Opa1
Grp75
b) ibrutinib
Ly1(BCR)
1/2 h
2 h
24 h
0 IBR 0 IBR 0 IBR
Opa1
Grp75
K422(OxPhos)
1/2 h
2 h
24 h
0 IBR 0 IBR 0 IBR
Opa1
Grp75
c) cal 101
Ly1(BCR)
1/2 h
2 h
24 h
0 CAL 0 CAL 0 CAL
Opa1
Grp75
K422(OxPhos)
1/2 h
2 h
24 h
0 CAL 0 CAL 0 CAL
Opa1
Grp75

Figure S1.

A

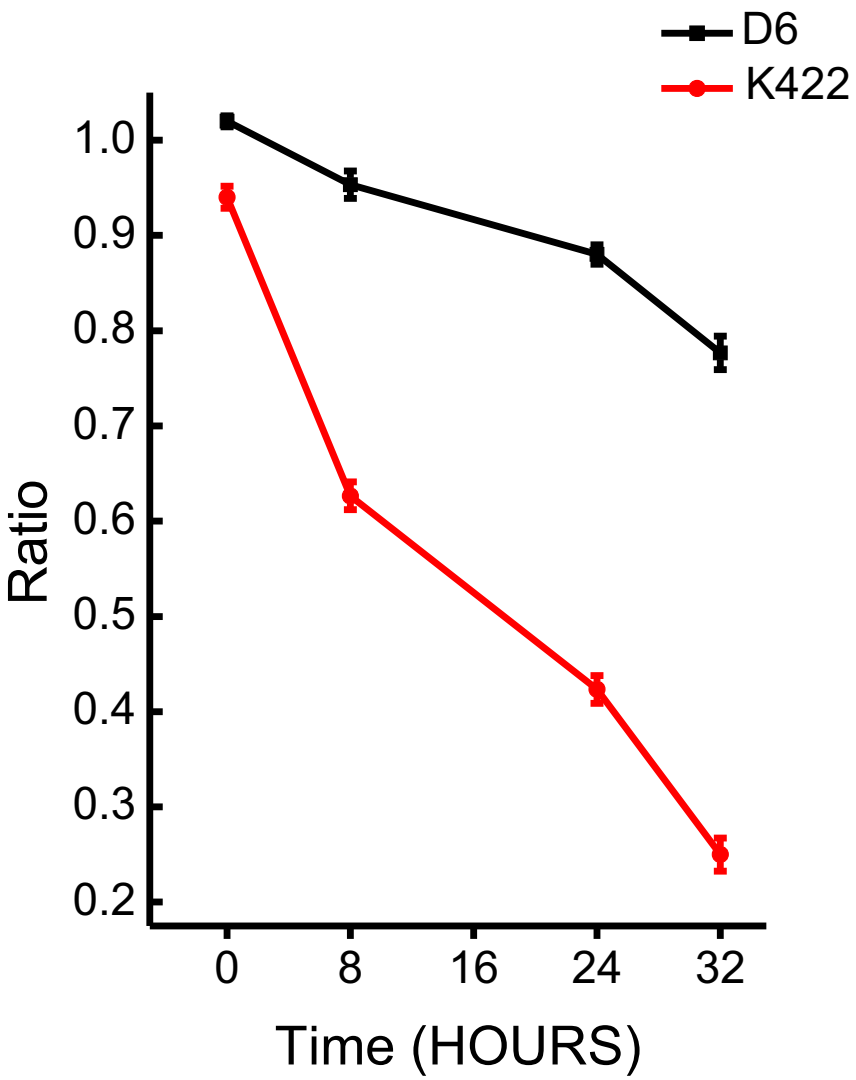
D6
K422
1.0
0.9
0.8
0.7
0.6
0.5
0.4
0.3
0.2
Ratio
0
8
16
24
32
Time (HOURS)

B

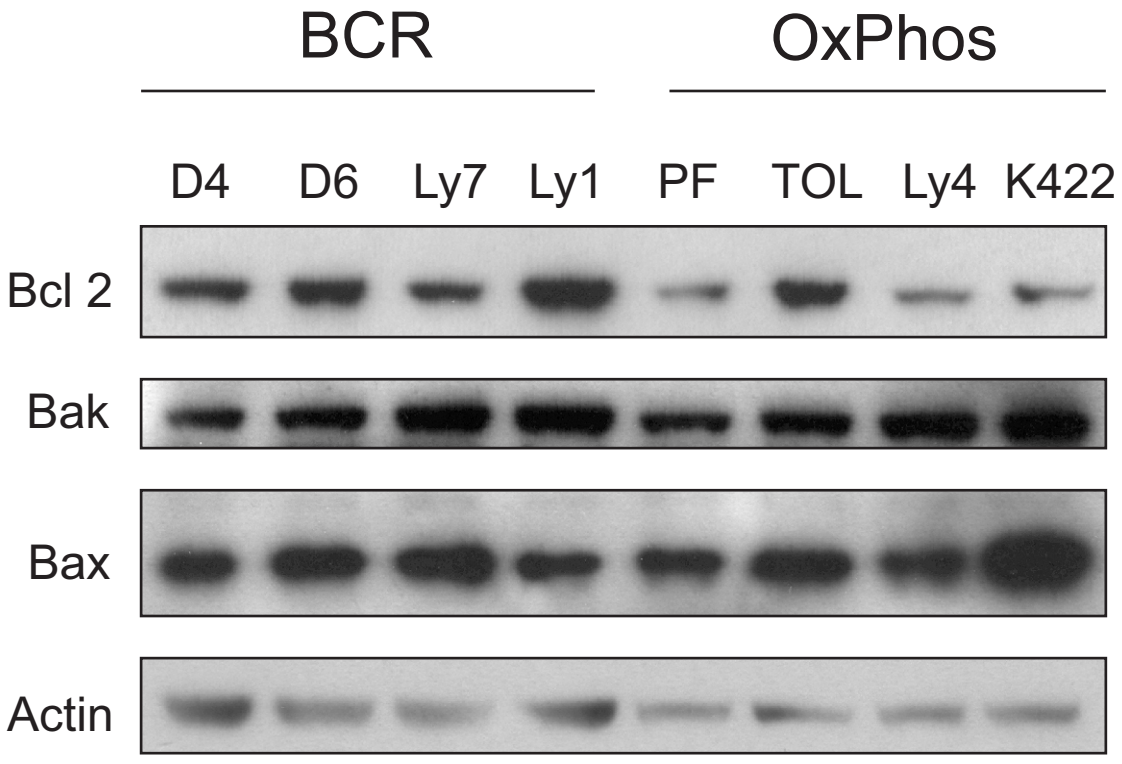
BCR
OxPhos
D4
D6
Ly7
Ly1
PF
TOL
Ly4
K422
Bcl 2
Bak
Bax
Actin

Figure S2.

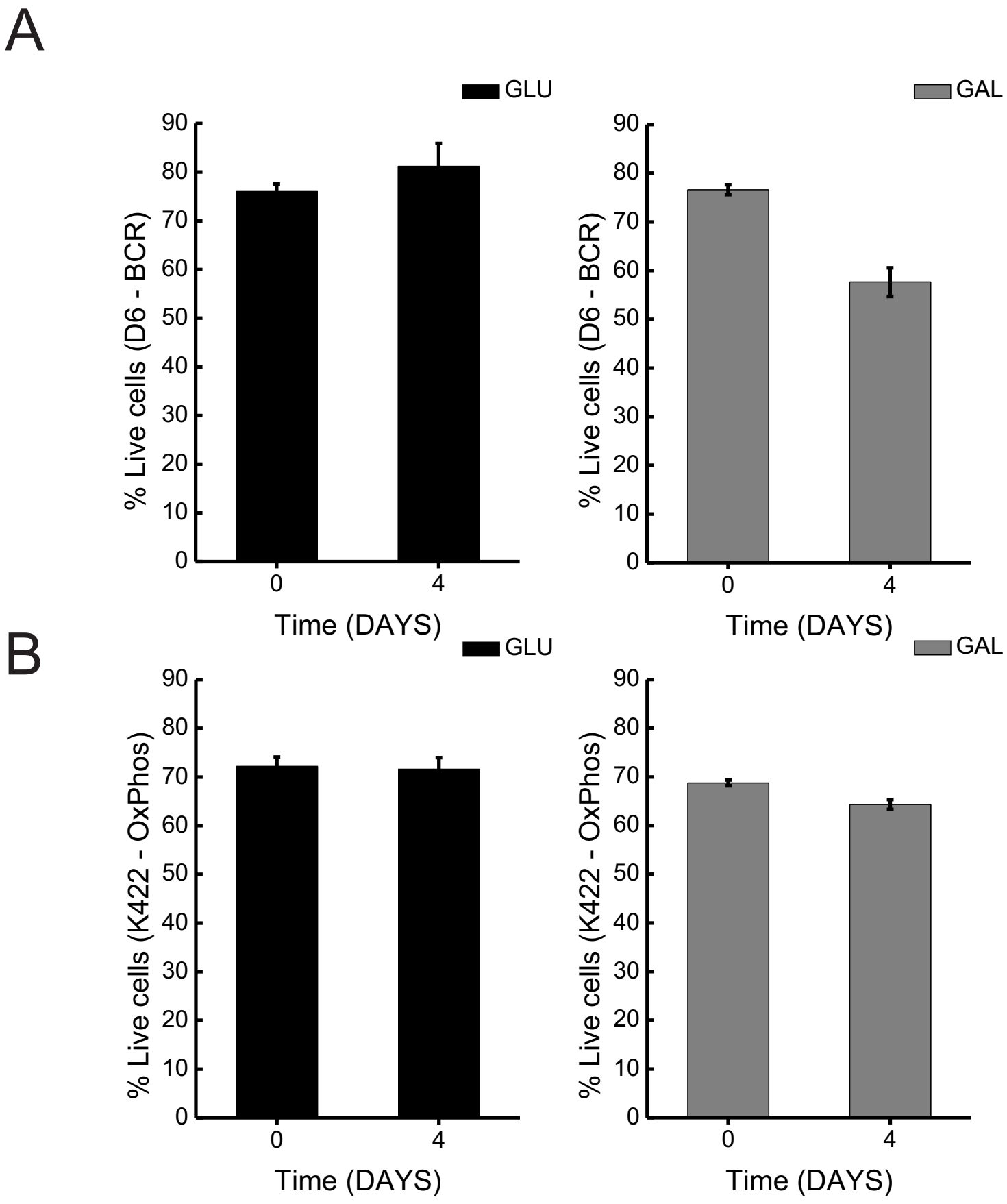
A
GLU
GAL
% Live cells (D6 - BCR)
90
80
70
60
50
40
30
20
10
0
0
4
Time (DAYS)
B
GLU
GAL
% Live cells (K422 - OxPhos)
90
80
70
60
50
40
30
20
10
0
0
4
Time (DAYS)

Figure S3.

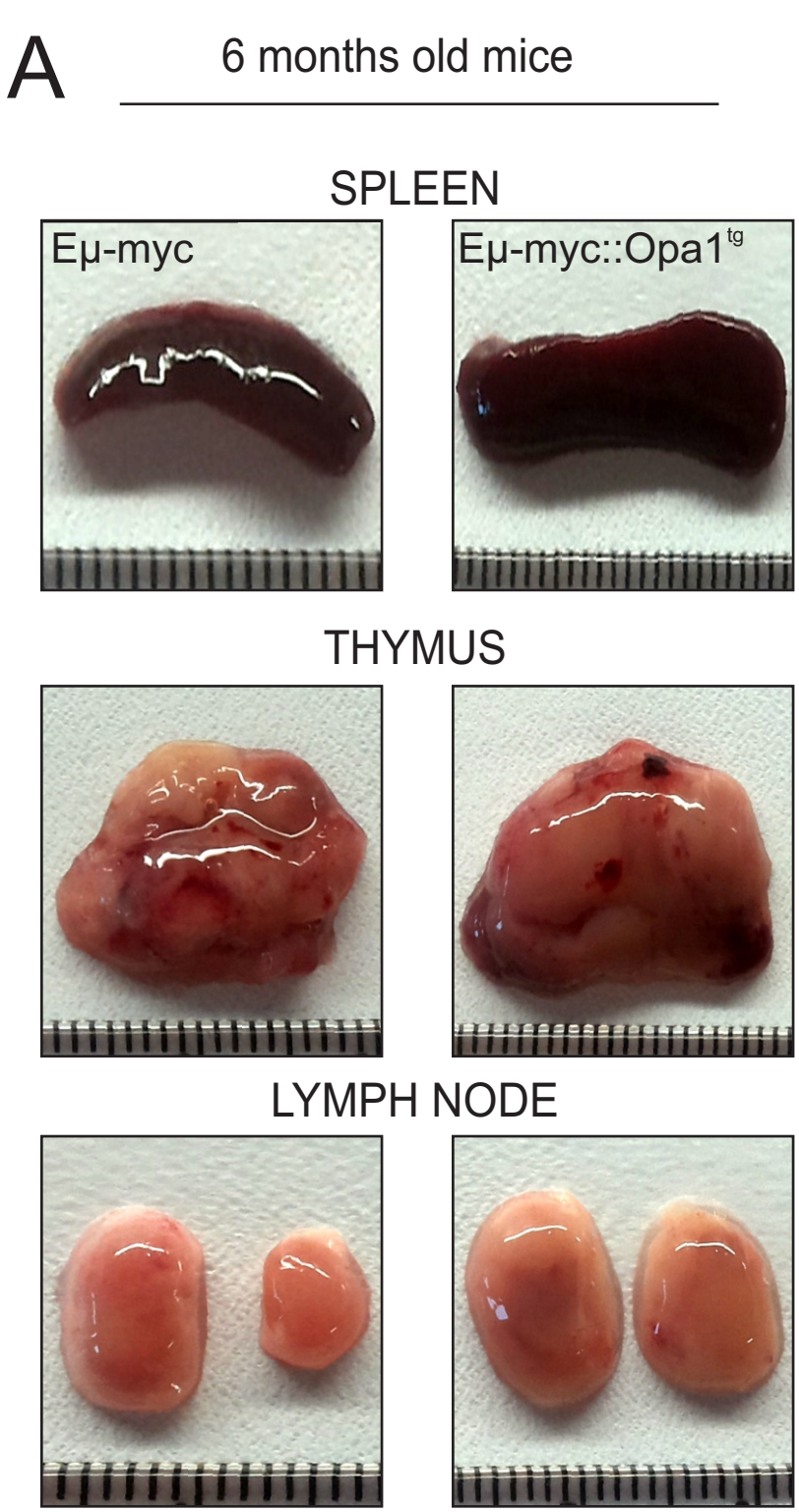
A
6 months old mice
SPLEEN
Eμ-myc
Eμ-myc::Opa1tg
THYMUS
LYMPH NODE

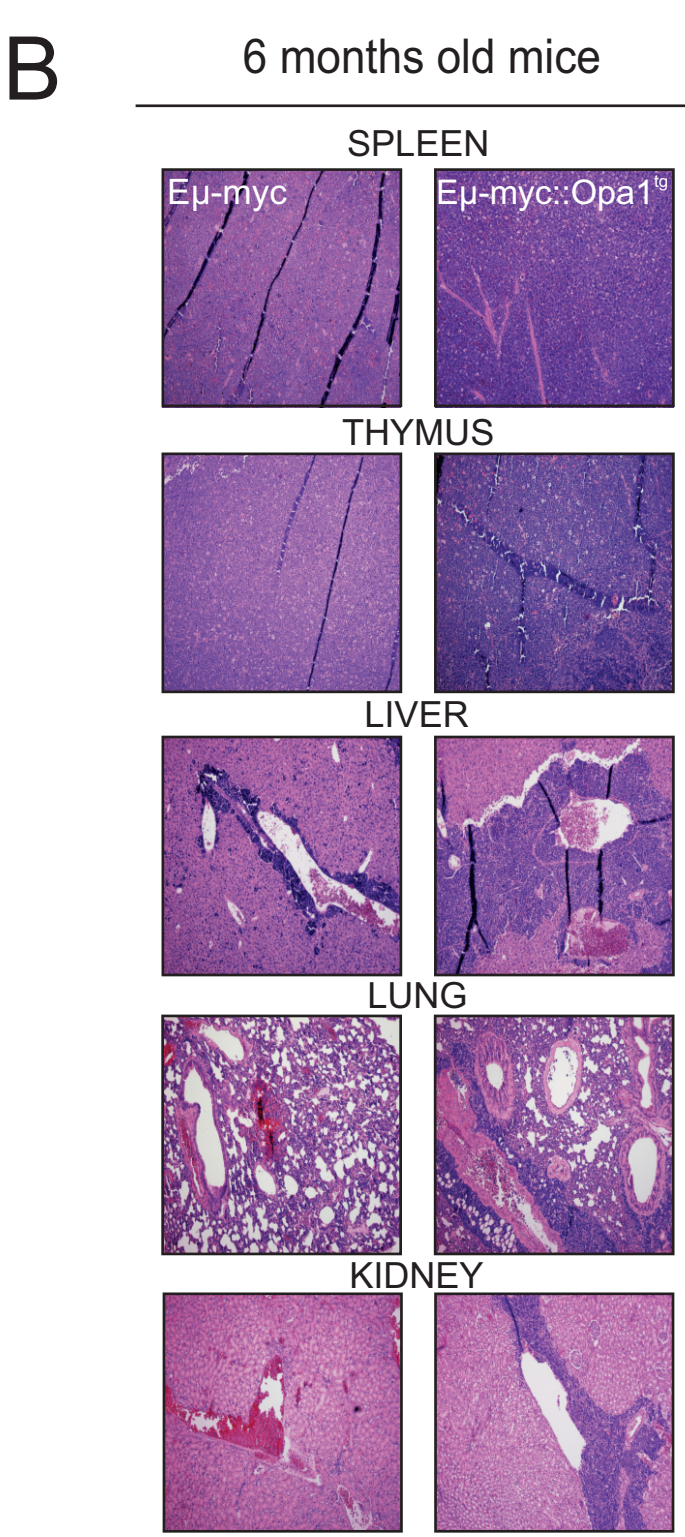
B
6 months old mice
SPLEEN
Eμ-myc
Eμ-myc::Opa1tg
THYMUS
LIVER
LUNG
KIDNEY

Figure S4.

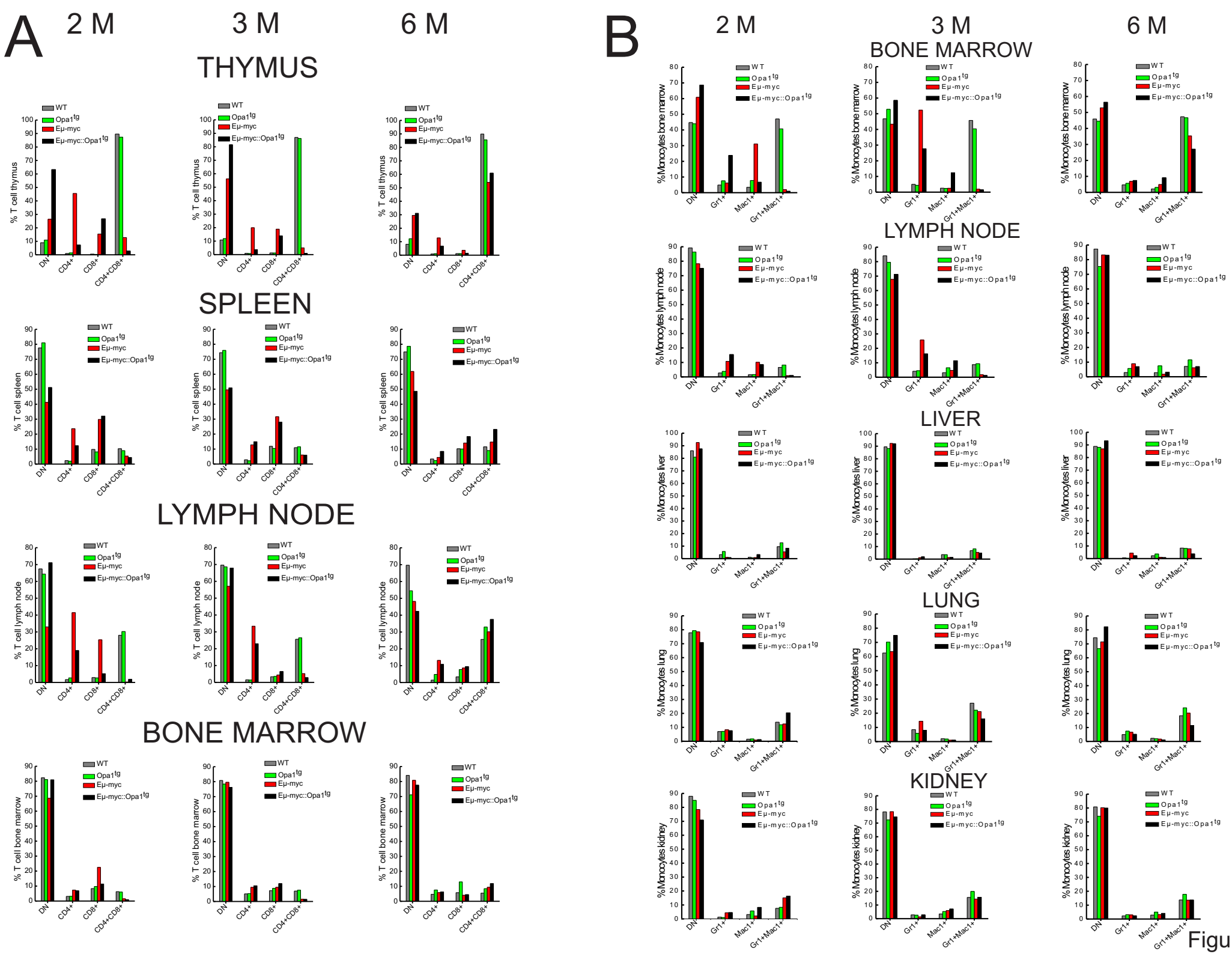
A
2 M
3 M
6 M
THYMUS
SPLEEN
LYMPH NODE
BONE MARROW
% T cell thymus
% T cell spleen
% T cell lymph node
% T cell bone marrow
WT
Opa1tg
Eμ-myc
Eμ-myc::Opa1tg
DN
CD4+
CD8+
CD4+CD8+
B
2 M
3 M
6 M
BONE MARROW
LYMPH NODE
LIVER
LUNG
KIDNEY
%Monocytes bone marrow
%Monocytes lymph node
%Monocytes liver
%Monocytes lung
%Monocytes kidney
Gr1+
Mac1+
Gr1+Mac1+

Figure S5.

5. CONCLUSIONS AND FUTURE PERSPECTIVES

In this Thesis we focused on understanding what role does Opa1 play in cancer.

In order to address this aim we reached out to in vitro and in vivo cancer models where we could explore the role of Opa1 in the acquisition and maintenance of the cancer phenotype. We analyzed what features of diffuse large B cell lymphoma cell subsets depend on Opa1, and what role does Opa1 play in the development and progression of cancer in an in vivo lymphoma mouse model with a controlled overexpression of Opa1.

In terms of the Opa1 status, a clear distinction between the two metabolic subsets of DLBCL was made according to the fact that Opa1 turned out to be increasingly processed in the BCR cell group, compared to the OxPhos, where contrary to the BCR, the balance between long and short Opa1 forms was maintained. The higher and overall more balanced levels of Opa1 in the OxPhos subset had an effect on cristae ultrastructure, making cristae tighter and more organized, compared to their BCR counterparts, while providing them with a proliferative advantage when they were forced to generate ATP in the process of oxidative phosphorylation by growth in galactose enriched media.

The difference in Opa1 levels in two DLBCL cell subsets didn't reflect on mitochondrial morphology in the steady state. Analysis of mitochondrial morphology of DLBCL cell lines that were previously grown in galactose, could be a way to distinguish whether changes in the mitochondrial architecture occur, compared to basal conditions, and whether this could be a feature which can be correlated to the observed differences in the Opa1 levels. The molecular

mechanism responsible for the increased Opa1 cleavage in the BCR subset, still remained unexplained, since chelation of intracellular calcium by BAPTA - AM and pharmacological blockage of BCR signaling kinases had no effect on Opa1 processing. It would be necessary to go back to the original proteomics data and investigate what other components of the DLBCL proteome are different between the two DLBCL subsets, which can be potentially correlated with the situation observed in terms of Opa1 processing.

Our results indicate that overexpression of Opa1 contributed to the progression and development of cancer in Eμ-myc mice. Eμ-myc::Opa1^{tg} mice were becoming terminally ill and were dying at a much faster rate compared to their Eμ-myc mice counterparts. Pathology and histopathology analysis revealed that a clinical picture observed in these mice corresponded to disseminated malignant lymphoma and that it was more severe in the doubly transgenic mouse, with severe cancer dissemination to the liver, kidney and lungs, indicating that Opa1 overexpression favored cancer spreading and severity. Immunophenotypic analysis revealed that overexpressing *Opa1* wasn't the driver of proliferation in the B cell lineage, but that was the task carried out by *Myc*, and that the bone marrows of these animals demonstrated higher levels of pro B and pre B cells, compared to the single transgenic Eμ-myc controls. In order to confirm that overexpression of *Opa1* doesn't drive proliferation it would be useful to stain histological sections of mouse organ tissues with the Ki-67 marker of proliferation, and assess the levels of positively stained sections between control Eμ-myc and Eμ-myc::Opa1^{tg} samples. This could be done together with performing a TUNEL assay in order to assess the rate of apoptosis in organs of these two mouse groups. In order to pinpoint the actual onset of the disease, it would be useful to analyze the positively stained cell subsets for the pan-B cell marker B220, in the peripheral

blood of these animals over time, narrowing down to the actual moment when hyperproliferation occurs.

It is also necessary to continue with the immunophenotypic characterization of Eμ-myc and Eμ-myc::Opa^{tg} lymphomas to understand better whether, and in what way *Opa1* overexpression changes the program of B cell differentiation.

Ultimate proof in understanding whether Opa1 is required for cancer maintenance is to ablate *Opa1* by Cre delivery in Eμ-myc::Opa1$^{flx/flx}$ Opa1^{tg} mice, which we get in the second generation after crossing Opa1$^{flx/flx}$Opa1^{tg} male mice with Eμ-myc::Opa1$^{flx/+}$::Opa1$^{tg/+}$ females.

The results of the already performed studies and expected results of the planed studies should ultimately serve the purpose of confirming Opa1 as gene / protein that displays oncogenic features, while validating it at the same time, as a promising therapeutic target. Mutations in the GTPase domain of Opa1 that abolish its GTPase activity impair its ability to protect from apoptosis. Therefore, development of chemical inhibitors that target the GTPase domain of Opa1, could mimic inactivating mutations in the GTPase domain, serving as drugs that can be used in cancer treatment.

Reference List

Abramson,J.S. and Shipp,M.A. (2005). Advances in the biology and therapy of diffuse large B-cell lymphoma: moving toward a molecularly targeted approach. Blood *106*, 1164-1174.

Acin-Perez,R., Fernandez-Silva,P., Peleato,M.L., Perez-Martos,A., and Enriquez,J.A. (2008). Respiratory active mitochondrial supercomplexes. Mol. Cell *32*, 529-539.

Adams,J.M., Harris,A.W., Pinkert,C.A., Corcoran,L.M., Alexander,W.S., Cory,S., Palmiter,R.D., and Brinster,R.L. (1985). The c-myc oncogene driven by immunoglobulin enhancers induces lymphoid malignancy in transgenic mice. Nature *318*, 533-538.

Akepati,V.R., Muller,E.C., Otto,A., Strauss,H.M., Portwich,M., and Alexander,C. (2008). Characterization of OPA1 isoforms isolated from mouse tissues. J. Neurochem. *106*, 372-383.

Alexander,C., Votruba,M., Pesch,U.E., Thiselton,D.L., Mayer,S., Moore,A., Rodriguez,M., Kellner,U., Leo-Kottler,B., Auburger,G., Bhattacharya,S.S., and Wissinger,B. (2000). OPA1, encoding a dynamin-related GTPase, is mutated in autosomal dominant optic atrophy linked to chromosome 3q28. Nat. Genet. *26*, 211-215.

Alexander,W.S., Bernard,O., Cory,S., and Adams,J.M. (1989). Lymphomagenesis in E mu-myc transgenic mice can involve ras mutations. Oncogene *4*, 575-581.

Alizadeh,A.A., Eisen,M.B., Davis,R.E., Ma,C., Lossos,I.S., Rosenwald,A., Boldrick,J.C., Sabet,H., Tran,T., Yu,X., Powell,J.I., Yang,L., Marti,G.E., Moore,T., Hudson,J., Jr., Lu,L., Lewis,D.B., Tibshirani,R., Sherlock,G., Chan,W.C., Greiner,T.C., Weisenburger,D.D., Armitage,J.O., Warnke,R., Levy,R., Wilson,W., Grever,M.R., Byrd,J.C., Botstein,D., Brown,P.O., and Staudt,L.M. (2000). Distinct types of diffuse large B-cell lymphoma identified by gene expression profiling. Nature *403*, 503-511.

Attardi,G. and Schatz,G. (1988). Biogenesis of mitochondria. Annu. Rev. Cell. Biol. *4*, 289-333.

Bedard,K. and Krause,K.H. (2007). The NOX family of ROS-generating NADPH oxidases: physiology and pathophysiology. Physiol Rev. *87*, 245-313.

Belenguer,P. and Pellegrini,L. (2013). The dynamin GTPase OPA1: more than mitochondria? Biochim. Biophys. Acta *1833*, 176-183.

Bojarczuk,K., Bobrowicz,M., Dwojak,M., Miazek,N., Zapala,P., Bunes,A., Siernicka,M., Rozanska,M., and Winiarska,M. (2015). B-cell receptor signaling in the pathogenesis of lymphoid malignancies. Blood Cells Mol. Dis. *55*, 255-265.

Borche,L., Lim,A., Binet,J.L., and Dighiero,G. (1990). Evidence that chronic lymphocytic leukemia B lymphocytes are frequently committed to production of natural autoantibodies. Blood *76*, 562-569.

Caro,P., Kishan,A.U., Norberg,E., Stanley,I.A., Chapuy,B., Ficarro,S.B., Polak,K., Tondera,D., Gounarides,J., Yin,H., Zhou,F., Green,M.R., Chen,L., Monti,S., Marto,J.A., Shipp,M.A., and Danial,N.N. (2012). Metabolic signatures uncover distinct targets in molecular subsets of diffuse large B cell lymphoma. Cancer Cell *22*, 547-560.

Cereghetti,G.M., Stangherlin,A., Martins de,B.O., Chang,C.R., Blackstone,C., Bernardi,P., and Scorrano,L. (2008). Dephosphorylation by calcineurin regulates translocation of Drp1 to mitochondria. Proc. Natl. Acad. Sci. U. S. A *105*, 15803-15808.

Chang,C.R. and Blackstone,C. (2007). Cyclic AMP-dependent protein kinase phosphorylation of Drp1 regulates its GTPase activity and mitochondrial morphology. J. Biol Chem. *282*, 21583-21587.

Chen,L., Monti,S., Juszczynski,P., Daley,J., Chen,W., Witzig,T.E., Habermann,T.M., Kutok,J.L., and Shipp,M.A. (2008). SYK-dependent tonic B-cell receptor signaling is a rational treatment target in diffuse large B-cell lymphoma. Blood *111*, 2230-2237.

Cheng,S., Coffey,G., Zhang,X.H., Shaknovich,R., Song,Z., Lu,P., Pandey,A., Melnick,A.M., Sinha,U., and Wang,Y.L. (2011). SYK inhibition and response prediction in diffuse large B-cell lymphoma. Blood *118*, 6342-6352.

Cipolat,S., Martins de Brito O., Dal Zilio B., and Scorrano,L. (2004). OPA1 requires mitofusin 1 to promote mitochondrial fusion. Proc. Natl. Acad. Sci. U. S. A *101*, 15927-15932.

Cipolat,S., Rudka,T., Hartmann,D., Costa,V., Serneels,L., Craessaerts,K., Metzger,K., Frezza,C., Annaert,W., D'Adamio,L., Derks,C., Dejaegere,T., Pellegrini,L., D'Hooge,R., Scorrano,L., and De Strooper,B. (2006). Mitochondrial Rhomboid PARL Regulates Cytochrome c Release during Apoptosis via OPA1-Dependent Cristae Remodeling. Cell *126*, 163-175.

Civiletto,G., Varanita,T., Cerutti,R., Gorletta,T., Barbaro,S., Marchet,S., Lamperti,C., Viscomi,C., Scorrano,L., and Zeviani,M. (2015). Opa1 overexpression ameliorates the clinical phenotype of two mitochondrial disease mouse models. Cell Metabolism.

Cogliati,S., Frezza,C., Soriano,M.E., Varanita,T., Quintana-Cabrera,R., Corrado,M., Cipolat,S., Costa,V., Casarin,A., Gomes,L.C., Perales-Clemente,E., Salviati,L., Fernandez-Silva,P., Enriquez,J.A., and Scorrano,L. (2013). Mitochondrial cristae shape determines respiratory chain supercomplexes assembly and respiratory efficiency. Cell *155*, 160-171.

Collins,T.J., Berridge,M.J., Lipp,P., and Bootman,M.D. (2002). Mitochondria are morphologically and functionally heterogeneous within cells. EMBO J. *21*, 1616-1627.

Colombini,M. and Mannella,C.A. (2012). VDAC, the early days. Biochim. Biophys. Acta *1818*, 1438-1443.

Corrado,M., Scorrano,L., and Campello,S. (2012). Mitochondrial dynamics in cancer and neurodegenerative and neuroinflammatory diseases. Int. J. Cell Biol. *2012*, 729290.

Craxton,A., Chuang,P.I., Shu,G., Harlan,J.M., and Clark,E.A. (2000). The CD40-inducible Bcl-2 family member A1 protects B cells from antigen receptor-mediated apoptosis. Cell Immunol. *200*, 56-62.

Cribbs,J.T. and Strack,S. (2007). Reversible phosphorylation of Drp1 by cyclic AMP-dependent protein kinase and calcineurin regulates mitochondrial fission and cell death. EMBO Rep. *8*, 939-944.

Dal Porto,J.M., Gauld,S.B., Merrell,K.T., Mills,D., Pugh-Bernard,A.E., and Cambier,J. (2004). B cell antigen receptor signaling 101. Mol. Immunol. *41*, 599-613.

Dalla-Favera,R., Migliazza,A., Chang,C.C., Niu,H., Pasqualucci,L., Butler,M., Shen,Q., and Cattoretti,G. (1999). Molecular pathogenesis of B cell malignancy: the role of BCL-6. Curr. Top. Microbiol. Immunol. *246*, 257-263.

Davidson,W.F., Giese,T., and Fredrickson,T.N. (1998). Spontaneous development of plasmacytoid tumors in mice with defective Fas-Fas ligand interactions. J. Exp. Med. *187*, 1825-1838.

Davis,R.E., Ngo,V.N., Lenz,G., Tolar,P., Young,R.M., Romesser,P.B., Kohlhammer,H., Lamy,L., Zhao,H., Yang,Y., Xu,W., Shaffer,A.L., Wright,G., Xiao,W., Powell,J., Jiang,J.K., Thomas,C.J., Rosenwald,A., Ott,G., Muller-Hermelink,H.K., Gascoyne,R.D., Connors,J.M., Johnson,N.A., Rimsza,L.M., Campo,E., Jaffe,E.S., Wilson,W.H., Delabie,J., Smeland,E.B., Fisher,R.I., Braziel,R.M., Tubbs,R.R., Cook,J.R., Weisenburger,D.D., Chan,W.C., Pierce,S.K., and Staudt,L.M. (2010). Chronic active B-cell-receptor signalling in diffuse large B-cell lymphoma. Nature *463*, 88-92.

de Brito,O.M. and Scorrano,L. (2008). Mitofusin 2 tethers endoplasmic reticulum to mitochondria. Nature. *456*, 605-610.

Delettre,C., Griffoin,J.M., Kaplan,J., Dollfus,H., Lorenz,B., Faivre,L., Lenaers,G., Belenguer,P., and Hamel,C.P. (2001). Mutation spectrum and splicing variants in the OPA1 gene. Hum. Genet. *109*, 584-591.

Delettre,C., Lenaers,G., Griffoin,J.M., Gigarel,N., Lorenzo,C., Belenguer,P., Pelloquin,L., Grosgeorge,J., Turc-Carel,C., Perret,E., Astarie-Dequeker,C., Lasquellec,L., Arnaud,B., Ducommun,B., Kaplan,J., and Hamel,C.P. (2000). Nuclear gene OPA1, encoding a mitochondrial dynamin-related protein, is mutated in dominant optic atrophy. Nat. Genet. *26*, 207-210.

DeVay,R.M., Dominguez-Ramirez,L., Lackner,L.L., Hoppins,S., Stahlberg,H., and Nunnari,J. (2009). Coassembly of Mgm1 isoforms requires cardiolipin and mediates mitochondrial inner membrane fusion. J. Cell Biol. *186*, 793-803.

Dimmer,K.S. and Scorrano,L. (2006). (De)constructing mitochondria: what for? Physiology. (Bethesda.) *21*, 233-241.

Donnou,S., Galand,C., Touitou,V., Sautes-Fridman,C., Fabry,Z., and Fisson,S. (2012). Murine models of B-cell lymphomas: promising tools for designing cancer therapies. Adv. Hematol. *2012*, 701704.

Ehses,S., Raschke,I., Mancuso,G., Bernacchia,A., Geimer,S., Tondera,D., Martinou,J.C., Westermann,B., Rugarli,E.I., and Langer,T. (2009). Regulation of OPA1 processing and mitochondrial fusion by m-AAA protease isoenzymes and OMA1. J Cell Biol *187*, 1023-1036.

Fang,H.Y., Chen,C.Y., Chiou,S.H., Wang,Y.T., Lin,T.Y., Chang,H.W., Chiang,I.P., Lan,K.J., and Chow,K.C. (2012). Overexpression of optic atrophy 1 protein increases cisplatin resistance via inactivation of caspase-dependent apoptosis in lung adenocarcinoma cells. Hum. Pathol. *43*, 105-114.

Frank,S., Gaume,B., Bergmann-Leitner,E.S., Leitner,W.W., Robert,E.G., Catez,F., Smith,C.L., and Youle,R.J. (2001). The role of dynamin-related protein 1, a mediator of mitochondrial fission, in apoptosis. Dev. Cell *1*, 515-525.

Frey,T.G. and Mannella,C.A. (2000). The internal structure of mitochondria. Trends Biochem. Sci. *25*, 319-324.

Frezza,C., Cipolat,S., Martins,d.B., Micaroni,M., Beznoussenko,G.V., Rudka,T., Bartoli,D., Polishuck,R.S., Danial,N.N., De Strooper,B., and Scorrano,L. (2006). OPA1 Controls Apoptotic Cristae Remodeling Independently from Mitochondrial Fusion. Cell *126*, 177-189.

Gandre-Babbe,S. and van der Bliek,A.M. (2008). The novel tail-anchored membrane protein Mff controls mitochondrial and peroxisomal fission in mammalian cells. Mol. Biol. Cell *19*, 2402-2412.

Gascoyne,R.D., Adomat,S.A., Krajewski,S., Krajewska,M., Horsman,D.E., Tolcher,A.W., O'Reilly,S.E., Hoskins,P., Coldman,A.J., Reed,J.C., and Connors,J.M. (1997). Prognostic significance of Bcl-2 protein expression and Bcl-2 gene rearrangement in diffuse aggressive non-Hodgkin's lymphoma. Blood *90*, 244-251.

Gilkerson,R.W., Selker,J.M., and Capaldi,R.A. (2003). The cristal membrane of mitochondria is the principal site of oxidative phosphorylation. FEBS Lett. *546*, 355-358.

Griparic,L., Kanazawa,T., and van der Bliek,A.M. (2007). Regulation of the mitochondrial dynamin-like protein Opa1 by proteolytic cleavage. J. Cell Biol *178*, 757-764.

Griparic,L., van der Wel,N.N., Orozco,I.J., Peters,P.J., and van der Bliek,A.M. (2004). Loss of the intermembrane space protein Mgm1/OPA1 induces swelling and localized constrictions along the lengths of mitochondria. J. Biol. Chem. *279*, 18792-18798.

Guan,K., Farh,L., Marshall,T.K., and Deschenes,R.J. (1993). Normal mitochondrial structure and genome maintenance in yeast requires the dynamin-like product of the MGM1 gene. Curr Genet *24*, 141-148.

Hackenbrock,C.R., Schneider,H., Lemasters,J.J., and Hochli,M. (1980). Relationships between bilayer lipid, motional freedom of oxidoreductase components, and electron transfer in the mitochondrial inner membrane. Adv. Exp. Med. Biol. *132*, 245-263.

Hanahan,D. and Weinberg,R.A. (2000). The hallmarks of cancer. Cell. *100*, 57-70.

Harder,Z., Zunino,R., and McBride,H. (2004). Sumo1 conjugates mitochondrial substrates and participates in mitochondrial fission. Curr. Biol. *14*, 340-345.

Harris,A.W., Pinkert,C.A., Crawford,M., Langdon,W.Y., Brinster,R.L., and Adams,J.M. (1988). The E mu-myc transgenic mouse. A model for high-incidence spontaneous lymphoma and leukemia of early B cells. J. Exp. Med. *167*, 353-371.

Harris,N.L., Jaffe,E.S., Stein,H., Banks,P.M., Chan,J.K., Cleary,M.L., Delsol,G., De Wolf-Peeters,C., Falini,B., Gatter,K.C., and . (1994). A revised European-American classification of lymphoid neoplasms: a proposal from the International Lymphoma Study Group. Blood *84*, 1361-1392.

Hartge,P. and Devesa,S.S. (1992). Quantification of the impact of known risk factors on time trends in non-Hodgkin's lymphoma incidence. Cancer Res. *52*, 5566s-5569s.

Herlan,M., Vogel,F., Bornhovd,C., Neupert,W., and Reichert,A.S. (2003). Processing of Mgm1 by the rhomboid-type protease Pcp1 is required for maintenance of mitochondrial morphology and of mitochondrial DNA. J. Biol. Chem. *278*, 27781-27788.

Herrmann,J.M. and Neupert,W. (2003). Protein insertion into the inner membrane of mitochondria. IUBMB Life *55*.

Hwang,S.K., Minai-Tehrani,A., Yu,K.N., Chang,S.H., Kim,J.E., Lee,K.H., Park,J., Beck,G.R., Jr., and Cho,M.H. (2012). Carboxyl-terminal modulator protein induces apoptosis by regulating mitochondrial function in lung cancer cells. Int. J. Oncol. *40*, 1515-1524.

Ishihara,N., Fujita,Y., Oka,T., and Mihara,K. (2006). Regulation of mitochondrial morphology through proteolytic cleavage of OPA1. EMBO J. *25*, 2966-2977.

Jones,B.A. and Fangman,W.L. (1992). Mitochondrial DNA maintenance in yeast requires a protein containing a region related to the GTP-binding domain of dynamin. Genes. Dev. *6*, 380-389.

Kong,B., Wang,Q., Fung,E., Xue,K., and Tsang,B.K. (2014). p53 is required for cisplatin-induced processing of the mitochondrial fusion protein L-Opa1 that is mediated by the mitochondrial metallopeptidase Oma1 in gynecologic cancers. J. Biol. Chem. *289*, 27134-27145.

Koshiba,T., Detmer,S.A., Kaiser,J.T., Chen,H., McCaffery,J.M., and Chan,D.C. (2004). Structural basis of mitochondrial tethering by mitofusin complexes. Science *305*, 858-862.

Kramer,M.H., Hermans,J., Wijburg,E., Philippo,K., Geelen,E., van Krieken,J.H., de,J.D., Maartense,E., Schuuring,E., and Kluin,P.M. (1998). Clinical relevance of BCL2, BCL6, and MYC rearrangements in diffuse large B-cell lymphoma. Blood *92*, 3152-3162.

Kraus,M., Alimzhanov,M.B., Rajewsky,N., and Rajewsky,K. (2004). Survival of resting mature B lymphocytes depends on BCR signaling via the Igalpha/beta heterodimer. Cell *117*, 787-800.

Kroemer,G. (2006). Mitochondria in cancer. Oncogene *25*, 4630-4632.

Kuppers,R. (2005). Mechanisms of B-cell lymphoma pathogenesis. Nat. Rev. Cancer *5*, 251-262.

Kurosaki,T. (2010). B-lymphocyte biology. Immunol. Rev. *237*, 5-9.

Lam,K.P., Kuhn,R., and Rajewsky,K. (1997). In vivo ablation of surface immunoglobulin on mature B cells by inducible gene targeting results in rapid cell death. Cell *90*, 1073-1083.

Langdon,W.Y., Harris,A.W., Cory,S., and Adams,J.M. (1986). The c-myc oncogene perturbs B lymphocyte development in E-mu-myc transgenic mice. Cell *47*, 11-18.

Lee,Y.J., Jeong,S.Y., Karbowski,M., Smith,C.L., and Youle,R.J. (2004). Roles of the mammalian mitochondrial fission and fusion mediators Fis1, Drp1, and Opa1 in apoptosis. Mol. Biol. Cell *15*, 5001-5011.

Lenz,G., Davis,R.E., Ngo,V.N., Lam,L., George,T.C., Wright,G.W., Dave,S.S., Zhao,H., Xu,W., Rosenwald,A., Ott,G., Muller-Hermelink,H.K., Gascoyne,R.D., Connors,J.M., Rimsza,L.M., Campo,E., Jaffe,E.S., Delabie,J., Smeland,E.B., Fisher,R.I., Chan,W.C., and Staudt,L.M. (2008). Oncogenic CARD11 mutations in human diffuse large B cell lymphoma. Science *319*, 1676-1679.

Levine,M.H., Haberman,A.M., Sant'Angelo,D.B., Hannum,L.G., Cancro,M.P., Janeway,C.A., Jr., and Shlomchik,M.J. (2000). A B-cell receptor-specific selection step governs immature to mature B cell differentiation. Proc. Natl. Acad. Sci. U. S. A *97*, 2743-2748.

Li,P., Nijhawan,D., Budihardjo,I., Srinivasula,S.M., Ahmad,M., Alnemri,E.S., and Wang,X. (1997). Cytochrome c and dATP-dependent formation of Apaf-1/caspase-9 complex initiates an apoptotic protease cascade. Cell *91*, 479-489.

Liu,X., Weaver,D., Shirihai,O., and Hajnoczky,G. (2009). Mitochondrial 'kiss-and-run': interplay between mitochondrial motility and fusion-fission dynamics. EMBO J. *28*, 3074-3089.

Liu,Y.J., Mason,D.Y., Johnson,G.D., Abbot,S., Gregory,C.D., Hardie,D.L., Gordon,J., and MacLennan,I.C. (1991). Germinal center cells express bcl-2 protein after activation by signals which prevent their entry into apoptosis. Eur. J. Immunol. *21*, 1905-1910.

Lohr,J.G., Stojanov,P., Lawrence,M.S., Auclair,D., Chapuy,B., Sougnez,C., Cruz-Gordillo,P., Knoechel,B., Asmann,Y.W., Slager,S.L., Novak,A.J., Dogan,A., Ansell,S.M., Link,B.K., Zou,L., Gould,J., Saksena,G., Stransky,N., Rangel-Escareno,C., Fernandez-Lopez,J.C., Hidalgo-Miranda,A., Melendez-Zajgla,J., Hernandez-Lemus,E., Schwarz,C., Imaz-Rosshandler,I., Ojesina,A.I., Jung,J., Pedamallu,C.S., Lander,E.S., Habermann,T.M., Cerhan,J.R., Shipp,M.A., Getz,G., and Golub,T.R. (2012). Discovery and prioritization of somatic mutations in diffuse large B-cell lymphoma (DLBCL) by whole-exome sequencing. Proc. Natl. Acad. Sci. U. S. A *109*, 3879-3884.

Mannella,C.A., Marko,M., Penczek,P., Barnard,D., and Frank,J. (1994). The internal compartmentation of rat-liver mitochondria: tomographic study using the high-voltage transmission electron microscope. Microsc Res Tech *27*, 278-283.

McQuibban,G.A., Saurya,S., and Freeman,M. (2003). Mitochondrial membrane remodelling regulated by a conserved rhomboid protease. Nature *423*, 537-541.

Meeusen,S., DeVay,R., Block,J., Cassidy-Stone,A., Wayson,S., McCaffery,J.M., and Nunnari,J. (2006). Mitochondrial inner-membrane fusion and crista maintenance requires the dynamin-related GTPase Mgm1. Cell *127*, 383-395.

Melchers,F., ten,B.E., Seidl,T., Kong,X.C., Yamagami,T., Onishi,K., Shimizu,T., Rolink,A.G., and Andersson,J. (2000). Repertoire selection by pre-B-cell receptors and B-cell receptors, and genetic control of B-cell development from immature to mature B cells. Immunol. Rev. *175*, 33-46.

Monti,S., Savage,K.J., Kutok,J.L., Feuerhake,F., Kurtin,P., Mihm,M., Wu,B., Pasqualucci,L., Neuberg,D., Aguiar,R.C., Dal,C.P., Ladd,C., Pinkus,G.S., Salles,G., Harris,N.L., Dalla-Favera,R., Habermann,T.M., Aster,J.C., Golub,T.R., and Shipp,M.A. (2005). Molecular profiling of diffuse large B-cell lymphoma identifies robust subtypes including one characterized by host inflammatory response. Blood *105*, 1851-1861.

Mori,S., Rempel,R.E., Chang,J.T., Yao,G., Lagoo,A.S., Potti,A., Bild,A., and Nevins,J.R. (2008). Utilization of pathway signatures to reveal distinct types of B lymphoma in the Emicro-myc model and human diffuse large B-cell lymphoma. Cancer Res. *68*, 8525-8534.

Niemann,C.U. and Wiestner,A. (2013). B-cell receptor signaling as a driver of lymphoma development and evolution. Semin. Cancer Biol. *23*, 410-421.

Olichon,A., Baricault,L., Gas,N., Guillou,E., Valette,A., Belenguer,P., and Lenaers,G. (2003). Loss of OPA1 perturbates the mitochondrial inner membrane structure and integrity, leading to cytochrome c release and apoptosis. J. Biol. Chem. *278*, 7743-7746.

Olichon,A., Elachouri,G., Baricault,L., Delettre,C., Belenguer,P., and Lenaers,G. (2007a). OPA1 alternate splicing uncouples an evolutionary conserved function in mitochondrial fusion from a vertebrate restricted function in apoptosis. Cell Death. Differ. *14*, 682-692.

Olichon,A., Emorine,L.J., Descoins,E., Pelloquin,L., Brichese,L., Gas,N., Guillou,E., Delettre,C., Valette,A., Hamel,C.P., Ducommun,B., Lenaers,G., and Belenguer,P. (2002). The human dynamin-related protein OPA1 is anchored to the mitochondrial inner membrane facing the inter-membrane space. FEBS Lett. *523*, 171-176.

Olichon,A., Landes,T., rnaune-Pelloquin,L., Emorine,L.J., Mils,V., Guichet,A., Delettre,C., Hamel,C., mati-Bonneau,P., Bonneau,D., Reynier,P., Lenaers,G., and Belenguer,P. (2007b). Effects of OPA1 mutations on mitochondrial morphology and apoptosis: relevance to ADOA pathogenesis. J. Cell Physiol *211*, 423-430.

Otera,H., Wang,C., Cleland,M.M., Setoguchi,K., Yokota,S., Youle,R.J., and Mihara,K. (2010). Mff is an essential factor for mitochondrial recruitment of Drp1 during mitochondrial fission in mammalian cells. J Cell Biol. *191*, 1141-1158.

Palade,G.E. (1952). The fine structure of mitochondria. Anat. Rec. *114*, 427-451.

Palmer,C.S., Osellame,L.D., Laine,D., Koutsopoulos,O.S., Frazier,A.E., and Ryan,M.T. (2011). MiD49 and MiD51, new components of the mitochondrial fission machinery. EMBO Rep. *12*, 565-573.

Pelloquin,L., Belenguer,P., Menon,Y., Gas,N., and Ducommun,B. (1999). Fission yeast Msp1 is a mitochondrial dynamin-related protein. J. Cell Sci. *112*.

Perez-Vera,P., Reyes-Leon,A., and Fuentes-Panana,E.M. (2011). Signaling proteins and transcription factors in normal and malignant early B cell development. Bone Marrow Res. *2011*, 502751.

Perkins,G., Renken,C., Martone,M.E., Young,S.J., Ellisman,M., and Frey,T. (1997). Electron tomography of neuronal mitochondria: three-dimensional structure and organization of cristae and membrane contacts. J. Struct. Biol. *119*, 260-272.

Pfanner,N. and Meijer,M. (1997). The Tom and Tim machine. Curr. Biol. *7*, R100-R103.

Pfanner,N. and Wiedemann,N. (2002). Mitochondrial protein import: two membranes, three translocases. Curr Opin Cell Biol *14*.

Pieper,K., Grimbacher,B., and Eibel,H. (2013). B-cell biology and development. J. Allergy Clin. Immunol. *131*, 959-971.

Reed,J.C., Haldar,S., Croce,C.M., and Cuddy,M.P. (1990). Complementation by BCL2 and C-HA-RAS oncogenes in malignant transformation of rat embryo fibroblasts. Mol. Cell Biol. *10*, 4370-4374.

Rhodes,D.R., Yu,J., Shanker,K., Deshpande,N., Varambally,R., Ghosh,D., Barrette,T., Pandey,A., and Chinnaiyan,A.M. (2004). ONCOMINE: a cancer microarray database and integrated data-mining platform. Neoplasia. *6*, 1-6.

Rojo,M., Legros,F., Chateau,D., and Lombes,A. (2002). Membrane topology and mitochondrial targeting of mitofusins, ubiquitous mammalian homologs of the transmembrane GTPase Fzo. J. Cell Sci. *115*, 1663-1674.

Sato,M. and Sato,K. (2011). Degradation of paternal mitochondria by fertilization-triggered autophagy in C. elegans embryos. Science *334*, 1141-1144.

Satoh,M., Hamamoto,T., Seo,N., Kagawa,Y., and Endo,H. (2003). Differential sublocalization of the dynamin-related protein OPA1 isoforms in mitochondria. Biochem. Biophys. Res. Commun. *300*, 482-493.

Schatz,D.G. and Swanson,P.C. (2011). V(D)J recombination: mechanisms of initiation. Annu. Rev. Genet. *45*, 167-202.

Schrader,M. (2006). Shared components of mitochondrial and peroxisomal division. Biochim Biophys Acta *1763*.

Scorrano,L. (2013). Keeping mitochondria in shape: a matter of life and death. Eur. J. Clin. Invest *43*, 886-893.

Scorrano,L., Ashiya,M., Buttle,K., Weiler,S., Oakes,S.A., Mannella,C.A., and Korsmeyer,S.J. (2002). A distinct pathway remodels mitochondrial cristae and mobilizes cytochrome c during apoptosis. Dev. Cell *2*, 55-67.

Sesaki,H., Southard,S.M., Yaffe,M.P., and Jensen,R.E. (2003). Mgm1p, a dynamin-related GTPase, is essential for fusion of the mitochondrial outer membrane. Mol. Biol. Cell *14*, 2342-2356.

Shaffer,A.L., Rosenwald,A., and Staudt,L.M. (2002). Lymphoid malignancies: the dark side of B-cell differentiation. Nat. Rev. Immunol. *2*, 920-932.

Shaffer,A.L., III, Young,R.M., and Staudt,L.M. (2012). Pathogenesis of human B cell lymphomas. Annu. Rev. Immunol. *30*, 565-610.

Sidman,C.L., Shaffer,D.J., Jacobsen,K., Vargas,S.R., and Osmond,D.G. (1993). Cell populations during tumorigenesis in Eu-myc transgenic mice. Leukemia *7*, 887-895.

SJOSTRAND,F.S. (1953). Electron microscopy of mitochondria and cytoplasmic double membranes. Nature *171*, 30-32.

Song,Z., Chen,H., Fiket,M., Alexander,C., and Chan,D.C. (2007). OPA1 processing controls mitochondrial fusion and is regulated by mRNA splicing, membrane potential, and Yme1L. J. Cell Biol *178*, 749-755.

Song,Z., Ghochani,M., McCaffery,J.M., Frey,T.G., and Chan,D.C. (2009). Mitofusins and OPA1 mediate sequential steps in mitochondrial membrane fusion. Mol. Biol. Cell *20*, 3525-3532.

Staudt,L.M. (2010). Oncogenic activation of NF-kappaB. Cold Spring Harb. Perspect. Biol. *2*, a000109.

Sthoeger,Z.M., Wakai,M., Tse,D.B., Vinciguerra,V.P., Allen,S.L., Budman,D.R., Lichtman,S.M., Schulman,P., Weiselberg,L.R., and Chiorazzi,N. (1989). Production of autoantibodies by CD5-expressing B lymphocytes from patients with chronic lymphocytic leukemia. J. Exp. Med. *169*, 255-268.

Strasser,A., Harris,A.W., Bath,M.L., and Cory,S. (1990). Novel primitive lymphoid tumours induced in transgenic mice by cooperation between myc and bcl-2. Nature *348*, 331-333.

Suzuki,M., Jeong,S.Y., Karbowski,M., Youle,R.J., and Tjandra,N. (2003). The solution structure of human mitochondria fission protein Fis1 reveals a novel TPR-like helix bundle. J. Mol. Biol. *334*, 445-458.

Taguchi,N., Ishihara,N., Jofuku,A., Oka,T., and Mihara,K. (2007). Mitotic phosphorylation of dynamin-related GTPase Drp1 participates in mitochondrial fission. J. Biol Chem. *282*, 11521-11529.

Tatsuta,T. and Langer,T. (2008). Quality control of mitochondria: protection against neurodegeneration and ageing. EMBO J. *27*, 306-314.

Teng,G. and Papavasiliou,F.N. (2007). Immunoglobulin somatic hypermutation. Annu. Rev. Genet. *41*, 107-120.

Thome,M. (2004). CARMA1, BCL-10 and MALT1 in lymphocyte development and activation. Nat. Rev. Immunol. *4*, 348-359.

Tsujimoto,Y. (1989). Stress-resistance conferred by high level of bcl-2 alpha protein in human B lymphoblastoid cell. Oncogene *4*, 1331-1336.

Uhlen,M., Bjorling,E., Agaton,C., Szigyarto,C.A., Amini,B., Andersen,E., Andersson,A.C., Angelidou,P., Asplund,A., Asplund,C., Berglund,L., Bergstrom,K., Brumer,H., Cerjan,D., Ekstrom,M., Elobeid,A., Eriksson,C., Fagerberg,L., Falk,R., Fall,J., Forsberg,M., Bjorklund,M.G., Gumbel,K., Halimi,A., Hallin,I., Hamsten,C., Hansson,M., Hedhammar,M., Hercules,G., Kampf,C., Larsson,K., Lindskog,M., Lodewyckx,W., Lund,J., Lundeberg,J., Magnusson,K., Malm,E., Nilsson,P., Odling,J., Oksvold,P., Olsson,I., Oster,E., Ottosson,J., Paavilainen,L., Persson,A., Rimini,R., Rockberg,J., Runeson,M., Sivertsson,A., Skollermo,A., Steen,J., Stenvall,M., Sterky,F., Stromberg,S., Sundberg,M., Tegel,H., Tourle,S., Wahlund,E., Walden,A., Wan,J., Wernerus,H., Westberg,J., Wester,K., Wrethagen,U., Xu,L.L., Hober,S., and Ponten,F. (2005). A human protein atlas for normal and cancer tissues based on antibody proteomics. Mol. Cell Proteomics. *4*, 1920-1932.

Varanita,T., Soriano,M.E., Romanello,V., Zaglia,T., Quintana-Cabrera,R., Semenzato,M., Menabò,R., Costa,V., Civiletto,G., Pesce,P., Viscomi,C., Zeviani,M., Di Lisa,F., Mongillo,M., Sandri,M., and Scorrano,L. (2015). The Opa1-Dependent Mitochondrial Cristae Remodeling Pathway Controls Atrophic, Apoptotic, and Ischemic Tissue Damage. Cell Metabolism *21*.

Vaux,D.L., Cory,S., and Adams,J.M. (1988). Bcl-2 gene promotes haemopoietic cell survival and cooperates with c-myc to immortalize pre-B cells. Nature *335*, 440-442.

Vogel,F., Bornhovd,C., Neupert,W., and Reichert,A.S. (2006). Dynamic subcompartmentalization of the mitochondrial inner membrane. J. Cell Biol. *175*, 237-247.

Wasiak,S., Zunino,R., and McBride,H.M. (2007). Bax/Bak promote sumoylation of DRP1 and its stable association with mitochondria during apoptotic cell death. J. Cell Biol. *177*, 439-450.

Wasilewski,M. and Scorrano,L. (2009). The changing shape of mitochondrial apoptosis. Trends Endocrinol. Metab *20*, 287-294.

Ye,B.H., Lista,F., Lo,C.F., Knowles,D.M., Offit,K., Chaganti,R.S., and Dalla-Favera,R. (1993). Alterations of a zinc finger-encoding gene, BCL-6, in diffuse large-cell lymphoma. Science *262*, 747-750.

Yu,T., Fox,R.J., Burwell,L.S., and Yoon,Y. (2005). Regulation of mitochondrial fission and apoptosis by the mitochondrial outer membrane protein hFis1. J. Cell Sci. *118*, 4141-4151.

Zhao,X., Tian,C., Puszyk,W.M., Ogunwobi,O.O., Cao,M., Wang,T., Cabrera,R., Nelson,D.R., and Liu,C. (2013). OPA1 downregulation is involved in sorafenib-induced apoptosis in hepatocellular carcinoma. Lab Invest *93*, 8-19.

Zhivotovsky,B., Orrenius,S., Brustugun,O.T., and Doskeland,S.O. (1998). Injected cytochrome c induces apoptosis. Nature *391*, 449-450.

ACKNOWLEDGEMENTS

As this exciting PhD journey is slowly coming to its end, from the first days in Geneva, over the move to Padova, I would like to take the opportunity to thank all the people whose help, support, guidance and inspiration made this Thesis possible.

I would like to thank my supervisor, professor Luca Scorrano, for giving me the opportunity to become part of such an incredible laboratory. I want to thank him for all the help and support he gave me over the course of these couple of years. I want to thank him for his patience, for believing in me in times when I maybe didn't believe in myself, for encouraging me to develop all my potentials, for being an inspiration to us all and for setting an example of what it means to be a true scientist and an extraordinary human being. Thank you very much Luca for everything!

I would like to thank my parents, my mother Mrs. Gordana Samardzic and my father Mr. Slobodan Samardzic, for being the biggest support in my life. I would like to thank them for all their love, for always being there for me, for encouraging me and supporting me every step of the way, from the day I was born. Mom and Dad, thank you very much, a person cannot ask for better parents then you, thank you so much for everything.

I would like to thank my sisters, for all the love, help and support over the years. A very special thank you goes to Ivana for being there for me in December, and a very special thank you goes to Aleksandra for being there for me in January. This wouldn't have been possible without you.

I would like to thank my aunt Maja for all her precious advice, guidance and encouragement over all these years.

I would like to thank my dear friend Bastien, for being there for me in Geneva and for playing a key role in something that turned out to completely change my life around. Thank you so much Bastien, I will never forget it.

I would like to thank all my lab members. It is an honor and pleasure to work side by side with such talented individuals on a daily basis. A very special thank you goes to Mauro and Francesca, for all their scientific help and input during this whole PhD experience. A special thank you goes to Alice, Charlotte, Christina, Sowmya and Elisa, my dear PhD girls with whom I shared good and bad over the course of these couple of years.

I would like to thank Matteo and Boris for their precious help when it came to fixing my computer.

I would like to thank Scambio Padova, and all my friends inside and outside the lab, for making my life here so interesting and exciting.

I would like to thank Irena for being such a great friend.

Lastly, a very special thank you goes to Ian, for being there for me, and for making my life so wonderful.

Thank you very much everyone.